AD-A110 835 SRI INTERNATIONAL. MENLO PARK CA F/G 7/4
STRATOSPHERIC REACTIONS OF PEROXYNITRIC ACID.(U)
APR 81 J R BARKER, P L TREVOR, R A KENLEY DOT-FA78WA-4228
UNCLASSIFIED SRI-7921-F FAA/EE-82-5 NL

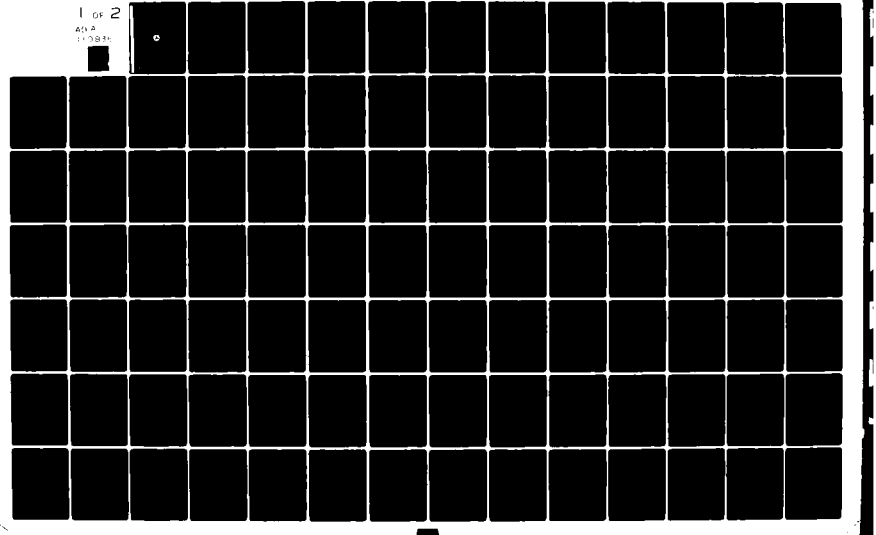

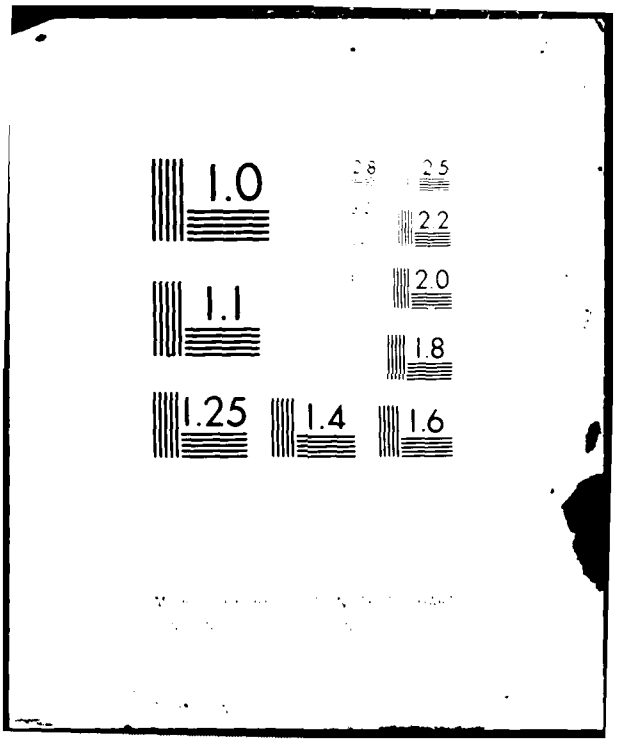
1.0
2.8
2.5
2.2
2.0
1.1
1.8
1.25
1.4
1.6

STRATOSPHERIC REACTIONS OF PEROXYNITRIC ACID

John R. Barker, Paula L. Trevor, Richard A. Kenley,
Jenq-Sian Chang, John E. Davenport, Bosco Y. Lan,
and Graham Black

SRI International
333 Ravenswood Avenue
Menlo Park, 94025

April 23, 1981

Final Report
Covering the Period September 29, 1978 to December 31, 1980

Document available to the U.S. public through the
National Technical Information Service,
Springfield, Virginia 22161.

Prepared for

U.S. DEPARTMENT OF TRANSPORTATION

FEDERAL AVIATION ADMINISTRATION
Logistics Service, Development Branch
800 Independence Avenue, SW
Washington, DC 20591

"This document is disseminated under the sponsorship of the Department of Transportation in the interest of information exchange. The U.S Goverment assumes no liability for its contents or use thereof.

The work reported in this document was conducted under Contract No. DOT-FA78WA-4228 for the U.S. Department of Transportation/Federal Aviation Administration. The publication of this report does not indicate endorsement by the Department of Transportation, nor should the contents be construed as reflecting the official position of that agency."

Technical Report Documentation Page

1. Report No.	2. Government Accession No.	3. Recipient's Catalog No.
FAA-EE-82-5	AD-A110 835	

4. Title and Subtitle	5. Report Date
STRATOSPHERIC REACTIONS OF PEROXYNITRIC ACID	April 23, 1981
	6. Performing Organization Code: 322
7. Author(s) John R. Barker, Paula L. Trevor, Richard A. Kenley, Jenq-Sian Chang, John E. Davenport, Bosco Y. Lan, and Graham Black	8. Performing Organization Report No.: 7921
9. Performing Organization Name and Address SRI International 333 Ravenswood Avenue Menlo Park, CA 94025	10. Work Unit No. (TRAIS)
	11. Contract or Grant No.: DOT-FA78WA-4228
12. Sponsoring Agency Name and Address U.S. Department of Transportation/Federal Aviation Administration, Logistics Service, Development Branch, 800 Independence Avenue, SW Washington, DC 20591	13. Type of Report and Period Covered Final Report 29 September 1978 through 31 December 1980
	14. Sponsoring Agency Code

15. Supplementary Notes

16. Abstract PNA($HOONO_2$) reactions have been studied because of their potential importance in the atmosphere. A new preparative procedure for PNA was developed, and experiments have been performed to measure the reaction rate constants for the following reactions:

$$O + HOONO_2 \rightarrow \text{Products} \quad (A)$$

$$H + HOONO_2 \rightarrow \text{Products} \quad (B)$$

$$OH + HOONO_2 \rightarrow \text{Products} \quad (C)$$

$$O_3 + HOONO_2 \rightarrow \text{Products} \quad (D)$$

The results were:

$(k_A \pm 1\sigma) = (7.0 \pm 12.2) \times 10^{-11} \exp(-3369 \pm 489/T)$ cm^3 s^{-1}, 3 K ≤ 297 K

$\sigma_{AB} = 5.97 \times 10^{-8}$

$(k_B \pm 2\sigma) = (2.46 \pm 0.35) \times 10^{-14}$ cm^3 s^{-1}, 248 K ≤ T ≤ 315 K

$(k_C \pm 2\sigma) = (4.0 \pm 1.0) \times 10^{-12}$ cm^3 s^{-1}, 246 K ≤ T ≤ 324 K

$k_D \leq 5 \times 10^{-20}$ cm^3 s^{-1}, 278 K

17. Key Words	18. Distribution Statement
Pernitric acid Stratospheric chemistry Oxygen atoms Hydrogen atoms Hydrogen radicals Ozone Bimolecular reactions	Unlimited

19. Security Classif. (of this report)	20. Security Classif. (of this page)	21. No. of Pages	22. Price
UNCLASSIFIED	UNCLASSIFIED	141	

Form DOT F 1700.7 (8-72) Reproduction of completed page authorized

ABSTRACT

PNA ($HOONO_2$) reactions have been studied because of their potential importance in the atmosphere. Experiments have been performed to measure the reaction rate constants for the following reactions:

$$O + HOONO_2 \rightarrow \text{Products} \quad (A)$$

$$H + HOONO_2 \rightarrow \text{Products} \quad (B)$$

$$OH + HOONO_2 \rightarrow \text{Products} \quad (C)$$

$$O_3 + HOONO_2 \rightarrow \text{Products} \quad (D)$$

The results were:

$(k_A \pm 1\sigma) = (7.0 \pm 12.2) \times 10^{-11} \exp(-3369 \pm 489/T)$ cm^3 s^{-1}, 228 K $\leq$ 297 K

$\sigma_{AB} = 5.97 \times 10^{-8}$

$(k_B \pm 2\sigma) = (2.46 \pm 0.35) \times 10^{-14}$ cm^3 s^{-1}, 248 K $\leq T \leq$ 315 K

$(k_C \pm 2\sigma) = (4.0 \pm 1.0) \times 10^{-12}$ cm^3 s^{-1}, 246 K $\leq T \leq$ 324 K

$k_D \leq 5 \times 10^{-20}$ cm^3 s^{-1}, 278 K

CONTENTS

ILLUSTRATIONS

Appendix E

TABLES

Appendix E

ACKNOWLEDGMENTS

Helpful suggestions were offered by many colleagues, including Dr. D. M. Golden, Dr. Mario Molina, Dr. J. V. Michael, Dr. L. Stieff, and Dr. B. Klemm. Thanks also go to E. Adkins and to our other colleagues at SRI.

I INTRODUCTION

Both HO_2 and NO_2 play crucial roles in the chemistry of the upper atmosphere. For several years, these two species were thought to react via a radical disproportionation reaction, although it was suggested[1] that a longer-lived complex could be formed according to reaction (1):

$$HO_2 + NO_2 + M \rightleftharpoons HOONO_2 + M \qquad (1)$$

The importance of reaction (1) has recently been verified by direct observation of HO_2NO_2 by Fourier transform infrared spectroscopy.[2] Moreover, the rate of reaction (1) has been measured,[3] and its reverse reaction (-1) has been studied.[4] Also, RRKM theory has been applied to these data for reaction (-1) so that its rate can be reliably estimated as a function of both temperature and pressure.[5] In another publication, the effect of HO_2NO_2 on tropospheric photochemical smog chemistry[6] was discussed.

A concerted effort is under way to investigate PNA and determine the rates of various loss mechanisms that affect its residence time in the stratosphere. In addition to the experimental studies reported on its thermal decomposition rate, results of investigations on optical absorption cross sections have been reported[7-9] that permit calculation of the photolysis rates appropriate for the atmosphere.

In our laboratory, reactions of PNA with several atmospheric species have been studied to determine bimolecular rate constants for the destruction of PNA. The rate constants for PNA reactions with O-atoms, H-atoms, O_3, and OH are reported here.

Although the primary reason for studying PNA reactions is their potential importance in the atmosphere, PNA also is an interesting chemical that is part of the fabric of H-N-O species. In this sense, it is a member of the homologous series of nitrogen acids (e.g., HONO, $HONO_2$, $HOONO_2$), as well as being the first member of a series of pernitrates (e.g., $HOONO_2$, CH_3OONO_2, $CH_3\overset{O}{\overset{\|}{C}}OONO_2$); in addition, it is a hydroperoxide (e.g., HOOH, HOOR, $HOONO_2$). All these species are important for various reasons, and data are needed on their reactions. Such data can then be used as a basis for predicting reaction rate constants for species that have not, as yet, been studied experimentally.

Each of the Appendices to this report has been submitted for publication in a technical journal and is intended to stand alone. Appendix A describes a convenient preparation of relatively pure PNA, and Appendices B-E give detailed descriptions of experiments designed to measure the rate constant for PNA reactions with O-atoms, OH, O_3, and H-atoms.

II SUMMARY AND CONCLUSIONS

This section summarizes the results of experimental work on the preparation of PNA and some of its reactions and discusses the implications of atmospheric chemistry.

A. Results

1. Preparation of PNA

Nitration of H_2O_2 with NO_2BF_4 provides a convenient method for preparing pure PNA in relatively large quantities. Aqueous PNA decomposes both by molecular elimination of O_2 and nitrite from the pernitrate anion and by acid-catalyzed decomposition of PNA molecules.

2. $O(^3P) + HOONO_2 \rightarrow$ Products

The rate constant was measured under O-atom-rich conditions as a function of temperature; the rate constant is given by $(k \pm 1\sigma) = (7.0 \pm 12.2) \times 10^{-11} \exp(-3369 \pm 489/T)$ cm^3 s^{-1}, covariance $\sigma_{AB} = 5.97 \times 10^{-8}$. Nine temperatures were studied ranging from 228 K to 297 K, and the uncertainties given are one standard deviation, based on a weighted least-squares analysis of the data. The products of the reaction could not be observed, but they are thought to be $OH + O_2 + NO_2$; HNO_3 can be ruled out since it was not observed.

3. $OH + HOONO_2 \rightarrow$ Products

Rate constants were measured under PNA-rich conditions by the flash-photolysis-resonance-fluorescence method for nine temperatures ranging from 246 K to 324 K. The rate constant was determined to be

$(k \pm 2\sigma) = (4.0 \pm 1.0) \times 10^{-12}$ cm^3 s^{-1}, independent of temperature. Products could not be observed, and several pathways are possible.

4. $O_3 + HOONO_2 \rightarrow$ Products

This reaction was investigated at 278 K under static conditions with O_3 in excess. The reaction rate was very slow, giving an upper limit to the rate constant of $k \leq 5 \times 10^{-20}$ cm^3 s^{-1}. Products were not observed.

5. $H + HOONO_2 \rightarrow$ Products

This reaction was studied under H-atom-rich conditions at seven temperatures ranging from 226 to 315 K, but at 226 K the rate was too fast to allow measurement of a rate constant and there were indications that wall reactions were important at temperatures lower than 248 K. For temperatures above 248 K, the rate constant was $(k \pm 2\sigma) = (2.46 \pm 0.35) \times 10^{-14}$ cm^3 s^{-1}, independent of temperature. The experimental technique appears to be free of problems and a tentative explanation is proposed for the very low A-factor. Products of the reaction were not observed, although they are expected to be analogous to those resulting from the reactions of H-atoms with H_2O_2 and CH_3OOH. Nitric acid was not observed and can be ruled out as a reaction product.

B. Implications for Atmospheric Chemistry

The potential importance of HO_2NO_2 is due to its ability to act as a reservoir for both HO_2 and NO_2. If HO_2NO_2 has a long lifetime, it will act as a radical trap and slow down the overall free radical chain mechanism; thus, ozone will probably not be destroyed as quickly. Acting as a reservoir, HO_2NO_2 can decompose slowly to release a steady stream of HO_2 radicals and NO_2, even in darkness. Thus, it can serve as a free radical

initiator as well as a trap. This unique role underlines its potential importance and makes it difficult to estimate its effects without detailed modeling calculations.

Although HO_2NO_2 can be shown not to influence tropospheric photochemical smog,[6] it potentially has a much more profound effect in the stratosphere because the lower temperatures and pressures combine to give it a much longer lifetime with respect to unimolecular decomposition. For example, at 220 K and 50 torr, its lifetime is estimated to be nearly 8 months, but at 280 K and 10 torr, the lifetime is only about 45 minutes.[4,5]

Reactions with atmospheric species must also be considered. Depending on the nature of such reactions, the net result might be to retard destructive stratospheric chemistry even further. For example, the potentially important reaction with OH can result in the net loss of an HO_2 radical as well as an OH radical:

$$\begin{aligned} HO_2 + NO_2 &\xrightarrow{M} HO_2NO_2 \\ OH + HO_2NO_2 &\xrightarrow{?} H_2O + NO_2 + O_2 \end{aligned}$$

$$\text{net:}\quad OH + HO_2 \rightarrow H_2O + O_2 \qquad (27)$$

For the reaction of O-atoms, however, the net result may have less effect on the ozone layer:

$$\begin{aligned} HO_2 + NO_2 &\xrightarrow{M} HO_2NO_2 \\ O + HO_2NO_2 &\xrightarrow{?} OH + O_2 + NO_2 \\ OH + O_3 &\rightarrow O_2 + HO_2 \end{aligned}$$

$$\text{net:}\quad O + O_3 \rightarrow 2O_2 \qquad (28)$$

These two reactions can be quite important because of the net chemical changes involved and because the shortened lifetime of HO_2NO_2 can influence the extent of diurnal effects; a long lifetime tends to damp them out.

Ozone and H-atoms might also react with HO_2NO_2 to cause chemical effects as well as to shorten the HO_2NO_2 lifetime:

$$O_3 + HOONO_2 \rightarrow HO + 2O_2 + NO_2 \qquad (22)$$

$$H + HOONO_2 \rightarrow \text{Products} \qquad (23)$$

As written, the ozone reaction products would have the following effect:

$$HO_2 + NO_2 \overset{M}{\rightarrow} HOONO_2$$

$$O_3 + HO_2NO_2 \rightarrow OH + 2O_2 + NO_2$$

$$OH + O_3 \rightarrow O_2 + HO_2$$

$$\text{net:} \quad 2O_3 \rightarrow 3O_2 \qquad (29)$$

Again, this would have less effect on atmospheric chemistry than destruction of OH or HO_2 radicals.

REFERENCES

1. R. Simonaitis and J. Heicklen, J. Phys. Chem., 80, 1 (1976).

2. H. Niki, P. D. Maker, C. M. Savage, and L. P. Breitenbach, Chem. Phys. Lett., 45, 564 (1977).

3. C. J. Howard, J. Chem. Phys., 67 5258 (1977).

4. R. A. Graham, A. M. Winer, and J. N. Pitts, Jr., Chem. Phys. Lett., 51, 215 (1977); J. Chem. Phys., 68, 4505 (1978).

5. A. C. Baldwin and D. M. Golden, J. Phys. Chem., 82, 644 (1978).

6. A. C. Baldwin, J. R. Barker, D. M. Golden, and D. G. Hendry, J. Phys. Chem., 81, 2483 (1977).

7. R. A. Graham, A. M. Winder, and J. N. Pitts, Geophys. Res. Lett., 5, 909 (1978).

8. R. A. Cox and K. Patrick, Int. J. Chem. Kinetics, 11, 635 (1979).

9. L. T. Molina and M. J. Molina, 14th Informal Conference on Photochemistry, March 30-April 3, 1980, paper C2; M. J. Molina, Report No. FAA-EE-80-07, U.S. Department of Transportation, Federal Aviation Administration, 1980.

Appendix A

PREPARATION AND THERMAL DECOMPOSITION OF PERNITRIC ACID IN AQUEOUS MEDIA

(Richard A. Kenley, Paula L. Trevor, Bosco Y. Lan)

A. Introduction

Pernitric acid (PNA), $HOONO_2$, can be viewed either as an inorganic peracid, ROOH (where R = NO_2), a mixed anhydride of two acids (HOOH and HNO_3) or as the parent member of the family of peroxynitrates, $ROONO_2$ (where R = H). As such, PNA can be expected to participate either in free radical or ionic reactions and it therefore affords the opportunity for some interesting kinetic and mechanistic investigations.

In 1911 D'An's and Friederich[1] reacted H_2O_2 with N_2O_5 and obtained a solution that liberated Br_2 from Br^-. They suggested that the solution contained $HOONO_2$, but did not offer definitive proof for the existence of PNA. Schwarz[2] reported similar observations in 1948.

In 1977 Niki et al.[3] studied the gas phase reaction of photochemically generated chlorine atoms with a mixture of H_2, O_2 and NO_2 and obtained the infrared spectrum of a species to which they assigned the formula HO_2NO_2. Other authors[4,5] have reported analogous photochemical methods for generating $HOONO_2$ in the gas phase. Graham et al.[6] condensed H_2O_2 in a 253°K trap and passed a mixture of 1% NO_2 in N_2 through the trap. They then degassed the trap under N_2 flow to yield PNA vapor.

The foregoing methods for generating $HOONO_2$ give a product that is contaminated with impurities and side products. As batch-type methods the existing procedures are not suitable for continuous generation of PNA, such as might be required for gas phase kinetic studies in flow systems. Moreover, the methods necessarily yield gaseous PNA, thereby precluding the possibility of investigating some interesting solution phase chemistry.

It is well-known[7-10] that direct nitration of organic hydroperoxides yields peroxynitrates. The reaction can be generalized as in equation (1),

$$ROOH + NO_2^+X^- \rightarrow ROONO_2 + HX \quad (1)$$

where R = alkyl, acyl, aroyl, and X = OH, NO_3 or BF_4, etc. The original method of D'Ans and Friederich can be considered as an example of this basic process if the reagents are written in an appropriate fashion, i.e. as in equation (2)

$$HOOH + NO_2^+NO_3^-(=N_2O_5) \rightarrow HOONO_2 + HNO_3 \quad (2)$$

Nitric acid can also be written as $NO_2^+OH^-$ and nitryl fluoroborate as $NO_2^+BF_4^-$ using this formalism.

In view of the foregoing we examined the potential utility of reaction (1) as a synthetic method for PNA. In this paper we describe the preparation of PNA in solution, and the suitability of flow methods for generating relatively pure PNA vapor from the reaction mixtures. We also report on some decomposition reactions of $HOONO_2$.

B. Experimental

Materials

NO_2BF_4 (Alfa Ventron), 90% H_2O_2 (FMC) and 70% HNO_3(Baker) were used as received.

Safety Hazards

The procedures used for preparation and analysis of PNA are potentially dangerous and certain safety precautions should routinely be observed.

We encountered one explosion in the course of our work. While PNA vapor was passed through the heated glass inlet system of the mass

spectrometer we raised the temperature of the inlet to 700°K. There was a sudden pressure increase in the mass spectrometer chamber followed by a violent explosion that shattered the inlet system. Fortunately the inlet was behind a safety shield and there were no injuries. In all subsequent work the inlet temperature was never raised above 600°K and there were no further incidents of this type. (Note: Schwarz[2] also reported a violent explosion apparently involving concentrated PNA vapor).

For PNA reaction mixtures made by method (1), see below, and allowed to stand at room temperature, gas evolution and the temperature of the reaction mixture increased over the period of a few hours. Eventually, gas evolution became so vigorous that the liquid bumped out of the reaction flask (again see reference 2). This behavior was not observed for PNA prepared by methods (2) and (3). The possibility of detonations due to large exotherms recommends that the synthetic reactions not be run on a scale exceeding ca. 5g. PNA reaction mixtures prepared by methods (1) and (2) are highly acidic and are powerful oxidizing agents. Skin contact results in painful burns. The reaction mixtures exhibit a sharp odor characteristic of many peroxides. One of us (RK) has complained of respiratory problems apparently associated with repeated exposure to PNA and other peroxynitrate vapors. These materials should be handled in a hood or other well-ventilated area.

Preparation of HO_2NO_2 from 90% H_2O_2 and 70% HNO_3 (Method 1)

A 2 g (2.2×10^{-2} mol) sample of 70% HNO_3 was added to a 1 dram specimen vial (A. H. Thomas) equipped with a 10-mm magnetic stirring bar. The acid was chilled in a small ice bath and 0.9 g (2.4×10^{-2} mol) of 90% H_2O_2 was added dropwise via a capillary pipette with vigorous agitation over a 10 minute period.

Preparation of HO_2NO_2 from 90% H_2O_2 and NO_2BF_4 (Method 2)

A 2 g (5.3×10^{-2} mol) sample of 90% H_2O_2 was chilled and stirred as described above. Solid NO_2BF_4, 0.4 g (3×10^{-3} mol) was added in approximately 5 to 10 mg portions using a spatula. Effervescence and evolution of brown fumes accompany addition of NO_2BF_4.

Preparation of HO_2NO_2 in CH_3CN (Method 3)

90% H_2O_2, 0.1 g (3×10^{-3} mol) was dissolved in 1 g of CH_3CN and cooled to 0°C with stirring. NO_2BF_4, 0.2 g (1.5×10^{-3} mol) was added as described in Method 2.

Characterization of HO_2NO_2

Infrared spectra of PNA vapor in Ar carrier were obtained using a Perkin Elmer Model 457 spectrophotometer and either a Wilks 20-m variable pathlength cell or a 2.5-cm ID x 10-cm pathlength Pyrex flow-through cell. Observed absorption maxima at 1745, 1715, 1390, 1300, 940, and 800 cm^{-1} compared favorably with literature values for $HOONO_2$.[3,6] Impurities in the sample included NO_2 (1620 cm^{-1}) and HNO_3 (840 cm^{-1}).

Procedures

Vapor phase samples of PNA for ir analysis were generated from liquid reaction mixtures as follows. A capillary pipette was used to transfer about 3 ml of reaction mixture from the specimen vial used as a reaction flash (and maintained at 273°K) to a 10-ml bulb equipped with an O-ring joint and a vacuum stopcock leading to an ebullation tube. The bulb was connected via the O-ring joint to the ir cell and allowed to warm to ambient temperature. Argon was admitted to the bulb via the stopcock at a rate of approximately 30 $cm^3\ s^{-1}$, bubbled through the reaction mixture, and used to carry PNA vapor through the cell.

Vapor samples for mass spectral analysis were handled similarly, except that the Argon flow was eliminated. Evolution of oxygen from decomposition of PNA in the reaction mixture was sufficient to sweep PNA vapors into the system. The mass spectrometer and inlet system have been described elsewhere.[24]

The evolution of oxygen from aqueous PNA solutions was monitored with a calibrated pressure transducer (Validyne model DP-7) connected via a three-way stopcock to a jacketed, 250-ml bulb equipped with magnetic stirring. To perform the experiments, 100.0 ml of buffer was added to the bulb and allowed to come to temperature while O_2 was vigorously bubbled through the solution. Next, the O_2 flow was stopped, 25 to 100 µl of a PNA reaction mixture were added via syringe, the stopcock closed and transducer output monitored with a strip chart recorder. For a 50 µl aliquot of preparative method (2), assuming 100% yield of PNA, the initial PNA concentration in 100 ml of buffer is calculated to be 7.5×10^{-4} M. For a 150 cm^3 gas volume, the final pressure of the system is calculated to be 9 torr, assuming complete decomposition to O_2. Consistent with these calculations, observed final pressures were typically 5 to 10 torr. Control experiments indicated significant oxygen evolution from excess H_2O_2 for PNA decompositions using preparative method (2) and pH $\leq$ 4. To circumvent this problem, we adopted preparative method (3), which does not require a large excess of H_2O_2.

Oxygen was identified as the reaction product by allowing a sample of PNA to decompose in a sealed, degassed, tube and then analyzing the gas over the frozen solution by mass spectroscopy.

Nitrite evolution was followed by monitoring the absorption at 365 nm with a Perkin-Elmer model 554 spectrophotometer. The buffer solution was first equilibrated to the desired temperature and 50-100 µl of PNA solution was then injected into the buffer and mixed well. The absorbance at 365 nm was monitored until completion of the reaction.

C. Results and Discussion

Preparation and Identification of PNA

We used three general procedures (see experimental section) for preparation of PNA at 273°K:

(1) reaction of neat 90% H_2O_2 with 70% HNO_3,

(2) reaction of neat 90% H_2O_2 with NO_2BF_4, and

(3) reaction of NO_2BF_4 and 90% H_2O_2 in CH_3CN.

Successful preparation of PNA was confirmed for methods (1) and (2) by warming the reaction mixtures to ambient temperature and passing a stream of Ar into the solutions and through a 10-cm pathlength ir cell or into a long-path cell. In both cases, the characteristic ir spectrum of PNA[3,6] was readily observed.

On the basis of the reported value of the $HOONO_2$ absorption coefficient at 803 cm^{-1},[11] we calculate that concentrations of $HOONO_2$ as high as 10^{-4} M were generated in the Ar stream using either method (1) or method (2). For method (1), we also observed variable, but large amounts (often exceeding the amount of PNA) of HNO_3 and NO_2 in the Ar stream. Using method (2), however, we found that the HNO_3 and NO_2 levels were normally less than 10% of the PNA level for cases where the concentration of PNA was on the order of 10^{-6} M.

For all three methods, PNA vapors could be continuously generated from a single reaction mixture for periods of up to 60 minutes. This suggested the possibility of developing a convenient flow method for

generation and analysis of gaseous PNA. Accordingly, we constructed a glass inlet system for admitting PNA/Ar mixtures to a mass spectrometer. The inlet was divided into two sections, one at ambient temperature and one heated to 600°K (Caution! See experimental details). We prepared PNA via method (2) and admitted PNA vapors from the reaction mixture into the inlet system. We similarly obtained reference spectra for possible impurities (NO_2 and HNO_3), and the data are given in Table 1.

The 300°K PNA mass spectrum does not exhibit a molecular ion at m/e = 79. We attribute the peaks at m/e = 46, 30, 18, and 17, respectively, to the fragmentation products $NO_2^{\bullet+}$, $NO^{\bullet+}$, $H_2O^{\bullet+}$, and $OH^{\bullet+}$. The m/e = 32 peak may derive either from fragmentation of the PNA molecular ion or from O_2 generated by decomposition of PNA in the reaction mixture (vide infra). At 600°K, the PNA mass spectrum shows the same mass ions as at 300°K; the relative intensities of the peaks differ, however. The thermal decomposition of PNA at 600°K should proceed as in reactions (3) and (4)[7,11-17]

$$HOO\text{-}NO_2 \rightleftharpoons HOO\bullet + NO_2 \qquad (3)$$

$$2HOO\bullet \rightarrow H_2O_2 + O_2 \qquad (4)$$

H_2O_2 would also decompose at this temperature via reactions (5) and (6)

$$HOOH \rightleftharpoons 2HO\bullet \qquad (5)$$

$$HO\bullet + HOO\bullet \rightarrow H_2O + O_2 \qquad (6)$$

The expected products of the PNA decomposition are thus NO_2, O_2 and H_2O. The 600°K PNA spectrum shows enhanced peaks at m/e = 32, 18, 17, and 16, consistent with O_2 and H_2O as decomposition products. Also for PNA the 30/46 mass ion ratio increases from 0.95 at 300°K to 3.4 at 600°K. By comparison, the mass spectrum of NO_2 at 600°K shows a 30/46 mass ion ratio

Table 1

MASS SPECTRAL DATA FOR PERNITRIC ACID (PNA), NO_2 AND HNO_3

Compound[a]	Inlet Temperature °K	Relative Intensity at m/e[b,c]							
		16	17	18	28	30	32	34	46
PNA	300	0.56	0.31	0.53	d	0.95	2.0	d	1
PNA	600	1.73	2.0	5.3	d	3.4	3.0	d	1
HNO_3	300	e	e	e	0.24	1.16	0.17	e	1
HNO_3	600	e	e	e	0.20	1.20	0.10	e	1
NO_2	600	e	e	e	0.10	4.1	e	e	1

[a] PNA prepared by method (2), see experimental details. HNO_3 prepared by reaction of H_2SO_4 with $NaNO_3$.

[b] Each mass spectrum is separately normalized to m/e = 46.

[c] Relative intensity ≤ 0.05 for m/e not listed.

[d] Relative intensity ≤ 0.20.

[e] Relative intensity ≤ 0.05.

of 4.1 while HNO_3 exhibits a mass ion ratio of 1.18 ± 0.02 at either 300 or 600°K. The value of 3.4 for PNA at 600°K is sufficiently close to the value of 4.1 for NO_2 to indicate the latter as a product of the decomposition. The presence of HNO_3 as an additional product (perhaps via wall reactions)[13] would account for the 30/46 ratio being somewhat lower for PNA than for pure NO_2. Thus, the change on heating of the 30/46 mass ion ratio serves to distinguish PNA from either NO_2 or HNO3.

Decomposition of PNA in Solution

PNA reaction mixtures continually evolve oxygen (identified by mass spectroscopy) over a period of several hours. We examined the kinetics of oxygen evolution by measuring the increase in pressure of a closed system containing the reaction mixture from preparative method (2). Semilog plots of pressure versus time were linear, and the corresponding observed first-order rate constant for oxygen evolution, k_{obs}, was 2.6 x 10^{-5} s^{-1} at 273°K and 1.2 x 10^{-4} s^{-1} at 293°K.

Two possible mechanisms can account for the evolution of oxygen from PNA solutions. In either mechanism PNA is assumed to participate in the acid-base equilibrium, reaction (7)

$$HOONO_2 \underset{k_{-7}}{\overset{k_7}{\rightleftharpoons}} H^+ + O_2NOO^- \qquad (7)$$

PNA decomposition could then proceed via either free radical or ionic reactions. In the latter case, pernitrate ion would undergo unimolecular elimination of O_2 and nitrite, reaction (8)

$$O_2NOO^- \xrightarrow{k_8} O_2 + NO_2^- \qquad (8)$$

In the free radical mechanism, reversible homolytic O-N bond scission, reaction (9)

$$HOO\text{-}NO_2 \underset{k_{-9}}{\overset{k_9}{\rightleftharpoons}} HOO\bullet + NO_2 \qquad (9)$$

is followed by hydroperoxyl radical disproprotionation, reaction (4). Oxygen and H_2O_2 are thus the expected free radical reaction products. Any NO_2 formed in reaction (9) would hydrolyze to a mixture of nitrite and nitrate.[18]

In an attempt to differentiate between the possible mechanisms we investigated the pH dependence of the kinetics of oxygen evolution from decomposition of 10^{-3} M PNA in aqueous buffer. Table 2 lists values of k_{obs} for PNA solutions at 283.6°K and various pH. From the table, it is evident that k_{obs} increases with increasing pH over the range investigated. The good agreement for k_{obs} values obtained in acetate buffer using both preparative methods (2) and (3) is taken as evidence that PNA was formed by the latter method. For PNA solutions prepared by method (3) and diluted in acetate buffer (pH = 4.7), nitrite formation was detected spectrophotometrically (λ_{max} = 365 nm). For two runs at 293°K, the observed first-order rate constant for production of nitrite was (22.5 ± 1.8) x 10^{-3} s^{-1}, which is in reasonable agreement with the rate constant for oxygen evolution at the same temperature, but higher pH.

To the extent that only reactions (7) and (8) are operative, applying the steady-state approximation to O_2NOO^- gives equations (10) and (11)

$$+d[O_2]/dt = [PNA]k_7k_8/([H^+]k_{-7} + k_8) = [PNA]k_{obs} \qquad (10)$$

$$(k_{obs})^{-1} = (k_7)^{-1} + [H^+](k_{-7}/k_7k_8) \qquad (11)$$

Table 2

OBSERVED FIRST-ORDER RATE CONSTANTS FOR OXYGEN EVOLUTION (k_{obs}) FROM 10^{-3} M PERNITRIC ACID IN AQUEOUS BUFFER AT 10.5°C [a]

Run	Preparative[b] Method	Buffer[c]	pH	k_{obs},[d] $s^{-1} \times 10^3$
1[e]	2	acetate	4.90	39.2 ± 2.9[f]
2	3	acetate	4.87	7.40
3	2	acetate	4.70	7.06 ± 0.75[g]
4	3	acetate	4.32	4.46
5	3	KH phthalate	3.80	3.21
6	3	KH phthalate	3.55	3.05
7	3	KH phthalate	3.28	2.47
8	3	KH phthalate	3.04	2.17
9	3	HCl	1.36	1.57

[a] Temperature control to ± 0.5° K.

[b] See experimental details.

[c] Buffer = 5×10^{-2} M, prepared according to standard formulations (reference 19) and made to ionic strength = 0.5 with $NaClO_4$.

[d] $k_{obs} = \ln 2 / t_{1/2}$, from semi-log plot of pressure vs. time.

[e] Temperature = 293°K.

[f] Average of three runs.

[g] Average of four runs.

Assuming the mechanism given by reactions (7) and (8) a plot of $(k_{obs})^{-1}$ versus $[H^+]$ will be linear. In actuality such a plot (Figure 1) shows pronounced downward curvature below pH = 5. This indicates O_2 evolution by an additional mechanism, and raises the possibility that PNA decomposition occurs at least in part by reactions (9) and (4).

It is interesting to compare the aqueous chemistry of PNA with that of other peroxynitrates. We have shown that formation of PNA via reaction (1) is entirely analogous to formation of alkyl, acyl, and aroyl peroxynitrates. There are also some interesting parallels in terms of decomposition mechanism. Alkaline hydrolysis of peroxyacetyl nitrate (PAN), $CH_3C(O)OONO_2$, yields stoichiometric amounts of acetate, nitrite, and (singlet) molecular oxygen.[20,21] Mudd[22] observed first-order kinetics for production of nitrite from hydrolysis of PAN (k_{obs} = 2 x 10^{-3} s^{-1} at pH = 7.6 and 300°K). On the basis of these results Stephens[23] postulated a mechanism for alkaline hydrolysis of PAN involving the intermediacy of pernitrate anion, i.e., reaction (10)

$$CH_3C(O)OONO_2 + OH^- \rightarrow CH_3C(O)OH + O_2NOO^- \qquad (10)$$

followed by reaction (8). Our results are consistent with this mechanism although a comparison of our kinetics with those of Mudd suggests that reaction (3), if it is involved in PAN hydrolysis, is not rate-limiting.

D. Conclusions

CONCLUSIONS

Nitration of concentrated H_2O_2 with NO_2BF_4 at 273°K yields PNA. PNA solutions thus prepared provide a convenient source of relatively pure PNA vapor. The analysis of PNA by infrared spectrophotometry or by mass spectroscopy in flow systems permits the study of reactions of PNA with radicals or other reactive species. These investigations are in progress and will be reported separately.

Aqueous PNA decomposes to molecular oxygen and nitrite. Unimolecular decomposition of the pernitrate anion to O_2 and NO_2^- seems a likely mechanism, though a free radical mechanism for decomposition of PNA may also be important.

Similarities in the hydrolytic chemistry of PNA and peroxyacetyl nitrate suggest that the pernitrate anion is an intermediate in both cases. PNA and peroyxacetyl nitrate both play important roles in the free radical chemistry of photochemical smog. One question that now remains is whether the ionic chemistry of these pernitrates in heterogeneous phases (aerosols, surfaces, etc.) is also of environmental concern.

ACKNOWLEDGEMENT

We gratefully acknowledge Dr. John R. Barker (SRI International) and Professor Mario Molina (University of California, Irvine) for their helpful discussions. This work was supported in part by DOT/FAA Contract No. DOT-FA78 WA-4228.

E. References and Notes (Appendix A)

1. D'Ans, J.; Friederich, W., Z. Anorg. Chem. 1911, 73, 325.

2. Schwarz, R., Z. Anorg. Chem. 1948, 256, 3.

3. Niki, H.; Maker, P. D.; Savage, C. M.; Breitenbach, L. P., Chem. Phys. Lett. 1977, 45, 564.

4. Hanst, P. L.; Gay, B. W., Environ. Sci. Technol. 1977, 11, 1105.

5. Levine, S. Z.; Uselman, W. M.; Chan, W. H.; Calvert, J. G.; Shaw, J. H., Chem. Phys. Lett. 1977, 48, 528.

6. Graham, R. A.; Winter, A. M.; Pitts, J. N., Chem. Phys. Lett. 1977, 51, 2-5.

7. Hendry, D. G., Kenley, R. A., "Atmospheric Chemistry of Peroxynitrates" in Nitrogenous Air Pollutants, Chemical and Biological Implications, D. Grosjean, Ed.; Ann Arbor Science, Ann Arbor, MI, 1979.

8. Louw, R.; Sluis, G. J.; Vermeeren, H.P.W., J. Amer. Chem. Soc. 1975, 97, 4396.

9. Duynstee, E.F.J.; Housmans, J.G.H.M.; Vleugels, J.; Voskuil, W., Tetrahedron Lett. 1973, 25, 2275.

10. Kenley, R. A.; Hendry, D. G., J. Amer. Chem. Soc. 1977, 99, 3198.

11. Graham, R. A.; Winer, A. M.; Pitts, J. N., Geophys. Res. Lett. 1978, 5, 909.

12. Graham, R. A.; Winer, A. M.; Pitts, J. N., J. Chem. Phys. 1978, 68, 4505.

13. Uselman, W. M., Levine, S. Z., Chon, W. H., Calvert, J. G., and Shaw, J. H., "A Kinetic Study of the Mechanism of Peroxynitric Acid Formation

in Irradiated Mixtures of Chlorine, Hydrogen, Nitrogen Dioxide, and Nitric Oxide in Air," in Nitrogenous Air Pollutants, Chemical and Biological Implications, D. Grosjean, Ed., ; Ann Arbon Science, Ann Arbor, MI, 1979.

14. Cox, R. A.; Derwent, R. G.; Hutton, A.J.L. Nature (Lon.), 1977, 270, 328.

15. Baldwin, A. C.; Golden, D. M., J. Phys. Chem. 1978, 82, 644.

16. Graham, R. A., Winer, A. M., Atkinson, R., Pitts, J. N., J. Phys. Chem., 83, 1563 (1979).

17. Cox, R. A., Patrick, K., Int. J. Chem. Kinetics, 1979, XI, 635.

18. Kaufman, F., Proc. Roy. Soc. (London), 1958, Ser. A 247, 123.

19. Handbook of Chemistry and Physics, 51st edition, R. C. Weast, Ed., Chemical Rubber Company, Cleveland, OH, 1971; p. D-104.

20. Nicksic, S. W., Harkins, J., Mueller, P. K., Atmos. Environ., 1967, 1, 11.

21. Stephens, E. R., Atmos. Environ., 1967, 1, 19.

22. Mudd, J. B., J. Biol. Chem., 1966, 241, 4077.

23. Stephens, E. R., Adv. Environ. Sci., 1969, 1, 119.

24. Chang, J. S.; Barker, J. R.; Davenport, J. E.; Golden, D. M., Chem. Phys. Lett. 1979, 60, 385.

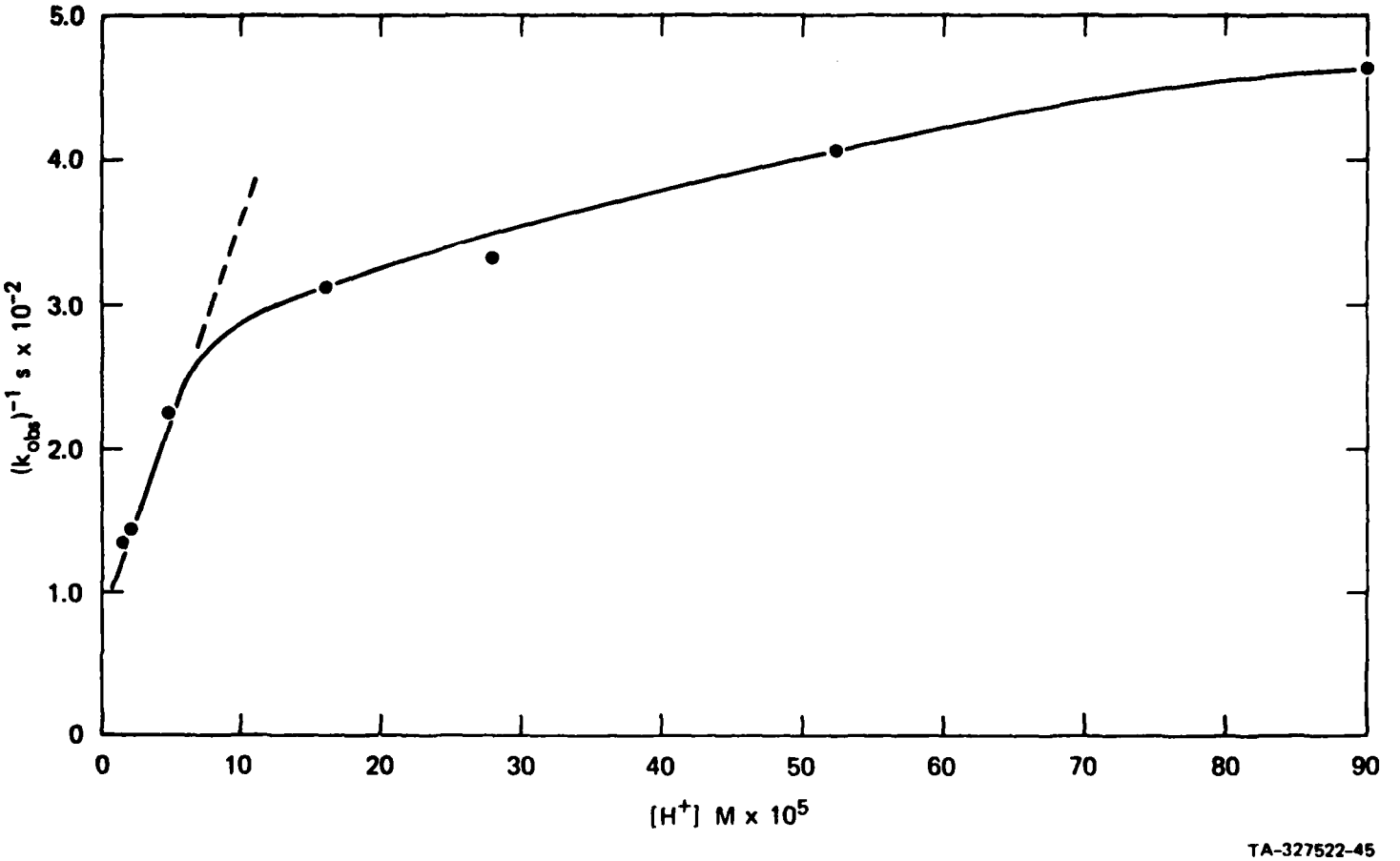

FIGURE 1 RECIPROCAL OBSERVED FIRST-ORDER RATE CONSTANT, $(k_{obs})^{-1}$ VERSUS HYDROGEN ION CONCENTRATION FOR DECOMPOSITION OF PERNITRIC ACID IN AQUEOUS BUFFER AT 283.6 K.

From data of Table 2.

Appendix B

$O(^3P) + HOONO_2 \rightarrow$ PRODUCTS: TEMPERATURE-DEPENDENT RATE CONSTANT

(Jenq-Sian Chang, Paula L. Trevor, and John R. Barker)

A. Introduction

Both HO_2 radicals and NO_2 play crucial roles in the chemistry of the atmosphere. Thus, it is not surprising that pernitric acid (PNA), the product of reaction (1), has received a good deal of recent attention:[1]

$$HOO + NO_2 \overset{M}{\rightleftarrows} HOONO_2 \qquad (1)$$

Because PNA couples the HO_x and NO_x catalytic cycles, its fate is of great importance for developing accurate computer models of atmospheric chemistry.[2] Oxygen atoms are present in the upper stratosphere and their reaction with PNA could affect its atmospheric lifetime:

$$O + HOONO_2 \rightarrow \text{Products} \qquad (2)$$

Although the primary impetus for studying PNA reactions is their potential importance in the atmosphere, PNA is also an interesting chemical species that is an important part of the fabric of H-N-O chemistry. In this sense, it is a member of the homologous series of nitrogen acids (i.e., HONO, $HONO_2$, $HOONO_2$), as well as being the first member of the series of pernitrates (i.e., $HOONO_2$, CH_3OONO_2, $CH_3\overset{O}{\overset{\|}{C}}OONO_2$, etc.); in addition, it is a hydroperoxide (i.e., HOOH, HOOR, $HOONO_2$). Each of these species may be important in atmospheric chemistry, as well as in other chemical systems, and data are needed on their reaction rate constants. Such data can then be used as a basis for predicting reaction rate constants for species that have not, as yet, been studied experimentally.

B. Experimental

Pernitric acid was prepared[3] by slowly and carefully dissolving 0.6 g of NO_2BF_4 in 2.0 g of 90% hydrogen peroxide. The solution was stirred vigorously, while immersed in an ice bath, and then maintained at $\sim 10^{\circ}C$; the PNA vapor that evolved was introduced into the reactor through a short

capillary tube. This preparative technique reliably gives relatively large yields of PNA with variable levels of contaminants. The level of NO_2 usually was found to be less than 10% of the PNA. Hydrogen peroxide, on the other hand, tended to be highly variable; in some batches it was not measurable, but in others it exceeded the concentration of PNA itself. Partly because of these impurities, the kinetics were studied under O-atom-rich conditions, so that effects on the rate constants due to secondary reactions were minimized.

Because of the slowness of the reaction between O and PNA, and because we wished to study the kinetics under O-atom-rich conditions, a 2-liter spherical stirred-flow reactor (SFR) was used, as shown in Figure 1. High purity helium (Liquid Carbonic) carried 1-5% molecular oxygen through a microwave discharge to produce $O(^3P)$ atoms. In the 1-meter flow tube[4] (prior to entry into the SFR), NO_2 could be added to the gas stream and the O-atom concentration could be determined by titration; the endpoint was signaled by extinction of the greenish-yellow glow due to $O + NO \rightarrow NO_2 + h\nu$.[5] A correction was applied to compensate for the formation of O_3 in the SFR, since it reduced the atom concentration from that measured in the flow tube (see below). An alternative method for measuring the O-atom concentration was to measure the O_2 flow rate, and then monitor the mass spectrometer signal at m/e = 32 to determine the fraction of O_2 dissociated in the microwave discharge. Both methods gave the same results within experimental uncertainty. Additional experiments were performed in which NO_2 titration of O-atoms was carried out at three different points in the apparatus: (a) in the flow tube prior to entry into the SFR, (b) in the SFR, and (c) at the exit of the SFR. Measured O-atom concentrations were the same at all three points, indicating that the O-atom wall loss rate constant is very slow and can be neglected. At higher O-atom concentrations, homogeneous O_3 formation depletes the atom concentration, as discussed below.

The helium carrier gas-flow rate was measured with a calibrated rotameter and the other gas flows (except for PNA itself) were measured by timing the pressure rise in calibrated volumes. Pressure rises were measured with calibrated variable reluctance pressure transducers (Validyne) and the total pressure in the reactor was measured with a calibrated Wallace and Tiernan gauge.

The gas stream was "turbulently" introduced in the SFR ($V = 2389\ cm^3$) through an inlet port that consisted of a 2-cm stub of tubing with four orifices oriented tangentially to the surface of the SFR. Reactant gases (such as PNA) were introduced through capillary inlets (1 cm x 1 mm) at C and D, located at the top of the SFR. The effluent gases passed through an outlet tube that was similar to the inlet port.

Due to the design of the experiment, O-atoms were intimately mixed with the carrier gas prior to introduction into the SFR. Since wall loss of O-atoms was negligible, the O-atom concentration was uniform within the reactor. For pseudo first order conditions, the rate of disappearance of PNA is controlled by the O-atom concentration, which is initially uniform, but which could be locally depleted due to non-homogeneous mixing of PNA and its subsequent reaction with O-atoms. Because mixing of PNA appears to be quite rapid compared to residence times in the SFR, it is unlikely that local depletion of O-atoms plays a role in the measurements. Moreover, the complete mixing tends to insure that PNA experiences the same residence time as the carrier gas.

The rate of mixing of PNA within the SFR was not measured directly, but even without turbulence, the diffusion mixing times were shorter than any of the nominal residence times employed in experiments. The diffusion coefficient can be estimated by assuming that helium and PNA have hard-sphere radii of 2.6 $\mathring{A}$ and 6 $\mathring{A}$, respectively, giving the binary

diffusion coefficient $D \approx 200/P_T$, where P_T is the pressure in torr. For diffusion in three dimensions, $< r^2 > \approx 6\ Dt_d$ and thus $t_d \approx (3V/4\pi)^{2/3}/(6D)$, where V is the volume of the reactor. At room temperature and for a pressure of 3 torr, $t_d \approx 0.2$ sec. All of the experiments reported were for residence times greater than 0.8 sec., sufficient time for diffusive mixing of PNA throughout the SFR. The turbulence in the SFR reduces the mixing time still further, very effectively giving well-stirred conditions even if the diffusive mixing times are somewhat longer than estimated. Experiments described in the next section were performed at 297K for residence times that varied from 0.853 sec. to 1.39 sec., and there was no measurable variation in the rate constant observed.

Concentrations of species in the reactor could be monitored by sampling through a small hole (~ 0.01 inch) drilled through a thin (~ 1 mm) Teflon plug into a modulated-molecular-beam-mass-spectrometer (MMB-MS), which has been described elsewhere.[4,6] Calibrations were performed daily for known concentrations of stable species that were introduced into the gas stream. The PNA concentration was determined by monitoring the intensity of m/e = 46 and comparing it to the intensity corresponding to a known concentration of NO_2. The relative sensitivities of PNA and NO_2 were determined by diverting the flow of PNA through a heated glass inlet and measuring the NO_2 produced in the thermal decomposition reaction, as described in great detail elsewhere.[7]

$$HO_2NO_2 \rightarrow HOO + NO_2 \qquad (-1)$$

$$2\ HOO \rightarrow H_2O_2 + H_2O \qquad (3)$$

For the present experiment, the PNA gave about six times as intense a signal at m/e = 46 as did the same concentration of NO_2. The addition of O-atoms to the gas stream during these measurements removed NO_2 impurities, and also constituted an independent check on the purity of each batch of PNA that

was used. The mass spectrometer was calibrated for HNO_3 with a sample of dry gas prepared by the reaction of $NaNO_3$ with concentrated H_2SO_4, and it was found that the sensitivities for HNO_3 and PNA are similar at m/e = 46. The presence of HNO_3 in our batches of PNA would be evidenced by the presence of a residual mass spectral intensity at m/e = 46 when the PNA is diverted through the heated inlet and O-atoms are added to remove NO_2. There was never any indication of such a residual signal, allowing us to rule out the presence of HNO_3.

Typically, experiments were performed at 1-3 torr total pressure, and residence times in the reactor were $\sim$ 0.8 to 2 seconds. Wall reactions were effectively discouraged by use of halocarbon wax (Halocarbon Products Corporation).

For temperature control, the reactor was enclosed in a special jacket and cold nitrogen gas was passed through the jacket. The special jacket consisted of a layer of heavy aluminum foil, followed by a porous layer of copper wool that allowed circulation of the cold nitrogen gas. The entire assembly was then enclosed in a thick layer of rigid foam insulation. The temperature control was less than perfect at the lower temperatures, and adequate stability was maintained for only two to three kinetic runs at a time. The temperature was monitored by seven chromel-constantan thermocouples located at various points on the reactor surface; they showed a temperature uniformity of $\pm$ 1 K at 270 K and $\pm$ 4 K at 240 K.

C. Results and Discussion

The stirred flow technique is a venerable one[8] that is especially useful for measuring relatively slow reaction rates. For the SFR used in the present experiments, data analysis is carried out for the well-stirred steady-state conditions assumed to be present in the reactor.

The average residence time, t, for gases in the reactor is related to the total flow rate F_T, the total concentration c_T, and the reactor volume V, by:

$$t = \frac{c_T V}{F_T}$$

The concentration of the i^{th} component of the mixture is given by

$$c_i = \frac{F_i}{F_T} c_T$$

where F_i is the flow rate of the i^{th} component and c_T is the total gas concentration as related to P_T by the ideal gas law.

For a general bimolecular reaction A + B → Products, where B is maintained in great excess so that pseudo-first-order conditions hold, a simple steady-state analysis gives the following equation:

$$\frac{[A]_0}{[A]} = 1 + k_{II}[B]_t \qquad (4)$$

where $[A]_0$ and $[A]$ are the concentrations of species A in the absence and in the presence of B, respectively; t is the residence time in the SFR, and k_{II} is the bimolecular rate constant for the reaction. Data for $[A]_0 / [A]$ plotted versus the product $t[B]$ should give a straight line of slope k_{II} and unit intercept.

As a pragmatic test of the SFR, a reaction with a known rate constant was investigated at room temperature. The reaction was:

$$O + Cl_2 \rightarrow ClO + Cl \qquad (5)$$

and the observed room temperature rate constant is $k_5 = (3.5 \pm 1.0) \times 10^{-14}$ cm^3 sec^{-1}, compared to the literature value[3] $k_5 = (4.2 \pm 0.6) \times 10^{-14}$ cm^3 sec^{-1}. This test shows that the SFR gives absolute rate constants in good agreement with those in the literature and that systematic errors are probably no greater than ± 30%.

As mentioned above, the O-atom concentrations were often measured in the flow tube (prior to entry into the SFR) by NO_2 titration, and thus a correction for ozone formation was applied to obtain the corresponding O-atom concentrations in the SFR. The correction was performed as part of the steady-state analysis for the entire reaction scheme:

$$\text{Flux} \xrightarrow{F_{NO_2}/V} O$$

$$O + HOONO_2 \longrightarrow OH + O_2 + NO_2 \qquad (2)$$

$$O + O_2 + M \longrightarrow O_3 + M \qquad (6)$$

$$O + O_3 \longrightarrow 2\,O_2 \qquad (7)$$

$$O + OH \longrightarrow O_2 + H \qquad (8)$$

$$H + HOONO_2 \longrightarrow H_2 + O_2 + NO_2 \qquad (9)$$

$$O + NO_2 \longrightarrow O_2 + NO \qquad (10)$$

The reaction rate constant k_9 has been measured in the companion paper and has been found to be $\approx 3 \times 10^{-14}$ cm^3 s^{-1} with only a slight temperature variation. If the fast secondary reactions (8) and (10) are grouped together with reaction (2) and a steady state analysis is performed, the steady-state oxygen atom concentration is given by

$$[O] = \frac{F_{NO_2}}{V}\left\{\frac{1}{t} + k_6[O_2][M]\left(1 + \frac{k_7[O]}{k_7[O] + t^{-1}}\right) + k_2[PNA]\left(3 + \frac{k_9[PNA]}{k_9[PNA] + t^{-1}}\right)\right\}^{-1} \qquad (11)$$

where F_{NO_2} is the flow of NO_2 necessary to titrate the O-atoms in the flow tube and is equal to the flow of atomic oxygen into the SFR; V is the SFR volume and t is the residence time. Rate constants k_6 and k_7 were taken from the Hampson and Garvin,[10] and Baulch et al.,[11] respectively.

The solution of equation (11) requires rate constant k_2 and must be performed iteratively as described below. Since secondary reaction (9) affects [PNA], equation (4) also must be modified. A steady state analysis gives

$$\frac{[PNA]_o}{[PNA]} = 1 + k_2 t[O] \left\{ \frac{t^{-1} + 2\, k_9[PNA]}{t^{-1} + k_9[PNA]} \right\} \qquad (12)$$

This expression can be rearranged to give

$$S = k_2 t[O] = \left(\frac{[PNA]_o}{[PNA]} - 1 \right) \left\{ \frac{t^{-1} + k_9[PNA]}{t^{-1} + 2k_9[PNA]} \right\} \qquad (13)$$

Since k_9, [PNA], $[PNA]_o$, and t are known or are measured, S is directly measured in each experimental run, giving an experimental value for k_2(run), if [O] is known, for each experimental run.

The effects of secondary reaction are explicitly taken into account in equations (11) and (13). The objective in the data analysis is to solve equations (11) and (13) in a self-consistent manner in order to devise [O] for each individual run and $k_2(T)$ for each set of runs at a given temperature. This goal was expedited since S does not depend on k_2 and [O] depends on k_2 only weakly. The analysis procedure was begun by taking the data for each individual experimental run and solving equations (11) and (13) iteratively for [O] and for a value of k_2: k_2(run). Convergence was rapid and was complete to within 0.1% after the five iterations used for each calculation. The second step of the analysis was to consider each set of several runs corresponding to the same temperature and average the derived values for k_2(run) to give $< k_2 >$. This approximate value for k_2 was then used to recalculate [O] for each run in the series so that the values of S and the recalculated [O] values could be used to derive a final self-consistent value for $k_2(T)$. In principle, this procedure could be extended further by using $k_2(T)$ in

place of $< k_2 >$ to produce a still more self-consistent value for $k_2(T)$, but this extension was not necessary, because of the weak dependence of $[O]$ on k_2, according to equation (11). The final value of $k_2(T)$ was derived from equation (13) according to either of two least-squares procedure, depending on the number of data points at a given temperature. If more than four data points were available, an unconstrained least-squares analysis was used, but the intercept was constrained to the origin if there were four or fewer data points. Values of $k_2(T)$ for a given data set never differed from $< k_2 >$ for that data set by more than 25%. A 25% variation in $< k_2 >$ was found to give a variation in $k_2(T)$ of $\sim 2\%$, far less than the other errors involved.

The data are presented in Table 1 along with the derived values for $[O]$, S, and $k_2(T)$. The values of $k_2(T)$ are summarized in Table 2. To determine the Arrhenius parameters for rate constant k_2, a weighted least-squares analysis was performed using the Taylor series method described by Cvetanovic and coworkers.[12] The uncertainties associated with k_2 at each temperature were adjusted[12b] by Student's t-factor according to the number of data points and the resulting "adjusted" standard deviations were used in the least-square analysis. The results were $(k_2 \pm \sigma) = (7.0 \pm 12.2) \times 10^{-11} \exp(-3369 \pm 489/T)$ cm^3 s^{-1}; covariance = 5.97×10^{-8}. This analysis does not take potential systematic errors into consideration, however, and such errors might change these results by an estimated factor of two, to be conservative.

Table 1 DATA SUMMARY

P_T (torr)	t (s)	F_{NO_2} [a]	F_{O_2} [b]	$[PNA]_o$ [c]	$\frac{[PNA]_o}{[PNA]}$	S	[O] [d]
297 K							
2.20	0.853	9.72	5.40	1.69	1.28	0.210	2.96
2.20	0.853	9.94	5.40	1.30	1.37	0.287	3.02
2.20	0.853	9.94	5.53	1.65	1.33	0.247	3.02
2.20	0.853	8.82	4.90	2.80	1.25	0.173	2.69
2.20	0.853	6.69	3.52	2.89	1.20	0.138	2.04
2.72	0.914	7.05	4.10	1.92	1.22	0.161	2.15
2.72	0.914	8.77	5.16	7.79	1.34	0.198	2.68
2.72	0.914	7.48	4.40	6.12	1.22	0.133	2.28
2.72	0.914	1.21	0.71	2.91	1.01	0.007	0.37
2.50	1.390	1.07	0.63	20.60	1.15	0.079	0.33
2.50	1.390	6.58	4.70	10.20	1.52	0.281	2.01
2.50	1.390	6.19	5.16	7.24	1.56	0.310	1.89
2.60	0.874	10.90	5.43	2.22	1.33	0.234	3.31
2.60	0.874	9.40	4.70	2.22	1.34	0.241	2.86
			$(k_2 \pm 1\sigma) = (9.39 \pm 1.30) \times 10^{-16}$ cm^3 s^{-1}				
282 K							
1.42	1.330	10.70	4.70	14.10	1.36	0.192	4.49
1.42	1.330	20.20	5.73	12.20	1.45	0.241	8.39
2.05	1.944	14.40	5.16	13.90	1.56	0.292	6.00
2.05	1.944	8.48	4.84	14.80	1.54	0.281	3.57
			$(k_2 \pm 1\sigma) = (2.98 \pm 0.83) \times 10^{-16}$ cm^3 s^{-1}				
268 K							
2.05	1.560	8.84	5.20	5.80	1.45	0.253	3.53
0.80	0.977	8.40	5.20	20.00	1.28	0.150	3.52
1.40	1.229	16.60	5.20	21.40	1.31	0.163	6.50
1.40	1.229	16.00	5.40	11.30	1.34	0.185	6.25
1.40	1.229	16.00	5.40	11.30	1.31	0.169	6.25
1.40	1.229	14.60	5.20	10.90	1.35	0.191	5.73
2.42	2.090	16.00	5.10	10.80	1.64	0.335	6.23
2.42	2.090	13.70	5.20	9.14	1.56	0.296	5.36
3.47	3.003	13.70	5.20	13.10	1.47	0.242	5.40
3.47	3.003	18.80	5.20	3.20	2.23	0.664	7.31
3.47	3.003	16.00	5.20	2.64	2.00	0.552	6.25
			$(k_2 \pm 1\sigma) = (2.53 \pm 0.45) \times 10^{-16}$ cm^3 s^{-1}				
263 K							
2.05	1.610	4.60	5.00	2.56	1.20	0.127	1.70
2.05	1.610	4.60	5.00	2.77	1.25	0.156	1.70
4.60	1.739	16.60	6.07	2.58	1.16	0.101	5.76
4.60	1.739	16.60	6.07	2.58	1.25	0.156	5.76
			$(k_2 \pm 2\sigma) = (3.23 \pm 2.30) \times 10^{-16}$ cm^3 s^{-1}				
244 K							
4.60	1.860	16.60	6.07	3.40	1.14	0.084	6.92
1.45	1.140	10.70	5.30	3.32	1.07	0.046	4.48
			$(k_2 \pm 1\sigma) = (0.78 \pm 0.17) \times 10^{-17}$ cm^3 s^{-1}				
228 K							
1.57	2.260	11.80	2.87	5.03	1.06	0.034	4.04
4.32	1.850	9.40	4.90	5.51	1.08	0.046	3.46
			$(k_2 \pm 1\sigma) = (0.54 \pm 0.24) \times 10^{-16}$ cm^3 s^{-1}				

[a] Units: 10^{17} molecules s^{-1}.
[b] Units: 10^{16} molecules s^{-1}.
[c] Units: 10^{13} molecules cm^{-3}.
[d] Units: 10^{14} molecules cm^{-3}.

Table 2 $O + HOONO_2 \rightarrow$ Products

T	Data Points	$(k_2 \pm 1\sigma_c)$ [a]
297	14	9.39 ± 1.35[b]
282	4	2.98 ± 1.00
268	11	2.53 ± 0.48[c]
263	4	3.23 ± 2.76
244	2	0.78 ± 0.31
228	2	0.54 ± 0.44

[a] Units are 10^{-16} cm^3 s^{-1}; uncertainties are one standard deviation, corrected by student's t factor.

[b] Linear least-squares result; (intercept ± 1σ) = −0.01 ± 0.03.

[c] Linear least-squares result; (intercept ± 1σ) = 0.01 ± 0.06.

Although the slow rate constant makes reaction (2) unimportant in most of the atmosphere, it is interesting to compare the Arrhenius parameters obtained for reaction of O + PNA to those obtained for other oxygen-atom reactions:

	$A \times 10^{12}$, $cm^3\ s^{-1}$	E/R	Ref
$O + H_2O_2$	2.75 ± 0.41	2125 ± 261	13
$O + HONO_2$	($k < 3 \times 10^{-17}$ at 300 K)		14
$O + HOONO_2$	70 ± 122	3369 ± 489	This work

Since A-factors for O-atom abstraction reaction are expected to be $\sim$ 1-5 x 10^{-11} $cm^3\ s^{-1}$, the A-factor determined in the present work is not unreasonable, although highly uncertain. That for $O + H_2O_2$ is unexpectedly low, but the activation energy is also low, leading to absolute rate constants within about a factor of 2-5 of those determined in the present study. Thus, the chemistry of PNA appears to be more similar to that of H_2O_2 than to that of nitric acid, which is quite unreactive.

Acknowledgement

Support by the High Altitude Pollution Program of the Office of Environment and Energy, Federal Aviation Administration, Department of Transportation under contract DOT/FA78WA-4228 is gratefully acknowledged.

We thank our colleagues here at SRI for useful discussions. We also thank M. Molina, D. Wuebbles, and R. Cicerone for general discussions concerning atmospheric chemistry.

This paper is dedicated to the late W. H. Duewer, who was active in investigating the role of PNA in atmospheric chemistry.

D. References (Appendix B)

1. (a) R. Simonaitis and J. Heicklen, J. Phys. Chem., 80, 1 (1976).

   (b) H. Niki, P. D. Maker, C. M. Savage, and L. P. Breitenbach, Chem. Phys. Letters, 45, 564 (1977).

   (c) C. J. Howard, J. Chem. Phys., 67, 5258 (1977).

   (d) R. A. Graham, A. M. Winer, and J. N. Pitts, Jr., Chem. Phys. Letters, 51, 215 (1977); J. Chem. Phys., 68, 4505 (1978).

   (e) A. C. Baldwin and D. M. Golden, J. Phys. Chem., 82, 644 (1978).

   (f) A. C. Baldwin, J. R. Barker, D. M. Golden, and D. G. Hendry, J. Phys. Chem., 81, 2483 (1977).

   (g) R. A. Graham, A. M. Winer, and J. N. Pitts, Geophys. Res. Lett., 5, 909 (1978).

   (h) R. A. Cox and K. Patrick, Int. J. Chem. Kinetics, 11, 635 (1979).

   (i) P. L. Trevor and J. R. Barker, Int. J. Chem. Kinetics, 00, 0000 (1981).

   (j) P. L. Trevor and J. E. Davenport, Geophys. Res. Lett., submitted.

2. J. S. Chang and W. H. Duewer, Ann. Rev. Phys. Chem., 30, 443 (1979).

3. R. A. Kenley, P. L. Trevor, and B. Y. Lan, J. Amer. Chem. Soc., in press.

4. J. S. Chang and J. R. Barker, J. Phys. Chem., 83, 3059 (1979).

5. F. Kaufman, Proc. Roy. Soc. (London), Ser. A247, 123 (1958).

6. J. S. Chang, J. R. Barker, J. E. Davenport, and D. M. Golden, Chem. Phys. Lett., 60, 385 (1979).

7. P. L. Trevor, G. Black, and J. R. Barker, J. Phys. Chem., submitted.

8. See K. G. Denbigh, Trans. Faraday Soc 40, 352 (1944); K. G. Denbigh, Discussions Faraday Soc., 2, 263 (1947).

9. R. T. Watson, J. Phys. Chem. Ref. Data, 6, 871 (1977).

10. For a summary of data, see R. F. Hampson, Jr. and D. Garvin, NBS Special Publication No. 513 (1977).

11. D. L. Baulch, D. D. Drysdale, J. Duxbury, and S. J. Grant, Evaluated Kinetic Data for High Temperature Reactions. Vol. 3: Homogeneous Gas-Phase Reactions for the O_2-O_3 System, the CO-O_2-H_2 System, and of Sulfur-Containing Species (Buttersworth, London, 1976).

12. (a) R. T. Cvetanovic, R. P. Overend, and G. Paraskevopoulos, Int. J. Chem. Kinetics, Symp. 1, 249 (1975).

(b) R. J. Cvetanovic, D. L. Singleton, and G. Paraskevopoulos, J. Phys. Chem., 83, 50 (1979).

13. D. D. Davis, W. Wong, and R. Schiff, J. Phys. Chem., 78, 463 (1974).

14. C. J. Chapman and R. P. Wayne, Int. J. Chem. Kinetics, 6, 617 (1974).

FIGURES

1 Low-Pressure Stirred-Flow Reactor

Note that the reactor is coupled to a discharge flow tube (for preparation of reactive species) and to the modulated-beam mass spectrometer.

2 Stirred-Flow Reactor Results for O + PNA → Products Plotted as S versus t [O] for (a) 297 K and (b) 268 K.

3 Arrhenius Plot for the Rate Constant for O + PNA → Products. Number associated with each data point shows the number of kinetic runs at each temperature. Confidence limits were derived from Propagation of Errors, including the covariance $\sigma_{AB} = 5.97 \times 10^{-8}$.

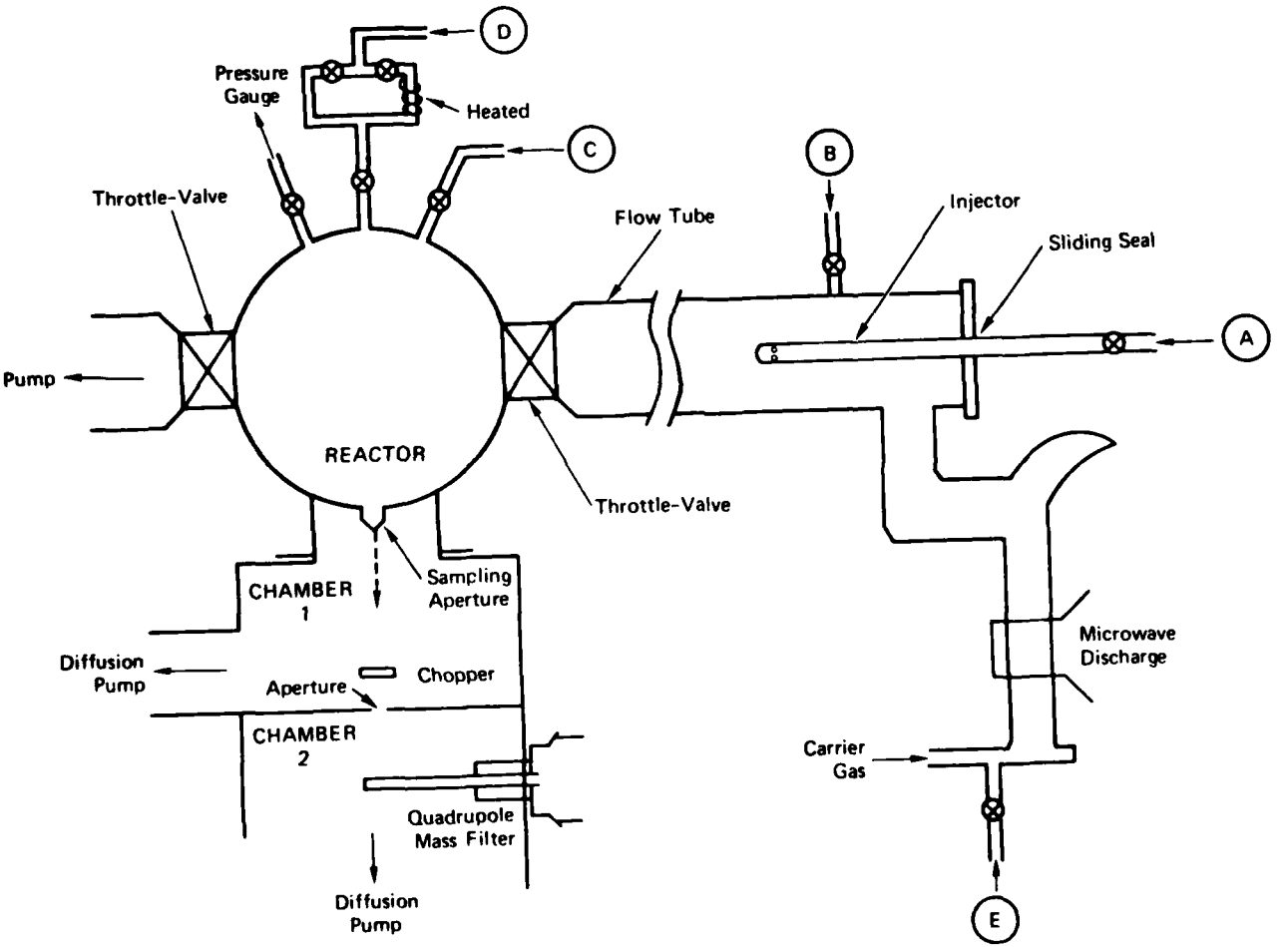
D
Pressure Gauge
Heated
C
B
Throttle-Valve
Flow Tube
Injector
Sliding Seal
A
Pump
REACTOR
Throttle-Valve
CHAMBER 1
Sampling Aperture
Microwave Discharge
Diffusion Pump
Aperture
Chopper
CHAMBER 2
Carrier Gas
Quadrupole Mass Filter
Diffusion Pump
E
SA-7921-3

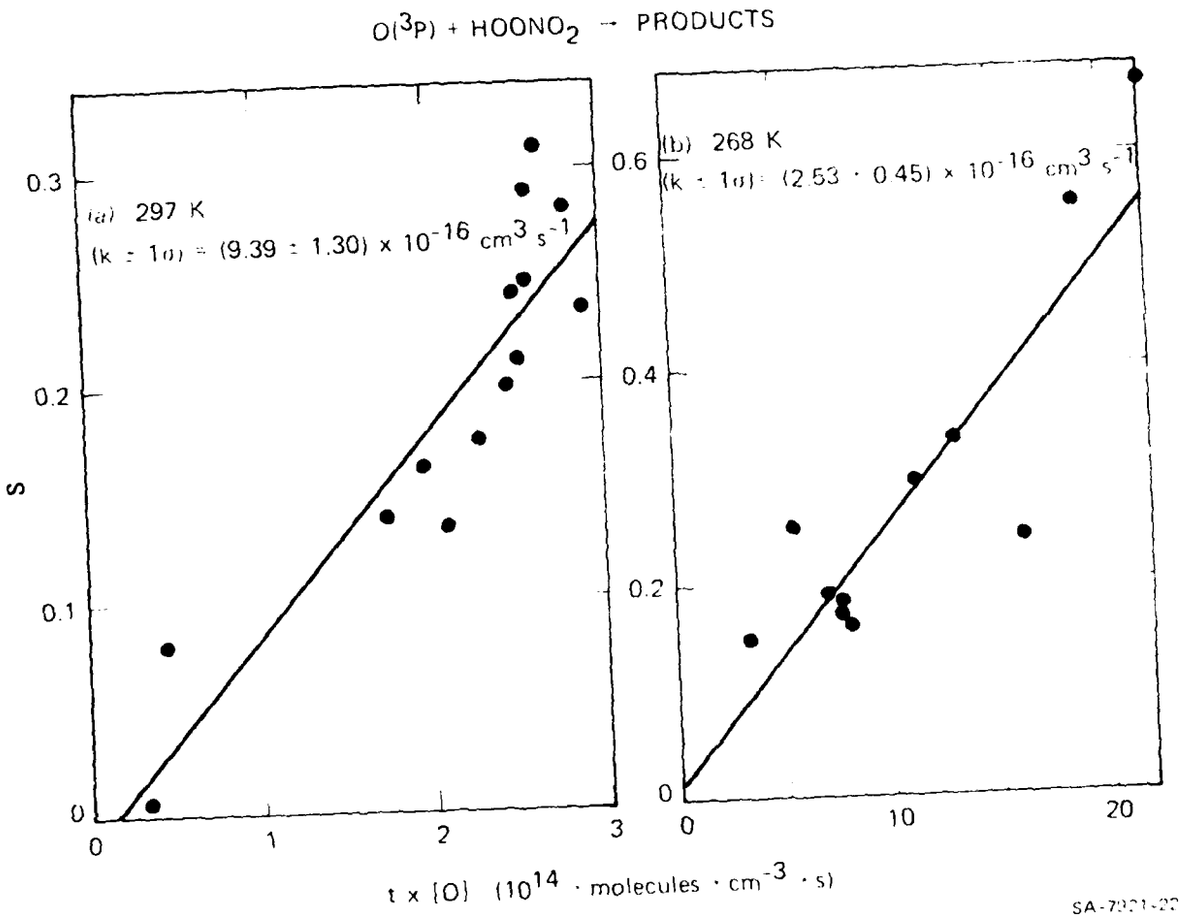
$O(^3P) + HOONO_2 \rightarrow$ PRODUCTS
(a) 297 K
(k ± 1σ) = (9.39 ± 1.30) x 10^{-16} cm^3 s^{-1}
(b) 268 K
(k ± 1σ) = (2.53 ± 0.45) x 10^{-16} cm^3 s^{-1}
S
0.3
0.2
0.1
0
0.6
0.4
0.2
0
1
2
3
10
20
t x [O] (10^{14} · molecules · cm^{-3} · s)
SA-7901-22

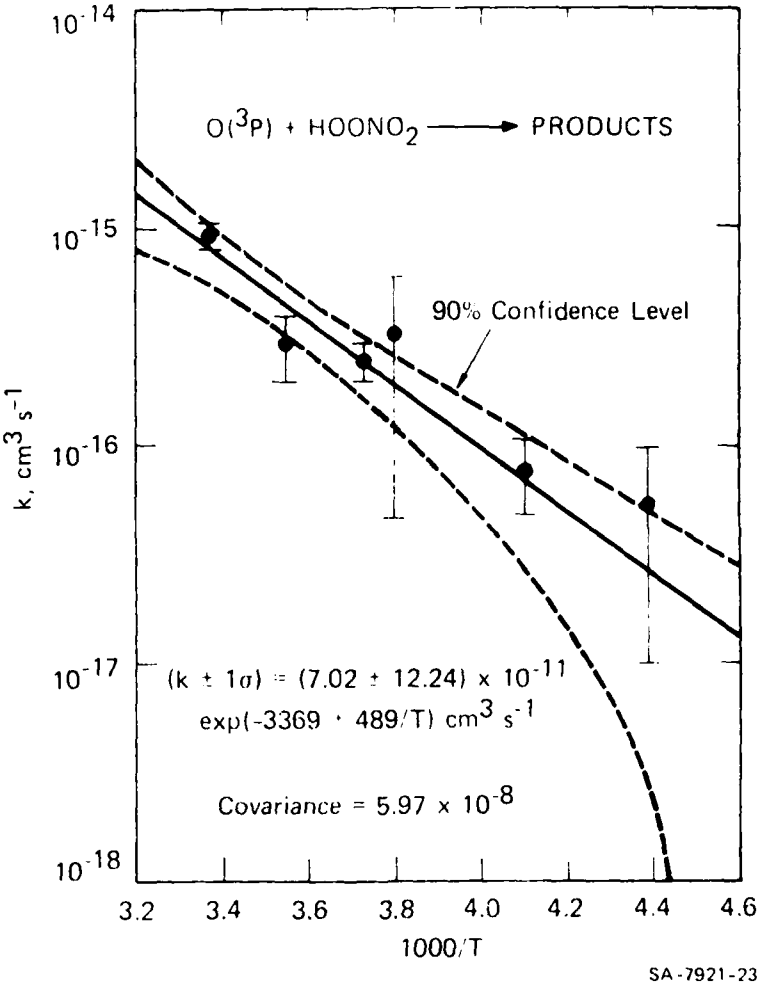
$O(^3P) + HOONO_2 \longrightarrow$ PRODUCTS
90% Confidence Level
$(k \pm 1\sigma) = (7.02 \pm 12.24) \times 10^{-11}$
$\exp(-3369 \pm 489/T)$ cm^3 s^{-1}
Covariance = 5.97×10^{-8}
k, cm^3 s^{-1}
10^{-14}
10^{-15}
10^{-16}
10^{-17}
10^{-18}
3.2
3.4
3.6
3.8
4.0
4.2
4.4
4.6
1000/T
SA-7921-23

Appendix C

$H + HOONO_2 \rightarrow$ PRODUCTS: TEMPERATURE-DEPENDENT RATE CONSTANT

(Paula L. Trevor and John R. Barker)

A. Introduction

Pernitric acid (PNA) is the product of the combination reaction of HO_2 radicals and NO_2:

$$HO_2 + NO_2 \longrightarrow HOONO_2 \qquad (1)$$

PNA has been the subject of considerable interest[1-6] since it represents a direct coupling pathway between the HO_x and NO_x catalytic cycles in the earth's atmosphere. In our laboratory, we have studied the reactions of OH,[7] O_3,[8] O atom,[9] and H atom with PNA in order to determine the chemical reaction rate constants and assess the relative importance of the various processes that affect PNA in the atmosphere. Recent measurements of the PNA absorption cross sections in the ultraviolet [10-12, 21] indicate that photolysis may be less important than chemical reaction. Since atomic hydrogen is present in the upper stratosphere, reaction (2) is an appropriate one for study.

$$H + HOONO_2 \longrightarrow H_2 + O_2NO_2 \qquad (2a)$$

$$\downarrow$$

$$O_2 + NO_2$$

$$\longrightarrow H_2O + NO_3 \qquad (2b)$$

$$\longrightarrow H_2O_2 + NO_2 \qquad (2c)$$

$$\longrightarrow HO + HONO_2 \qquad (2d)$$

Although its possible importance in the atmosphere was the primary reason for studying reactions (2), PNA is an interesting chemical species that represents several homologous series, including the nitrogen acids, the peroxides and the hydroperoxides. We are not yet able to identify the reaction products (although we can rule out $HONO_2$) and so it was hoped that the reaction rate constant could provide clues to the dynamical pathways involved, giving us some insight into the chemistry of the various homologous series of which PNA is a member. As described below, the measured rate constants exhibit such unusual behaviour that interpretation is tenuous and uncertain, but it is also clear that the reaction is too slow to be important in the stratosphere.

B. Experimental

The reaction of hydrogen atoms with PNA was studied under hydrogen-atom-rich conditions due to the ubiquitous presence of NO_2 as an impurity in the PNA. The PNA was prepared as described in detail elsewhere[13] by slowly and carefully dissolving 0.6-g NO_2BF_4 in 2.0-g 90% H_2O_2 that was stirred vigorously at 0^0C. The solution temperature was maintained at 0^0C or slightly above in order to obtain the desired rate of evolution of PNA, and the vapor that evolved was introduced into the reactor via a short capillary tube. This preparative technique gives gas-phase PNA that contains NO_2 and H_2O_2, as well as O_2 and H_2O, which were not measured.

Because of the NO_2 impurity and because NO_2 is one of the likely products of the reaction of H-atoms with PNA, the kinetics were studied under atom-rich conditions, where the atom concentration is not significantly affected reactions with the NO_2 impurity. The kinetics were studied in a stirred-flow reactor (SFR), as depicted in Figure 2. A very similar reactor was used previously for the study of the oxygen atom reaction[9] with PNA, and all of the experimental details are quite similar in both studies.

Briefly, the SFR is coupled to a modulated molecular-beam mass spectrometer (MMBMS) that has been described elsewhere.[14,15] Hydrogen atoms were generated by a microwave discharge and swept by the helium carrier gas into the SFR of volume 2106 cm^3. Wall reactions were inhibited by a halocarbon wax coating (Halocarbon Products Corp.). The helium flow rate was measured with a calibrated rotameter, and the flow rates of minor species were measured by the rate of pressure increases in calibrated volumes. The total pressure in the SFR was measured with a calibrated Wallace and Tiernan gauge.

Pernitric acid concentrations were monitored with the MMBMS at m/e = 46 and the absolute concentration was determined relative to the NO_2 sensitivity, as described in detail previously.[7] The hydrogen-atom flux into the SFR was measured by adding ~ 2-fold excess of ClNO and observing the resulting concentration of HCl product:

$$H + ClNO \longrightarrow HCl + NO \qquad (3)$$

A weakness of this method is that the H-atom reaction with ClNO is so fast[16] that potential wall reactions of H-atom cannot compete; thus, this method gives only a measure of the flux of H-atom into the reactor, not the true steady-state concentration encountered by the PNA. This may not be a severe weakness, however, since wall reactions of H-atom are usually relatively slow as measured in flow-tube reactors, and the SFR has a much lower surface/volume ratio than do flow-tube reactors. For typical flow-tube reactors (2.5 cm i.d.), the first-order wall-loss rate constants usually range from 0-5 sec^{-1}; for the flow tube coupled to the SFR in the present experiments, no wall loss could be observed, implying $k_w \lesssim 1\ sec^{-1}$. (It should be pointed out, however, that the halocarbon wax coating on the flow tube has a melting point of 150°C, and the wax coating on the SFR has a melting point of 80°C. Thus, although the waxes are chemically similar, they have different average molecular weight and are from different batches.) For the flow tube, $S/V = 1.6\ cm^{-1}$, whereas that for the SFR is $\sim 0.38\ cm^{-1}$; thus, if the wall-reaction rate constant for the flow tube is conservatively estimated to be $k_w = 2 \pm 2\ sec^{-1}$, that for the SFR will be $k_w' = 0.5 \pm 0.5\ sec^{-1}$. Since the residence time in the SFR was sometimes as short as one second, the higher value of k_w' could cause a factor of 2 error in the H-atom concentration, but the error is expected to be much less. Oxygen atoms

also do not combine rapidly on walls treated with halocarbon wax. In our study[9] of the O + PNA reaction, k_w for O-atoms was too slow to be detected in the SFR. If H-atoms are similar, k_w for H-atoms is negligible. After the data for this study was collected, another inlet was attached to the system immediately before the throttling stopcock and after the SFR. A photomultiplier tube (RCA 1P28) was mounted so as to view the region just beyond this additional inlet. Nitric oxide was introduced into the system (in excess of the H-atom concentration) at three different points, namely, the flow tube, the SFR, and the additional inlet while the intensity of the red HNO^* emission was recorded. No difference in the HNO^* emission was detected (± 20%) regardless of the titration point. Also, no change was observed whether or not PNA was being added to the system. These data further evidence the fact that wall loss of H-atoms probably is not a problem in the kinetic study.

Because NO_2 is present as an impurity and is also a possible product of the reaction between H-atom and PNA, we added carbon monoxide to the gas stream to act as an OH-radical scavenger that converts OH back to H:

$$H + NO_2 \longrightarrow OH + NO \qquad (4)$$

$$OH + CO \longrightarrow H + CO_2 \qquad (5)$$

Typically, $\sim$ 1-2 x 10^{15} molecules/cm^3 of CO were added, leading to a rate for reaction (5) that is far greater than other potential losses of OH in this system.[17] Thus, the observed extent of reaction should not reflect contributions due to OH attack on PNA.

Typically, experiments were performed at 1-3 torr total pressure, and residence times in the reactor were 1-2 seconds. For temperature control, the reactor was covered with heavy aluminum foil and was then closely wrapped with a coil of Tygon tubing through which a cooling fluid was circulated from a constant temperature bath (Neslab, Model LT-50). A closed-cell flexible foam sheet was then used as insulation. The temperature was monitored by seven chromel-constantan thermocouples attached to the surface of the bulb; they showed excellent temperature uniformity: ± 1 K at 230 K.

C. Results and Discussion

The data analysis for the SFR was performed as described earlier.[9] Briefly, the residence time t is related to the total gas flow rate F_T, the total concentration C_T, and the reactor volume V by:

$$t = \frac{C_T V}{F_T} \quad . \tag{6}$$

The concentration of the i^{th} component of the mixture is given by:

$$C_i = \frac{F_i}{F_T} C_T \tag{7}$$

where F_i is the flow rate of the i^{th} component, and C_T is the total gas concentration as related to P_T by the ideal gas law.

The input flux of H-atoms was measured by ClNO titration, as discussed earlier. Using this technique, the H-atom concentration is given by:

$$[H] = [HCl]\left(\frac{1}{1 + tk_w'}\right) \qquad (8)$$

where $[HCl]$ is the concentration of HCl as measured with the calibrated MMBMS at m/e = 36, and k_w' is the first-order wall reaction rate for loss of H-atoms in the SFR. As mentioned earlier, an estimated upper limit to k_w' is $\sim 1\ sec^{-1}$, but it is probably much lower. We will assume $k_w' \approx 0$ and $[H] = [HCl]$ as determined in the ClNO titration.

For bimolecular reaction (1) where $[H]$ is maintained in great excess so that pseudo-first-order conditions prevail, a simple steady-state analysis gives:

$$\frac{I_o}{I} = \frac{[PNA]_o}{[PNA]} = 1 + tk_2[H] \qquad (9)$$

where I_o and I are mass spectral intensities at m/e = 46 and $[PNA]_o$ and $[PNA]$ are the concentrations of PNA in the absence and in the presence of $[H]$, respectively; t is the residence time in the SFR, and k_2 is the bimolecular reaction rate constant. Data for $[PNA]_o/[PNA]$ plotted versus $t[H]$ should give a straight line of slope k_2 and unity intercept. A sufficient excess of $[H]$ was used so that even if the primary products reacted further with H-atoms, there was no significant variation in $[H]$. Moreover, if OH is a reaction product, it is converted back to H atoms by reaction with the added CO.

The data obtained in the present study are presented in Table 1 and are plotted in Figure 1, where the lines shown were computed by least squares analysis. Slopes and intercepts obtained from such data for all of the temperatures studied are summarized in Table 2. The slopes may be identified with the overall rate constant for reaction (2). The calculated intercepts are unity (within one standard deviation) for all except the three lowest temperatures. At these temperatures, long periods of time were necessary for stabilization of the PNA intensity at m/e = 46 and there appeared to be a systematic variation toward higher extents of reaction (for the same [H])over a period of time; this pathological behavior may be symptomatic of heterogeneous reactions, and thus the data for the lowest three temperatures are somewhat suspect. At 226 K, all of the PNA reacted, and the rate constant could not be determined. On the other hand, the data for the higher temperatures were found to be reproducible.

Aside from the lower temperature data points, the apparent bimolecular rate constant shows a remarkable constancy with temperature. Considering the rather low average value for k_2, the constancy with temperature is difficult to explain. This is because the constancy with temperature implies that the measured rate constant corresponds to the A-factor, and the activation energy is zero. Typical A-factors for H-atom reactions are usually $\gtrsim 10^{-11}$ cm^3 sec^{-1}, nearly three orders of magnitude larger than the observed rate constant. Thus, a puzzle exists.

Table 1

$HOONO_2 + H \rightarrow$ PRODUCTS;
STIRRED-FLOW REACTOR EXPERIMENTAL DATA

T (K)	P_T (torr)	t (sec)	$[HOONO_2]_o$ (molecule·cm^{-3})	$[H]_o$ (molecule·cm^{-3})	I_o/I
315	2.00	1.00	3.2×10^{12}	3.51×10^{13}	1.84
	2.00	1.00	3.2×10^{12}	4.62×10^{13}	2.15
	2.00	1.00	3.2×10^{12}	6.35×10^{13}	2.48
	2.00	1.00	3.2×10^{12}	7.83×10^{13}	2.74
	2.00	1.00	3.2×10^{12}	9.35×10^{13}	3.17
	2.00	1.00	3.2×10^{12}	1.54×10^{14}	4.23
	2.00	1.00	3.2×10^{12}	1.91×10^{14}	5.81
				$k_2 = (2.38 \pm 0.16) \times 10^{-14}$	
297	2.00	1.06	2.0×10^{12}	2.38×10^{13}	1.71
	2.00	1.06	2.0×10^{12}	3.42×10^{13}	1.80
	2.00	1.06	2.0×10^{12}	4.04×10^{13}	2.53
	2.00	1.06	2.0×10^{12}	6.92×10^{13}	2.72
	2.00	1.06	2.0×10^{12}	4.50×10^{13}	3.14
	2.00	1.06	2.0×10^{12}	4.50×10^{13}	2.53
	2.05	1.24	1.0×10^{12}	9.20×10^{13}	4.41
	2.05	1.24	1.4×10^{12}	4.40×10^{13}	2.27
	2.05	1.24	1.4×10^{12}	2.30×10^{13}	1.68
				$k_2 = (2.87 \pm 0.50) \times 10^{-14}$	
274	2.00	1.15	2.5×10^{12}	2.16×10^{13}	1.72
	2.00	1.15	2.5×10^{12}	2.79×10^{13}	1.82
	2.00	1.15	2.5×10^{12}	7.81×10^{13}	2.50
	2.00	1.15	2.5×10^{12}	1.14×10^{14}	4.95
	2.00	1.15	2.5×10^{12}	9.86×10^{13}	4.90
	2.00	1.15	2.5×10^{12}	4.63×10^{13}	2.27
	2.00	1.15	2.5×10^{12}	5.41×10^{13}	2.92
	2.00	1.15	2.5×10^{12}	6.61×10^{13}	3.60
	2.20	1.15	2.5×10^{12}	8.71×10^{13}	4.44
				$k_2 = (3.28 \pm 0.56) \times 10^{-14}$	
258	2.00	1.22	2.6×10^{12}	1.41×10^{14}	4.48
	2.00	1.22	2.6×10^{12}	1.03×10^{14}	4.30
	2.00	1.22	2.6×10^{12}	4.40×10^{13}	2.05
	2.00	1.22	2.6×10^{12}	5.98×10^{13}	3.09
	2.00	1.22	2.0×10^{12}	1.40×10^{14}	5.00
	2.00	1.22	2.0×10^{12}	7.62×10^{13}	1.88
	2.00	1.22	2.0×10^{12}	5.61×10^{13}	1.84
	2.00	1.22	2.0×10^{12}	3.77×10^{13}	1.49
	2.00	1.22	2.0×10^{12}	1.76×10^{13}	1.36
	2.00	1.22	2.0×10^{12}	4.01×10^{13}	1.85
	2.00	1.22	2.0×10^{12}	5.61×10^{13}	2.62
	2.00	1.22	2.0×10^{12}	4.46×10^{13}	2.46
				$k_2 = (2.35 \pm 0.32) \times 10^{-14}$	

continued . . . . . .

Table 1 (concluded)

T (K)	P_T (torr)	t (sec)	$[HOONO_2]_0$ (molecule·cm^{-3})	$[H]_0$ (molecule·cm^{-3})	I_0/I
248	2.00	1.27	3.0×10^{12}	4.04×10^{13}	1.92
	2.00	1.27	3.0×10^{12}	2.14×10^{13}	1.47
	2.00	1.27	3.0×10^{12}	4.34×10^{13}	2.36
	2.00	1.27	3.0×10^{12}	1.06×10^{14}	7.11
	2.00	1.27	3.0×10^{12}	3.56×10^{14}	4.94
				$k_2 = (3.84 \pm 2.94) \times 10^{-14}$	
238	2.00	1.32	2.5×10^{12}	4.30×10^{13}	5.25
	2.00	1.32	2.5×10^{12}	2.46×10^{13}	2.57
	2.00	1.32	2.5×10^{12}	3.38×10^{13}	4.09
				$k_2 = (6.41 \pm 1.40) \times 10^{-14}$	
226	2.00	1.39	2.7×10^{12}	1.69×10^{14}	LARGE
	2.00	1.39	2.7×10^{12}	9.80×10^{13}	LARGE
	2.00	1.39	2.7×10^{12}	2.35×10^{13}	LARGE
				k_2 = FAST	

Table 2

$HOONO_2 + H \rightarrow$ PRODUCTS;
SUMMARY OF APPARENT BIMOLECULAR RATE CONSTANTS

T (K)	$k_2 \pm 1\sigma$ ($cm^3 \cdot molecule^{-1} \cdot sec^{-1}$)	Intercept $\pm 1\sigma$	Data Points
315	$(2.38 \pm 0.16) \times 10^{-14}$	0.95 ± 0.18	7
297	$(2.87 \pm 0.50) \times 10^{-14}$	1.03 ± 0.29	9
274	$(3.28 \pm 0.56) \times 10^{-14}$	0.77 ± 0.46	9
258	$(2.35 \pm 0.32) \times 10^{-14}$	0.75 ± 0.30	12
248	$(3.84 \pm 2.94) \times 10^{-14}$	0.55 ± 1.33	5
238	$(6.41 \pm 1.40) \times 10^{-14}$	- - -	3
226	(too large for measurement)	- - -	3

Weighted average from 248 K to 315 K:

$$(k_2 \pm 2\sigma) = (2.46 \pm 0.35) \times 10^{-14} \text{ cm}^3 \text{ s}^{-1} .$$

Based upon analogy with H_2O_2 + H and CH_3OOH + H,[17] several reaction paths are possible for reaction (2). The simple abstraction reaction (a) is expected to have an A-factor near 10^{-11} cm^3 sec^{-1} and an activation energy. The three "addition" or "displacement" paths will give the products shown. The Arrhenius parameters for such addition reactions are difficult to estimate, since few examples are known for this class of compounds. However, if res s for H + H_2O_2 and H + CH_3OOH are taken at face value, the addition reactions can contribute from 10% to 70% of the total reaction.

For the case H + $HOONO_2$, reaction channel (d) can be immediately ruled out because we observe no evidence for nitric acid formation. Because of the slow reaction between H and HNO_3, nitric acid should survive under our conditions and, if present, it would be detected at m/e = 46. At this cracking peak, HNO_3 gives a signal $\sim$ 90% as intense as that of $HOONO_2$, for the same concentration. If nitric acid were formed the plots of I_o/I versus [H]t would show nonlinearity, tending to level off at high [H]t. Inspection of the data shown in Figures 1(a) and 1(b) shows no tendency toward nonlinear behavior, and thus reaction channel (d) must contribute less than 10% of the total reaction. Under our conditions, it was not possible to detect the products of the other channels due to their fast reaction with the excess [H]. (Thus, there is also no interference at m/e = 46 due to product NO_2, for example.)

In the absence of the identification of reaction products, the observed rate constant does not provide sufficient information for an unambiguous interpretation of the reaction dynamics. Nevertheless, several reasonable conclusions can be reached although they cannot be proved.

First of all, the reaction is probably <u>not</u> a simple H-atom abstraction reaction since such reactions usually have A-factors of about $1\text{-}5 \times 10^{-11}$ $cm^3 s^{-1}$ and activition energies of $\sim$ 5-10 kcal/mole. An abstraction reaction with these Arrhenius parameters might make itself evident at a temperature of $\sim$ 400 K, but at the temperatures of the present study it would be too slow to be observed. These considerations suggest, however, that if additional studies were performed at higher temperatures, the observed reaction rates might reflect the presence of the abstraction channel (2a).

The "addition" or " isplacement" reactions can be written

$$H + PNA \underset{-a}{\overset{a}{\rightleftharpoons}} [H_2NO_4]^* \xrightarrow{b} \text{Products} \qquad (10)$$

where the $H_2NO_4^*$ complex is a vibrationaly excited species formed by chemical activation. For this reaction scheme, the observed rate constant will be[18]

$$k_{obs} = \frac{k_a k_b}{k_{-a} + k_b} = \epsilon k_a, \qquad (11)$$

where ϵ in an "efficiency factor".

Since k_a is expected to be $\sim 1 \times 10^{-11}$ cm^3 s^{-1}, similar to other H-atom addition reactions, the efficiency factor at room temperature is $\epsilon(300) \approx 2 \times 10^{-3}$ and we may conclude that $\epsilon \approx k_b/k_{-a}$. Since reaction (-a) and (b) are unimolecular reactions almost certainly at the low pressure limit, we can use classical RRK theory and write

$$\epsilon = \frac{k_b}{k_{-a}} = \frac{A_b\left(\frac{E-E_b}{E}\right)^{s-1}}{A_{-a}\left(\frac{E-E_{-a}}{E}\right)^{s-1}} = \frac{A_b}{A_{-a}}\left[\frac{E-E_b}{E-E_{-a}}\right]^{s-1} \qquad (12)$$

where E is the internal energy, E_b and E_{-a} are the respective critical energies for the two reaction channels, and s is the effective number of oscillators, which is usually about $^2/_3$ of the actual number of oscillators in the molecule. The energy E is given by $E \approx E_{-a} + skT$; therefore

$$\epsilon \approx \frac{A_b}{A_{-a}}\left[1 - \frac{\Delta E}{skT}\right]^{s-1} \qquad (13)$$

where $\Delta E = E_{-a} - E_b$, the difference in reaction critical energies.

To evaluate the A-factors,[19] we must estimate the entropy of activation. Forreaction (-a), the A-factor is expected to be similar to those for other H-atom bond fissions and we can estimate $\log A_{-a} \approx 13.5$. For reaction (-b), we can invoke a cyclic transition state:

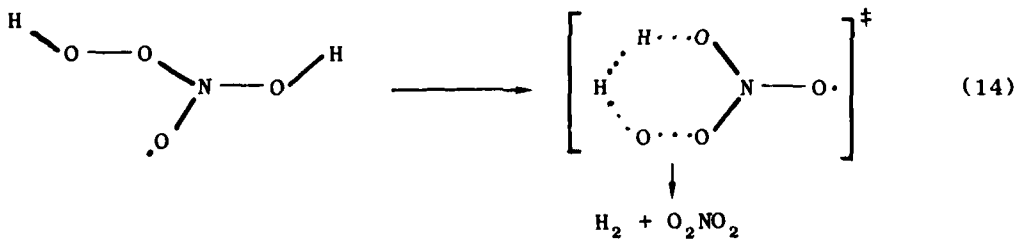

(14)

If the three internal rotors in H_2NO_4 are free rotors with no barriers, the major contribution to $\Delta S^{\pm}$ will be the loss of entropy due to tying them up. This represents a limiting case (i.e. lowest estimate for k_b) since significant barriers to internal rotation in H_2NO_4 will reduce the amount of entropy lost in going to the cyclic transition state. For the three rotors, $S_{int}^{max} \cong 10$ Gibbs/mole, giving log $A_b \gtrsim 11$. Thus $A_b/A_{-a} \gtrsim 3 \times 10^{-3}$ and equation (13) becomes

$$\epsilon \gtrsim 3 \times 10^{-3}\left[\frac{skT - \Delta E}{skT}\right]^{s-1} \qquad (15)$$

Since the observed efficiency factors appear to be virtually independent of temperature for the more reliable higher temperature data, this analysis indicates that $\Delta E \approx 0$. A similar analysis using quantum RKK theory leads to the same general result.

The magnitude of ϵ predicted by equation (15) is within a factor of two of that deduced from the experimental data, indicating that this picture of the reaction dynamics is not inconsistent with experiment. On the other hand, the uncertainties in this analysis are difficult to estimate and are probably large. The idea that H-atoms can attach to the O-atom of the NO_2 group does not seem outlandish, but there is no clear precedent for this behavior.

Other dynamical reaction pathways are also conceivable, but in invoking them, it is more difficult to reproduce the value of ϵ determined from experiment. For example, there exists some evidence that H-atoms attack the O-atom in H_2O_2 and in $HOOCH_3$.[17] If this were the case for the reaction

of H + PNA, one could write a transition state involving a 3 or 4 member ring. Such structures do not tie up as many free-rotors and thus the $\Delta S^{\pm}$ values would lead to larger values for A_b, requiring $\Delta E > 0$ to reproduce the value of ϵ at room temperature. This leads to an inconsistency, however, since it would also predict that ϵ increases with temperature, contrary to experiment.

In conclusion, the interpretation of the experimental results is not straight forward, although addition of H to PNA followed by a cyclic elimination reactors appear to be consistent with the data. More extensive data over a wider temperature range may help to elucidate the reaction mechanism and, specifically, the simple abstraction reaction should become apparent at higher temperatures. A careful reaction product study might also clear up this issue.

Considering the concentration of H-atoms at various altitudes in the atmosphere, it is estimated that at 40 km, $[H] \approx 10^5$ cm^{-3} [20]; below 40 km, [H] is insignificant. Taking the measured rate constant from this study, the estimated lifetime of PNA with respect to reaction with H-atoms is $\tau \gtrsim 13$ years. Thus, this reaction is not expected to have any significant effect on the PNA concentration in the upper atmosphere. It is also worth noting that even if systematic errors have affected our rate constant measurements, the measured rate constants must be too slow by a factor of 10^3 or more for the reaction of H-atoms to affect the atmospheric PNA concentration.

Acknowledgements

We are appreciative of helpful discussions with our colleagues here at SRI. We are grateful for financial support from the High Altitude Pollution Program of the Office of Environment and Energy, Federal Aviation Administration, Department of Transportation under contract DOT-FA78WA-4228.

D. References (Appendix C)

1. R. Simonaitis and J. Heicklen, J. Phys. Chem., 80, 1 (1976).

2. H. Niki, P. D. Maker, C. M. Savage, and L. P. Breitenbach, Chem. Phys. Letters, 45, 564 (1977).

3. C. J. Howard, J. Chem. Phys., 67, 5258 (1977).

4. R. A. Graham, A. M. Winer, and J. N. Pitts, Jr., Chem. Phys. Letters, 51, 215 (1977); J. Chem. Phys., 68, 4505 (1978).

5. A. C. Baldwin and D. M.Golden, J Phys. Chem., 82, 644 (1978).

6. A. C. Baldwin, J. R. Barker, D. M. Golden, and D. G. Hendry, J. Phys. Chem., 81, 2483 (1977).

7. P. L. Trevor, G. Black, and J. R. Barker, J. Phys. Chem., submitted.

8. P. L. Trevor and J. E. Davenport, manuscript in preparation.

9. J. S. Chang, P. L. Trevor, and J. R. Barker, Int. J. Chem. Kinetics, submitted (preceding paper).

10. R. A. Graham, A. M. Winer, and J. N. Pitts, Geophys. Res. Lett., 5, 909 (1978).

11. R. A. Cox and K. Patrick, Int. J. Chem. Kinetics, 11, 635 (1979).

12. L. T. Molina and M. J. Molina, 14th Informal Conference on Photochemistry, March 30-April 3, 1980, paper C2; M. J. Molina, Report No. FAA-EE-80-07, US Department of Transportation, Federal Aviation Administration, 1980.

13. R. L. Kenley, P. L. Trevor, and B. Y. Lan, J. Amer. Chem. Soc., in press.

14. J. S. Chang and J. R. Barker, J. Phys. Chem., 83, 3059 (1979).

15. J. S. Chang, J. R. Barker, J. E. Davenport, and D. M. Golden, Chem. Phys. Lett., 60, 385 (1979).

16. (a) M.A.A. Clyne and D. H. Stedman, Trans. Faraday Soc., 62, 2164 (1960);
(b) M. R. Dunn, M. M. Sutton, C. G. Freeman, M. J. McEwan, and L. F. Phillips, J. Phys. Chem., 75, 722 (1971).
(c) H. Gg. Wagner, U. Welzbacher, and R. Zellner, Bensenges, Phys. Chem., 80, 1023 (1976).

17. For a summary of data, see R. F. Hampson, Jr., and D. Garvin, NBS Special Publication No. 513 (1977); also see R. D. Hudson and E. I. Reed, Eds., The Stratosphere: Present and Future (NASA Ref. Pub. No. 1049, 1974), p. 12.

18. A convenient summary is found in D. M. Golden, J. Phys. Chem. 83, 108 (1979).

19. S. W. Benson, Thermochemical Kinetics, 2nd Ed. (John Wiley and Sons, New York, 1976).

20. O_3 concentration from F. M. Luther, J. S. Chang, W. H. Duewer, J. E. Penner, R. L. Tarp, and D. J. Wuebbles, Potential Environmental Effects of Aircraft Emissions, Lawrence Livermore Laboratory Report No. UCRL-52861, 1979, as quoted from United States Standard Atmosphere, ICAO, Geneva, Switzerland, 1976.

21. O. Morel, R. Simonaitis, and J. Heicklen, Chem. Phys. Lett., 73, 38 (1980).

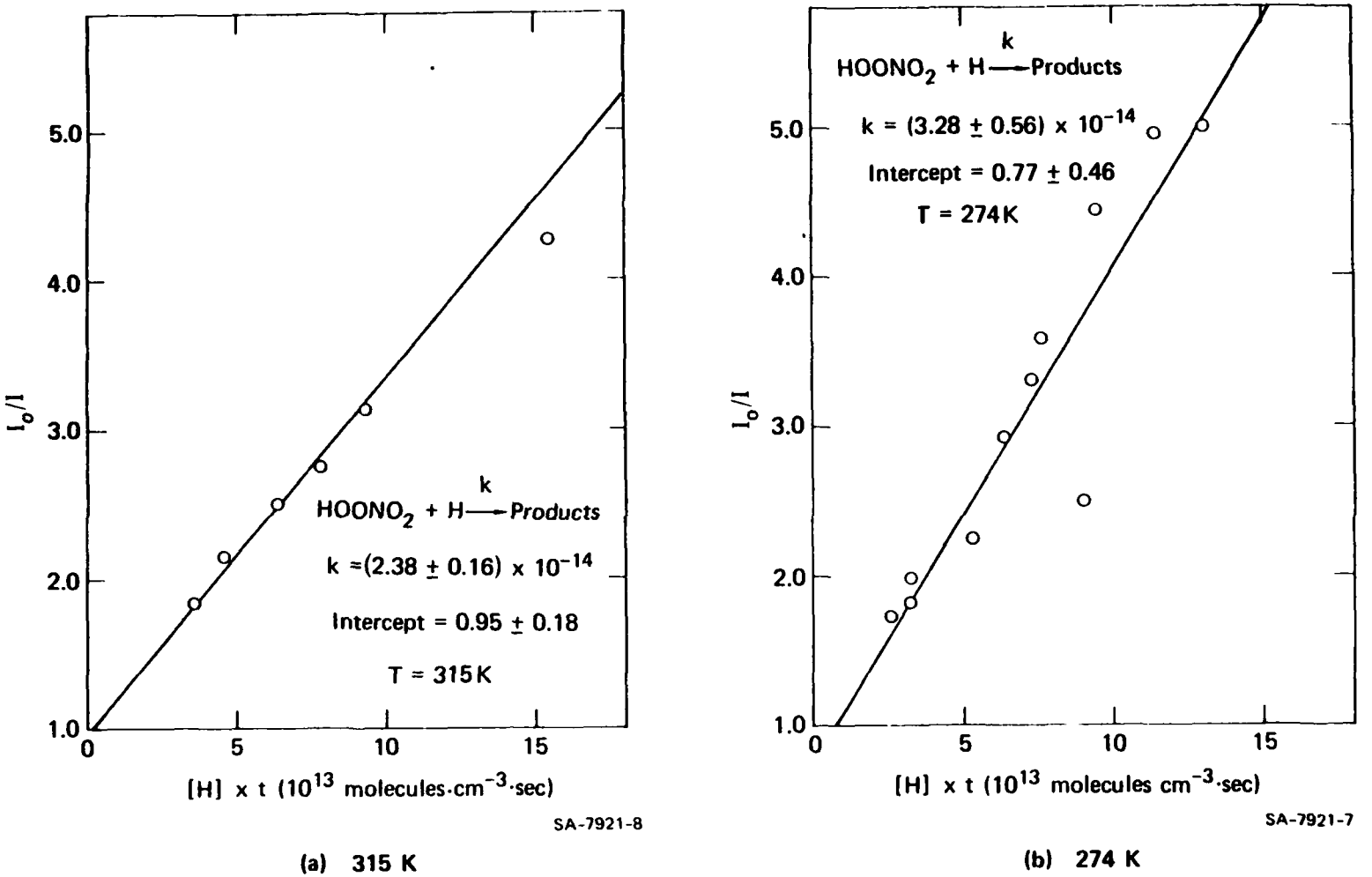

(a) 315 K (b) 274 K

FIGURE 1 STIRRED-FLOW REACTOR RESULTS FOR H + PNA → PRODUCTS PLOTTED AS I_o/I (AT m/e = 46) VERSUS t·[H] FOR (a) 315 K AND (b) 274 K

Appendix D

$OH + HOONO_2 \rightarrow$ PRODUCTS:

TEMPERATURE-DEPENDENT RATE CONSTANT

(Paula L. Trevor, Graham Black, and John R. Barker)

A. Introduction

Both HO_2 and NO_2 play crucial roles in the chemistry of the upper atmosphere. For several years, these two species were thought to react via a radical disproportionation reaction, although it was suggested[1] that a longer-lived complex could be formed according to reaction (1):

$$HO_2 + NO_2 + M \rightleftarrows HOONO_2 + M \qquad (1)$$

The importance of reaction (1) has been verified by direct observation of HO_2NO_2 using Fourier transform infrared spectroscopy.[2] Moreover, the rate of reaction (1) has been measured,[3] and its reverse reaction (−1) has been studied.[4] Also, RRKM theory has been applied to these data for reaction (−1) so that its rate can be reliably estimated as a function of both temperature and pressure.[5] In another publication, the effect of HO_2NO_2 on tropospheric photochemical smog chemistry[6] was discussed.

A concerted effort is under way to investigate pernitric acid (PNA) and determine the rates of various loss mechanisms that affect its residence time in the stratosphere. In addition to the experimental studies reported on its thermal decomposition rate, results of investigations on optical absorption cross sections have been reported,[7-9] permitting calculation of the photolysis rates appropriate for the atmosphere.

In our laboratory, reactions of PNA with several atmospheric species have been studied to determine bimolecular rate constants for the destruction of PNA, including reactions with O-atoms,[10] H-atoms,[11] and O_3.[12] Each of these three reactions is too slow to be important for atmospheric chemistry.

Of the atmospheric species, the OH radical is probably the most reactive, and its reaction with PNA can have a profound effect on the chemistry of the stratosphere. The reaction products are not known, but several set are thermochemically possible:

$$OH + HOONO_2 \rightarrow H_2O + O_2NO_2 \quad (2a)$$
$$\downarrow$$
$$O_2 + NO_2$$

$$\rightarrow H_2O_2 + NO_3 \quad (2b)$$

$$\rightarrow HO_2 + HNO_3 \quad (2c)$$

If the reaction products are given by equation (2a), model calculations[13] show the net result of reactions (1) and (2) is the NO_2-catalyzed disproportionation of OH and HO_2 radicals. The effect of this reaction is to reduce the calculated depletion of the stratospheric ozone column by about a factor of two.[13] Because of the sensitivity of stratospheric chemistry calculations to the rate and products of reaction (2), we have made a great effort to obtain a reliable experimental measurement of the reaction rate constant.[14] Unfortunately, we are not yet able to identify the reaction products.

Although the primary reason for studying PNA reactions is their potential importance in the atmosphere, PNA also is an interesting chemical that is part of the fabric of H–N–O species. In this sense, it is a member of the homologous series of nitrogen acids (e.g., HONO, $HONO_2$, $HOONO_2$), as well as being the first member of a series of pernitrates (e.g., $HOONO_2$, CH_3OONO_2, $CH_3\overset{O}{\overset{\|}{C}}OONO_2$); in addition, it is a hydroperoxide (e.g., HOOH, HOOR, $HOONO_2$). All these species are important for various reasons, and data are needed on their reactions. Such data can then be used as a basis for predicting reaction rate constants for species that have not, as yet, been studied experimentally.

B. Experimental

The experiments were performed in four series, each differing from the other in various ways, mostly due to improvements in technique. The Series A was performed using a flow-tube apparatus and was essentially unsuccessful, but Series B, C, and D were performed using variations on the flash-photolysis resonance-fluorescence (FPRF) technique coupled with mass spectrometric measurement of (PNA), and they were fully successful. Although the flow-tube experiments were relatively unsuccessful, much of the apparatus is common to the other series.

Series A: Flow-Tube Apparatus[14]

The apparatus[15] consists of two main parts, the flow system and the mass spectrometric detection system. The flow system consists of a flow tube, a gas-metering system, a mass spectrometric-sampling device, and a high-capacity pump. As shown in Figure 1, the main flow tube is a Pyrex tube, 1-meter long and 2.5-cm i.d., equipped with a manifold to prepare the main flow mixture before it is introduced into the flow tube. Typically, helium mixed with a small amount of hydrogen constitutes the main flow which is then passed through a microwave discharge (2450 MHz) before being introduced into the flow tube. A Wood's horn is used to prevent light generated by the microwave discharge from entering the main flow tube. The He flow is controlled with a needle valve and is measured by a Fisher-Porter rotameter, and reactant flows are measured by the pressure change in a calibrated volume fitted with a Validyne pressure transducer ($\pm$ 0.1 psi).

It is important to maintain the purity of the helium carrier gas because minor impurities easily produce hydrogen-atom concentrations in excess of 10^{12} cm^{-3}. For this purpose, ultra-high purity helium (99.999%, Matheson Gas Products, Inc.) was used as carrier gas. Before the helium was admitted to the flow tube, hydrogen-containing impurities were removed by passing the gas over a catalyst (No. R3-11, Chemical Dynamics Corp.) at 200°C followed by three liquid nitrogen-cooled molecular sieve (No. 5A) traps to remove water, CO_2, or other byproducts. The resulting purity was such that hydrogen-atom concentrations less than 10^{10} cm^{-3} were obtained from discharging the carrier gas alone.

A coaxial sliding injector inside the flow tube is used to add the reactant to the main flow. The injector is composed of a 0.3-cm o.d. Pyrex tube, O-ring-sealed to the main flow tube at the upstream end. A stainless-steel valve and a length of 0.25-inch Teflon tubing connects the injector to the PNA generator. At the end of the Pyrex injector, a small Teflon tip (cap) that has radial pinholes is used to provide mixing of the reactant into the main flow. Both the inside surface of the main flow tube and the outside surface of the movable injector were coated with halocarbon wax (Halocarbon Products Corp., Type No. 15-00) to minimize wall reactions of OH radicals.

To determine the wall-loss rate of the OH, the radicals were generated at different axial positions along the flow tube. In this experiment, helium carrying a small amount of hydrogen was discharged to generate H-atoms at a concentration of $\sim 2 \times 10^{11}$ cm^{-3}. A fixed amount of NO_2, usually on the order of 10^{12} cm^{-3}, is then added through the movable injector to generate known amounts of OH radicals through the reaction $H + NO_2 \rightarrow OH + NO$ at different positions along the length of the flow tube. The first-order wall-loss rate constants obtained in this manner are usually less than 15 s^{-1}.

The pressure in the main flow tube is monitored by a Wallace-Tiernan gauge or by a pressure transducer (Validyne, ± 1 psi) connected to upstream and/or downstream pressure ports.

The temperature of the reaction region is controlled by the use of heavy aluminum foil and a coil of tubing that circulates fluid from a constant temperature bath. The temperature is monitored by three chromel-constantan thermocouples attached to the outside surface of the main flow tube. The temperatures were constant within ± $2^{o}C$ during the experiment.

Sampling of the reactants and the products from the flow tube to the mass spectrometer is accomplished by a Teflon cap that is situated at the downstream end of the flow tube. In the center of the Teflon cap, a 0.010-inch-diameter pinhole, situated close to the center of the flow tube, serves as a molecular beam source; the beam is modulated by a mechanical chopper and detected by the mass spectrometer. The pressure in the first pumping chamber after the pinhole is typically $\sim$ 1–3 x 10^{-5} torr, while the pressure in the second chamber (containing the Finnigan quadrupole) is $\sim$ 10^{-6} torr. The same modulated-beam mass spectrometer has been used for detection in various other studies, such as very low-pressure pyrolysis and very low-pressure photolysis, and a description can be found elsewhere.[16]

Pumping of the main flow is achieved by a mechanical pump (Alcatel 1P4A or Welch 1397) connected to the system through a stopcock and ballast bulb to damp-out any pressure fluctuations caused by the pump. Molecular sieve (Union Carbide 4X) is placed in the bulb to prevent pump-oil vapor from diffusing back into the flow system. Velocities of 500 to 1000 cm/s are achieved by adjusting both the flow rate of gases and the stopcock openings.

Although not shown in Figure 1, the flow tube is also equipped with a resonance-fluorescence detection system for OH radicals. The resonance lamp is fitted with a quartz window and is powered by a microwave generator (Opthos Instrument Company) that is operated in a chopped mode. Helium at $\sim$ 2.5 torr is passed over water prior to flowing into the lamp. The OH radical resonance-fluorescence is detected through a window in the flow tube situated at 90° to the orientation of the lamp. An interference filter centered at 3100 Å (100 Å FWHM; Corion Corporation) helps to eliminate scattered light and the fluorescence light is detected by a photomultiplier tube (EMI Model 6255B) whose output is amplified by a lock-in amplifier. For a lock-in amplifier averaging time constant of 10 seconds, the detection limit for OH is $\sim 2 \times 10^{10}$ particle/cm^3. The resonance-fluorescence cell is situated about 2-3 cm upstream from the mass spectrometer sampling point.

Pernitric acid was prepared[17] by slowly and carefully dissolving 0.6 g NO_2BF_4 in 2.0 g 90% H_2O_2 that was stirred vigorously and maintained in an ice bath. The solution temperature was then adjusted, and the PNA vapor that evolved was introduced into the flow tube through the movable glass injector. This preparative technique will be described below in more detail. The PNA concentration was determined by monitoring the intensity of m/e = 46 and comparing it to the intensity of a known concentration of NO_2. The relative sensitivities of PNA and NO_2 were determined by diverting the flow of PNA through a heated inlet and measuring the NO_2 produced in the thermal decomposition of PNA, as described below.

Series B: 248-nm Flash-Photolysis Resonance-Fluorescence (FPRF)

The apparatus used in experiment Series B, C, and D is shown schematically in Figure 2. For this setup, the flow tube described above was coupled to a resonance-fluorescence cell as shown in the figure. The cell is not the same one used for Series A and is 70 cm on the long axis to reduce scattered light from the CaF_2 windows that transmit the laser beam. The top and side windows are quartz to transmit the OH radical resonance-fluorescence light centered near 3100 Å. Light from the OH resonance lamp (2450 MHz; 9 torr He; H_2O) is collimated or weakly focussed with a quartz lens and directed through the side window of the cell. The flow tube is coupled to the cell directly opposite the side window. Since the long axis of the cell is oriented at $\sim 35^0$ from the axis of the flow tube, the light from the resonance lamp does not pass down the length of the tube, but is stopped by the bend of the coupling tubulation. This arrangement acts as a crude Wood's horn to reduce scattered light from the lamp.

The photomultiplier tube was rewired for single photon counting and viewed the OH fluorescence through the top window of the cell. The 3100 Å interference filter was used to reduce scattered light. Output from the photomultiplier was amplified and an amplifier/discriminator was used to detect single-photon pulses. The output of the discriminator was stored in a multichannel analyzer (Nuclear Data, Model ND100) that was operated in the multi-channel scaling mode. After several thousand laser shots, the memory contents were recorded on an x-y chart recorder and were then analyzed to determine the fluorescence decay rate.

The gas flow entered the cell at the port opposite the side window and then turned 90^0 downward through the exit tube that is opposite the top window. About 8 cm from the optical center, the gas stream was sampled through a Teflon cap, perforated with a hole $\sim$ 0.008-inch in

diameter that acted as the originating orifice of the modulated molecular-beam mass spectrometer described above. At the exit port of the cell (see Figure 2), a 10-mm glass or Teflon-bore stopcock fitted with viton O-rings was used as a throttle valve to control gas flow velocity and total pressure. From this valve, the gas flow was conducted directly to the main flow-tube pump.

In these experiments, the flow tube was used primarily as a gas-mixing manifold; linear flow velocities were usually of the order of 0.5-3 m/s. but faster velocities were used occasionally. Concentration calibrations for NO_2, H_2, and HNO_3 were performed by measuring the rate of pressure increase in calibrated volumes, as described previously. Dry HNO_3 was prepared by mixing $NaNO_3$ with concentrated H_2SO_4 in an evacuated bulb. Ozone concentration calibrations were performed daily by measuring the attenuation[18] of light from a Hg 2537 Å penlight source viewed through an interference filter by a 1P28 photomultiplier down the long axis of the photolysis cell.

Ozone was prepared in a separate vacuum line by an electric discharge in O_2 and was trapped and stored in a silica gel-packed trap maintained at -78^0C. The ozone concentration was controlled by sweeping it out of the trap with a stream of helium diverted from the main flow. Mass spectrometric analysis showed that H_2O vapor was released from the trap along with O_2 and O_3.

Pulses of OH radicals were generated according to the following scheme:

$$O_3 + h\nu(249\ nm) \rightarrow O(^1D) + O_2 \quad (3)$$

$$O(^1D) + H_2 \rightarrow OH + H \quad (4)$$

$$O(^1D) + PNA \xrightarrow{?} OH + O_2 + NO_2 \quad (5)$$

$$H + O_3 \rightarrow OH(vib) + O_2 \quad (6)$$

The 248-nm light was generated by a Lambda-Physik excimer laser (Model EMG 101) operated with a mixture of krypton, fluorine, and helium. Output energies were measured with a Scientech calorimeter-type power meter (Model 360203) and averaged $\sim$ 80 mJ/pulse, of which energy about 25% actually entered the cell after collimation. Typically, pulse repetition frequencies used were $\sim$ 5-10 Hz. Since gas residence times in the cell body were $\sim$ 1/2 sec, the O_3 was significantly depleted by the laser beam, but the PNA concentration showed less than $\sim$ 5% depletion, demonstrating the validity of pseudo-first-order conditions. It was found by experimentation that the observed OH fluorescence decay rates were independent of O_3 pressures (at this laser pulse energy) as long as they were less than $\sim$ 1 mTorr, corresponding to an initial OH concentration of $\lesssim 2 \times 10^{13}$ radicals/cm^3. Hydrogen concentrations were high enough (2×10^{15} atoms/cm^3) so that all of the O(^{1}D) reacted by reaction (4) within $\sim$ 10 μsec after the laser pulse.[19]

The troublesome probability existed that vibrationally excited OH was present initially, and an observed spectrum showed our resonance lamp could excite OH(v = 1), if present. Thus, the fluorescence data for times shorter than 2.5 msec after the laser pulse were ignored to allow some time for vibrational relaxation of OH(vib). Several spikes due to electronic pickup from the laser appeared on each decay curve, providing a convenient time marker for the 2.5 msec delay.

The relative mass spectrometric sensitivities of PNA and NO_2 at m/e = 46 were measured in a series of experiments described below, and these data were used with the daily measurements of absolute NO_2 sensitivity to determine the absolute PNA concentrations.

In this series of experiments, it was found that PNA decomposition on the pyrex surface could be somewhat inhibited by application of a thin coating of halocarbon wax. This treatment permitted the incorporation of

a cold-trap in the PNA preparation train that helped to reduce unwanted H_2O_2. Moreover, higher total pressures were obtainable without excessive decomposition of the PNA. The primary high pressure limitation, however, was the residual gas pressure tolerable for the mass spectrometer.

Series C: 266-nm FPRF[20]

This series of experiments was performed in a manner similar to Series B, with a few differences. The light source for this series was a Quanta Ray Nd:YAG laser whose output was quadrupled in frequency to give 266-nm light (~ 20 *mJ/pulse*, 90% *of* which entered the cell). The source of OH was:

$$O_3 + h\nu(266\ nm) \rightarrow O(^1D) + O_2 \qquad (3)$$

$$O(^1D) + H_2O \rightarrow 2OH \qquad (7)$$

This source of OH was "cleaner" than in Series B, because the initial vibrational excitation in OH produced by reaction (7) is quite low,[21] and there is no subsequent reaction of $H + O_3$ to produce highly vibrationally-excited radicals. Due to the absence of vibrationally-excited radicals, the data analysis could be carried out for all data from t = 0. The initial OH concentration is estimated to be $\lesssim 2 \times 10^{13}$ radicals/cm^3 for 1 mTorr O_3.

PNA was prepared and its concentration was determined as described previously, except that a new quadrupole mass spectrometer (Balzers Models 311, 140) was substituted for the Finnigan instrument. The new equipment performed very well, and a new series of relative mass spectrometer sensitivity *measurements* was performed.

One additional change was made in the data analysis procedure. The trigger sequence was arranged so that background fluorescence was recorded for several tenths of a millisecond before the laser was pulsed, enabling

us to digitally subtract the background light intensity. After subtraction of background, the memory contents of the MCA were passed through a logarithmic amplifier prior to the x-y recorder. These steps considerably reduced the time consumed in the data analysis process.

Series D: 266-nm FPRF

This series of experiments was performed in just the same way as Series C, except that the lens elements of the mass spectrometer were cleaned and the electron multiplier was rejuvenated (because of an accidental vacuum failure), necessitating a new series of relative sensitivity measurements.

PNA Preparation, Purity, and Concentration Determination

The preparation, purity, and concentration determination of PNA require a separate section because this aspect of the experiments is the single largest source of error and uncertainty.

Our experience is that PNA tends to decompose relatively rapidly (seconds) on pyrex and metal surfaces. Halocarbon wax and teflon tend to be more inert, but some decomposition still takes place. Due to this behavior by PNA, we did not use static mixtures of PNA in storage bulbs, but generated the PNA batch-wise and mixed it with the gas stream in the flow tube. Small preparative batches of PNA are advised because, during this study (CAUTION!!) two minor explosions took place, one of which destroyed a heated glass tube, even though the partial pressure of PNA was probably less than 5 Torr, and the total pressure was less than 20 Torr.

As described elsewhere, PNA was prepared[17] by cautiously and slowly adding 0.6 g NO_2BF_4 (Alfa-Ventron) to 90% H_2O_2 maintained at 0^oC and rapidly stirred. This preparative solution was kept at 0^oC until the

small vessel ($\sim$ 25 cm^3) was O-ring sealed to the preparative train and pumped down to the flow tube pressure. PNA was carried out of the preparative vessel by a stream of helium (diverted from the main flow) that was passed over the liquid surface. Bubbling the carrier gas through the solution did not significantly improve the PNA yield. The flow-tube PNA concentration was controlled by varying the helium flow rate and by varying the bath temperature of the PNA preparative solution up to $\sim 15^{\circ}C$; it was deemed too dangerous to allow the temperature to go higher.

In experimental Series B, C, and D, a U-trap followed the preparation vessel, and when held at a temperature of $\sim -15^{\circ}C$, it seemed to reduce the relative amount of impurity H_2O_2 that was released.

Potential impurities, such as NO_2, H_2O_2, and HNO_3, were specifically sought using the mass spectrometer, and it was found that HNO_3 either was not present or its level was < 5% of the PNA (see below). Hydrogen peroxide appeared as a highly variable impurity, ranging from undetectable levels (m/e = 34) up to concentrations several times as large as the PNA concentration. NO_2 was often present as an impurity, but its level was usually $\lesssim$ 10%, and never more than $\sim$ 50% of the PNA concentration. As discussed later, the reaction rate of OH with NO_2 at the total pressures of He used here are slow, and thus the effect of NO_2 is small. H_2O and O_2 were also impurities, but were not monitored.

The basic idea behind the relative mass spectral sensitivity measurements for PNA and NO_2 is that the thermal decomposition of PNA quantitatively yields NO_2:

$$HOONO_2 \xrightarrow{\text{heat}} HOO + NO_2 \qquad (8)$$

$$2\ HO_2 \longrightarrow H_2O_2 + O_2 \qquad (9)$$

$$H_2O_2 \longrightarrow H_2O + 1/2\ O_2$$

The experimental procedure was as follows:

For a constant flow of PNA,

(1) Measure the mass spectral intensity at m/e = 46: I_1

(2) Using the flow-tube microwave-discharge, add O-atoms and titrate away any NO_2 impurity using the NO_2^* afterglow technique; measure the mass spectral intensity: I_2

(3) With the O-atom concentration from step (2), divert the PNA flow through the heated bypass [a 1/4-inch x 50-cm stainless steel (because of explosion hazard) U-tube maintained at 300°C], and measure the mass spectral intensity: I_3

(4) Add more O-atoms to titrate any NO_2 produced by the thermal decomposition of PNA, and measure the mass spectral intensity: I_4 (Titration of NO_2 by O-atoms is an effective technique, because the rate constant O + NO_2 is about three orders of magnitude faster than that of the reaction O + PNA. As long as a modicum of care is taken, PNA is not depleted by reaction with O-atoms under these conditions.)

The difference $(I_3 - I_4)$ is proportional to the amount of NO_2 produced by the thermal decomposition of PNA. The difference $(I_2 - I_4)$ is proportional to the amount of PNA decomposed. The ratio of these quantities is related to the mass spectrometer sensitivities for the two compounds:

$$\frac{I_3 - I_4}{I_2 - I_4} = S^{-1} \qquad (8)$$

and, $[PNA] = S^{-1} \alpha_{NO_2} \cdot I_2$, where α_{NO_2} is the measured NO_2 sensitivity (molecules cm^{-3}/millivolt).

To determine whether HNO_3 contributes to the observed mass spectral intensity of m/e = 46, the PNA is diverted through the heated bypass and a great excess of O-atoms (i.e., $> 10^{14}$ atom/cm^3) is added. Under these conditions (reaction time ~ 1 sec), it is observed that virtually all of the intensity at m/e = 46 disappears, indicating the absence of HNO_3 since

HNO_3 does not thermally decompose under these conditions, and it reacts only very slowly with O-atoms. On the other hand, PNA both thermally decomposes and reacts with O-atoms at a moderate rate ($k \sim 10^{-15}$ cm^3 sec^{-1} at 300 K).[10] All experiments of this type that were performed showed negligible amounts of HNO_3.

It was concluded that the thermal decomposition of PNA under our conditions quantitatively gives NO_2 for the following reasons:

(1) HNO_3 was shown not to be a significant product.

(2) The ratio of intensities at m/e = 46 and at m/e = 30 were consistent with product NO_2, although the experimental scatter was large due to PNA interference and due to taking the differences of relatively noisy values.

(3) Experiments in which mixtures of NO_2 and H_2O_2 were passed through the heated bypass showed that the NO_2 was unaffected by the treatment.

(4) In the highly oxidizing environment containing $HOONO_2$ and H_2O_2, it seems unlikely that the PNA decomposition product would be HONO or other reduced forms of nitrogen.

The results obtained for the relative sensitivities of NO_2 and PNA in experiment Series B, C, and D, are presented in Table 1.

Table 1 RELATIVE MASS SPECTROMETER SENSITIVITIES FOR PNA AND NO_2

Experimental Series	S ± 1σ	Data Points	Mass Spectrometer
B	7.48 ± 1.05	21	Finnigan
C	4.44 ± 0.74	9	Balzers
D	5.07 ± 0.34	14	Balzers

C. Results and Discussion

To attain pseudo-first-order conditions, PNA was used in excess in all the experiments. Under these conditions, the reaction can be written:

$$OH + PNA_{(excess)} \xrightarrow{k_2} \text{Products} \qquad (2)$$

where k_2 is the bimolecular rate constant for the reaction. The rate expression for the removal of OH can be written:

$$\frac{d[OH]}{dt} = -k_2[OH][PNA] = -k^I[OH] \qquad (10)$$

where k^I is the pseudo-first-order constant and equal to k_2 x [PNA]. For the flow-tube experiment Series A, the plug flow approximation is valid, and time resolution is achieved by varying the mixing distance of the two reacting species. Therefore, k^I is expressed as:

$$k^I = -\frac{d\ln[OH]}{dt} = -\frac{1}{\bar{v}}\frac{d\ln[OH]}{dx} \qquad (11)$$

where the average flow velocity, $\bar{v}$, depends on temperature, pressure, total flow rate, and the cross section of the flow tube. Therefore, k^I is the product of the average flow velocity and the slope of the semi-log plot of disappearance of [OH] versus mixing distance. The bimolecular rate constant, k_2, is then obtained from the slope of the plot of k^I versus [PNA]. As an alternative method to varying the reaction time for fixed concentrations of PNA, the time may be held fixed while the concentration of PNA is varied:

$$k_2 \frac{x}{\bar{v}} = -\frac{\ln([OH]/[OH]_0)}{[PNA]} = k_2 t = z \qquad (12)$$

Therefore, the slope of the plot of ln[OH] versus [PNA] for fixed time gives the product $k_2 t$. The bimolecular rate constant is then obtained from the slope of a linear plot of z versus t. The latter method was used in the present study, because it was found that an inordinate amount of time was necessary for the signal to stabilize after moving the probe position. This behavior is symptomatic of wall reactions involving OH, PNA, or both species. Moreover, the use of the second method was necessitated because during the long periods of time necessary for a complete experiment, the PNA concentration often varied significantly, necessitating corrections for such variations.

It is noteworthy that although the first-order plots of [OH] decay in the flow tube were very well behaved, the second-order plots show considerable scatter. Indeed, the second-order plot for 275 K showed two distinct groups of data and, for any given day, the data seemed to fall in one or the other of them at random.

Considerable effort was spent in attempting to isolate the cause of the data scatter or to eliminate it. In most of our other work with PNA, the major source of error and experimental scatter is in measurements of the PNA concentration. If this was the cause of the scatter in the present work, the first-order plots according to Method II should show such scatter, since the PNA concentration enters directly. But for these experiments, there is not an inordinate amount of scatter, and the plots give good straight lines. Thus, uncertainties in PNA concentration are probably not at fault.

Another potential problem is the possible production of major quantities of impurities in some batches of PNA. This possibility can be eliminated, however, since two or more batches of PNA were used on each day of experiments, and all of the experiments for any single day were self-consistent.

In an effort to test our general technique, we measured the reaction rate constant for the reaction OH + isobutane → products. Good linear first-order plots and second-order plots were obtained that gave ($k \pm 1\sigma$) = (2.2 ± 0.3) x 10^{-12} cm^3 sec^{-1}, in good agreement with literature values.[22] The agreement indicates that our experimental techniques are satisfactory and that there are no unrecognized errors of technique that are affecting the rate constants obtained when PNA is a reactant.

After many efforts to eliminate the anomalous scatter in the data, we have concluded that this behavior may be due to a wall reaction of OH and PNA that is dependent on the PNA concentration and/or H_2O_2 concentration and the history of the flow tube. Although we cleaned the flow tube and recoated it with a fresh layer of halocarbon wax several times, the problem persisted. We feel that of the various wall coatings available, halocarbon wax is among the least likely to cause adsorption of PNA, and thus is one of the best for inhibiting wall reactions. Since it has turned out that this coating is not effective, we concluded that further experiments using the flow-tube technique on this reaction would not be fruitful, and we turned to the FPRF approach. In anticipation of the FPRF results, it is of interest to note that the flow-tube results give a bimolecular rate constant ($k_2 \pm 1\sigma$) = (3.3 ± 0.9) x 10^{-12} cm^3 sec^{-1} at room temperature.

For the FPRF technique, the OH concentration change with time is conventionally written:[23]

$$\frac{d[OH]}{dt} = -(k_2[PNA] + k_p)[OH] \qquad (13)$$

and the inverse decay lifetime of the fluorescence intensity I_f is:

$$\tau^{-1} = k_2[PNA] + k_p \qquad (14)$$

where k_2 is the bimolecular reaction rate constant, and k_p is a parameter that describes the effective "rate constant" for loss of OH due to physical processes. For the particular conditions in the present experiments, the physical processes include the translational motion of gas parcels as they pass into and out of the intersection of the detector field of view and the region illuminated by the resonance lamp. Such motions are due to the gas-stream velocity as it is pumped through the cell and to mass diffusion of [OH]. Neither of these processes is exactly represented by the first-order "rate constant" k_p since the pumping velocity is clearly independent of the OH concentration and spherical diffusion subsequent to excitation in a cylindrical profile coupled with crossed-optical-beam detection is not expected to be so simple. Nevertheless, equation (14) is a good, pragmatic representation as long as the expression is employed for data taken at the same average elapsed time following the laser pulse.

Under pseudo-first-order conditions, a plot of log I_f versus time will give a nearly straight line, if k_p is only slightly dependent on time. Two such plots are shown in Figure 3 for experiment Series C. For Series C and D, the protocol was established that the initial slopes on first-order plots be taken; this protocol is supported because second-order plots of τ^{-1} versus reactant concentrations give good straight lines. Two such examples are presented in Figures 4 and 5 for the reaction:

$$OH + H_2O_2 \rightarrow H_2O + HO_2 \qquad (15)$$

and for

$$OH + NO_2 + He \rightarrow HONO_2 + He \qquad (16)$$

Both second-order plots show very good straight-line behavior. The absolute rate constant for reaction (15) was not determined only because the mass spectrometer could not easily be calibrated for sensitivity to

H_2O_2. The absolute rate constant for reaction (16), determined from the data in Figure 5, is 1.6 x 10^{-30} cm^6 $molecule^{-2}$ s^{-1}, in excellent agreement with literature data.[24] Similar tests were performed using isobutane as reactant, also leading to rate constants in excellent agreement with literature values.[22] The test reaction rates determined are summarized in Table 2.

Table 2 TEST REACTIONS

Reaction	T(K)	Results of Present Study P(torr)	k^{II}_{obs} (cm^3 s^{-1})
OH + iC_4H_{10}	298	9.2	3.6 x 10^{-12}
	324	10.1	(3.62 ± 0.40) x 10^{-12}
	267	10.1	(2.70 ± 0.20) x 10^{-12}
OH + NO_2 + He	246	15.1	(9.23 ± 0.22) x 10^{-13}

For experiment Series B, the protocol for data treatment was somewhat different for two reasons. First, because it was felt that OH(vib) could cause problems, the first 2.5 msec of data from each run were ignored, and the first-order plots were constructed from data beginning at 2.5 msec after the laser pulse. The second reason for this procedure was that two or three "spikes" due to electronic pickup from the excimer laser appeared in each run, causing some interference. The last spike occurred at 2.5 msec after the laser pulse, providing a convenient time marker.

Because the data for Series B corresponded to lower OH concentrations (due to decay after the pulse), the fluorescence data were significantly

noisier than those of Series C and D, but they, again, gave good straight second-order plots and absolute rate constants, in good agreement with the literature. This finding tends to support the use of the approximately accurate equation (14) for the second-order plots.

In all these series--B, C, D--the intercept of the second-order plots can be identified with k_p. It was observed that k_p is larger at lower pressures, as expected for diffusive loss, and it seemed to depend upon day-to-day variation in optical alignment and linear flow velocity through the optical intersection region. No further significance is placed on k_p in the present work.

When H_2O_2 and NO_2 are present as impurities, equation (14) must be generalized to:

$$\tau^{-1} = k_2[PNA] + k_{16}[He][NO_2] + k_{15}[H_2O_2] + k_p \qquad (17)$$

As mentioned earlier, the NO_2 impurity is relatively small, and at the pressures and temperatures of the present study, its effect on the observed τ is also small and can be neglected (see below). Since k_p varies on a day-to-day basis, the best way of combining all of the data for a given temperature and pressure is to consider only the net first-order rate constant resulting from the following expression:

$$k^I_{net} = k_2[PNA] = \tau^{-1} - k_{15}[H_2O_2] - k_p \qquad (16)$$

For experimental runs performed using just H_2O_2, we have:

$$k^I_{H_2O_2} = k_{15}[H_2O_2] + k_p \quad . \qquad (17)$$

For each set of conditions, runs were carried out using only H_2O_2 as reactant, and a linear least-squares analysis gave values for k_{15} and k_p. Since H_2O_2 concentration was measured in arbitrary units, k_{15} has units

AD-A110 835 SRI INTERNATIONAL MENLO PARK CA F/G 7/4
STRATOSPHERIC REACTIONS OF PEROXYNITRIC ACID.(U)
APR 81 J R BARKER, P L TREVOR, R A KENLEY DOT-FA78WA-4228
UNCLASSIFIED SRI-7921-F FAA/EE-82-5 NL

2 OF 2
AD A
110 835

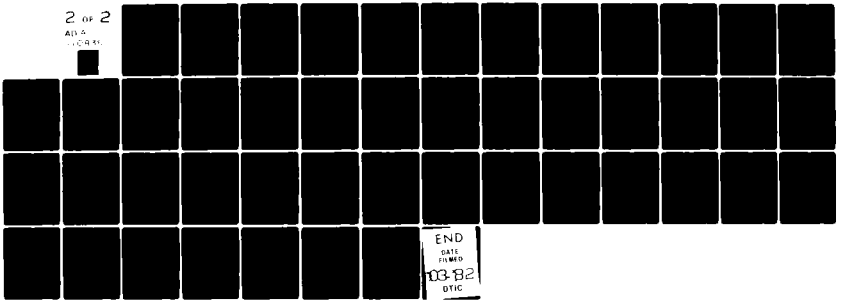

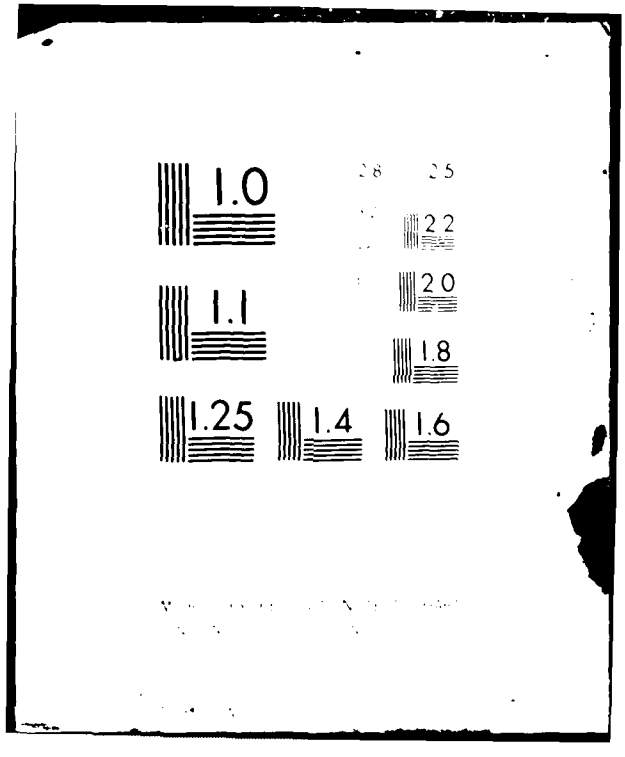
1.0
2.8
2.5
2.2
2.0
1.1
1.8
1.25
1.4
1.6

of (arbitrary unit)$^{-1}$ s^{-1}; k_P is obtained in units of s^{-1}. Once k_P and k_{15} are known, H_2O_2 and PNA concentrations are measured mass spectrometrically and recorded along with τ^{-1}. From these quantities, k^I_{net} is determined, and second-order plots of k^I_{net} versus [PNA] can be constructed as shown in Figure 6.

All of the data obtained in experiment Series B, C, and D are tabulated in the Appendix.

The data for 298 K presented in Figure 6 were obtained on several different days for three different total pressures and several different linear flow velocities. Clearly, the data are quite consistent with one another, showing no significant dependence on total pressure. For the purpose of illustration, the data for 246 K are presented in Figure 7, and again, there is no significant dependence on total pressure.

From the O_3 concentration, laser energy, and ozone absorption coefficient,[18] we can estimate that the initial OH concentration does not exceed $\sim 2 \times 10^{13}$ radicals/cm^3. Several tests were performed to determine whether the observed fluorescence decay rates depended upon either the source of OH radicals or on their initial concentration. In experiment Series B, the O_3 partial pressure was varied from 0.23 to 0.8 mtorr with no perceptable variation in either decay rate or in the shape of the fluorescence decay curve, although the absolute fluorescence intensity varied. When the O_3 partial pressure was raised to 3 mTorr, a faster decay rate occurred at early times, but by the 2.5 msec time marker, there was little effect.

In experiments Series C, more extensive tests were performed. With 80 mTorr H_2O, the O_3 partial pressure was varied from 0.4 to 4.0 mTorr, resulting in a variation of $\sim$ 10% in the OH + H_2O_2 bimolecular rate constant. The 4 mTorr O_3 data for OH + PNA may have been $\sim$ 15% lower than the usual, but this variation is not significant and the data were included in the overall data set.

In another series of test runs in Series C, H_2 was substituted for H_2O, to reproduce the conditions of experiment Series B. Substitution of 85 mTorr H_2 for the usual H_2O gave no significant difference in observed rate constant. Indeed, runs with no H_2 or H_2O added to the gas stream also agreed with the rest of the data. This result can be understood, since reaction of $O(^1D)$ with PNA may give OH and since H_2O was observed evolving both from the PNA preparation train and from the O_3 trap. Thus, it appears that H_2O was always present in significant quantities. Since $H_2O + O(^1D)$ gives relatively "cool" OH, and because H_2O is an efficient quencher for vibrationally excited OH, it appears that if any residual vibrational excitation remained, it played no significant role in the observed rate constants.

In addition to varying the O_3, H_2O, and H_2 partial pressures, the laser power was also varied in experiment Series C. When the laser pulse energy was reduced by about a factor of 10 from the usual 20 mJ/pulse, there was a reduction in fluorescence intensity, but no significant variation in observed rate constant. Thus, we may conclude that (1) secondary reactions of OH and reaction products are not significant, (2) depletion of PNA concentration is not significant, and (3) OH disproportionation is not significant. Thus, the system appears to be kinetically well behaved.

The measured bimolecular rate constants for each temperature are summarized in Table 3 and Figure 8, along with least-squares and propagation of errors estimates of the associated experimental uncertainties. The first uncertainty listed for each rate constant is just the statistical uncertainty associated with the second-order plot of k^I_{net} versus nominal [PNA]. The second uncertainty listed is that associated with the PNA/NO_2 relative mass spectrometric sensitivity. The third uncertainty listed is the propagation of errors combination of these two sources of error.

Table 3 OH + PNA → PRODUCTS: RATE CONSTANTS

T(K)	Data Points	10^{12} k cm^3/sec	$10^{12}\ \sigma_{FPRF}$	$10^{12}\sigma_{NO_2/PNA}$	$10^{12}\ \sigma_{net}$
Series B: 248 nm FPRF					
251	11	3.84	0.28	0.54	0.61
273	17	4.60	0.41	0.65	0.77
298	23	6.05	0.52	0.84	0.99
316	12	4.95	0.31	0.69	0.76
Series C: 266 nm FPRF					
246	42	4.80	0.46	0.80	0.92
267	22	4.83	0.21	0.81	0.84
298	58	3.61	0.16	0.60	0.62
324	20	3.79	0.21	0.63	0.66
Series D: 266 nm FPRF					
254	21	3.24	0.30	0.22	0.37
Total =	226	data points			

The effect of any NO_2 impurity can be shown to be small. In the worst case, for our lowest temperature (246 K) and highest pressure (15.1 torr), the effective bimolecular rate constant for reaction of NO_2 with OH is $k_{16}[He] = (9.23 \pm 0.22) \times 10^{-13}$ cm^3 sec^{-1} (Figure 4). If, for our worst case estimate, the NO_2 impurity is 50% of the PNA concentration, the relative contribution of NO_2 to the observed rate constant is less than 10%. Since this worst case scenario is intended to be pessimistic and the effect is smaller than the other sources of error, effects due to the small NO_2 impurity have been neglected.

The data from Table 3 show very little variation with temperature, but a weighted least-squares calculation[25] of the Arrhenius parameters was performed, giving $(k \pm 1\sigma) = (8.05 \pm 5.69) \times 10^{-12} \exp(-193 \pm 194/T)$ cm^3 s^{-1}, covariance = 1.098×10^{-9}; at the center of our temperature range, these parameters give a one standard deviation uncertainty of about 8%.

Because the temperature dependence of the rate constant is so small, a simple weighted average of the nine rate constants in Table 3 may be of equal usefulness. Such an average gives $(k \pm 1\sigma) = (3.97 \pm 0.27) \times 10^{-12}$ cm^3 s^{-1}. Since the uncertainties quoted refer only to statistical fluctuation and do not include systematic errors, our recommended rate constant and 95% limit uncertainty is:

$$(k \pm 2\sigma) = (4.0 \pm 1.0) \times 10^{-12} \text{ cm}^3 \text{ s}^{-1}$$

where the uncertainty is assigned by a subjective estimate of systematic error.

Our recommended value of $(4.0 \pm 1.0) \times 10^{-12}$ can be compared to the Series A[14] result of $(k \pm 1\sigma) = (3.3 \pm 0.9) \times 10^{-12}$ that was rejected due to our suspicions that wall reactions played a role in those experiments.

Similarily, it can be compared to the "upper limit" rate constant of $\sim 3 \times 10^{-12}$ estimated by Graham, Winer, and Pitts[4] on the basis of a competitive rate measurement in a smog chamber. More recently, an excellent molecular-modulation spectroscopy study was reported by Littlejohn and Johnston[26] that gave a rate constant $k_2 = (2\ ^{+2}_{-1}) \times 10^{-12}$. This last result is noteworthy since it depends upon the accuracy and completeness of a reaction mechanism consisting of more than a dozen reactions, and yet the result is in good agreement with the present study. Moreover, the PNA in that study was prepared by an entirely different technique and the reaction mixture was analyzed spectroscopically, rather than by mass spectrometry. Thus, the agreement of these two very different studies is quite satisfactory. Further experiments using the molecular modulation technique may give information on the reaction products, as well.

Table 4 RATE CONSTANT COMPARISONS

Reaction	Rate Constant ($cm^3\ s^{-1}$)	Reference
$OH + H_2O_2$	$(2.51 \pm 0.6) \times 10^{-12} \exp(-126 \pm 76/T)$	29
	$(2.96 \pm 0.50) \times 10^{-12} \exp(-164 \pm 52/T)$	30
$OH + HOONO_2$	$\lesssim 3 \times 10^{-12}$	4
	$(4.0 \pm 1.0) \times 10^{-12}$ independent of T	present work
	$(2\ ^{+2}_{-1}) \times 10^{-12}$	26
$OH + HONO_2$	$(1.52 \pm 0.38) \times 10^{-14} \exp(649 \pm 69/T)$	27
$OH + HONO$	7×10^{-12}	31

In Table 4 the present results are compared to rate constants measured for H_2O_2, HONO, and $HONO_2$. The most perplexing of these rate constants is the recent result[27] for OH + HNO_3, since it exhibits a "negative activation energy." (The Arrhenius form of data expression is probably not appropriate for such reaction rate constants, but it is convenient in the present context.) Although the reaction products are not beyond question, indications are that it is a simple abstraction reaction[28] making interpretation of the reaction dynamics even more obscure (a displacement reaction could be explained on the basis of long-range chemical attraction). The OH + PNA reaction rate constant seems to be unexceptional in this group, since no clear trends or interpretations are apparent. The A-factor is appropriate either for abstraction or for displacement or complex formation. Further work should be done on this series of reactions to elucidate the dynamical pathways involved.

Acknowledgements

We gratefully acknowledge conversations with our colleagues here at SRI. We are also appreciative of the loan of photon-counting equipment from PAR Corporation. The Nd:YAG laser was rented from the San Francisco Laser Center,[32] and this work was funded primarily by the High Altitude Pollution Program of the Office of Environment and Energy, Federal Aviation Administration, Department of Transportation under contract DOT-FA78WA-4228. Supplemental funding was provided by the National Aeronautics and Space Administration under contract 954815/NAS7-100.

D. Data Tables

Each of the following tables summarizes the experimental data obtained on a given day and set of conditions. Within each set of data are experiments run with [PNA] = 0, and these were analyzed by the method of least-squares to obtain the slope and intercept for the equation:

$$\tau^{-1} = k_{15}[H_2O_2] + k_P ,$$

where τ^{-1} is the observed first-order rate, k_{15} is the slope, and k_P is the intercept, as recorded in the table.

The absolute mass spectrometric sensitivity for NO_2 is determined daily and used along with the NO_2/PNA sensitivity ratio to give absolute [PNA], as described in the text. The approximate NO_2/H_2O_2 sensitivity ratio was determined using the phenomenological H_2O_2 rate constant, the assumed absolute rate constant 1.6×10^{-12} cm^3/sec, and the measured NO_2 sensitivity. The "net rate" is given by:

$$k^I_{net} = \tau^{-1} - k_{15}[H_2O_2] - k_P$$

All of the data were used in the evaluation of the rate constants unless otherwise indicated. Specifically, the "test data" of 18 November 1980 were not used, although they are consistent with the rest of the data. Also, data were arbitrarily rejected if $k^I_{net} \leq 0.5\ k_{15}[H_2O_2]$ for any given run.

OH + PERNITRIC ACID DATA--Series B

TEMP = 298. KELVIN
HELIUM TOTAL PRESSURE = 3.40 TORR
NO2 SENSITIVITY = 2.894E+11 MOLECULES/CC/MV
NO2/PNA SENSITIVITY RATIO = 7.48

APPROXIMATE NO2/H2O2 SENSITIVITY RATIO = 0.4466

H2O2 PHENOMENOLOGICAL RATE LEAST-SQUARES:
SLOPE = 6.4800
INTERCEPT = 285.0 SEC-1

O3(MTORR)	H2X E-15	H2O2(ARB. UNITS)	PNA(MOLEC./CC)	OBS. RATE(SEC-1)	NET RATE(SEC-1)	
0.27	2.10	0.00	0.000E-01	226.	-59.	
2.30	2.10	0.00	0.000E-01	363.	78.	
1.80	2.10	3.95	3.332E+13	423.	112.	
0.87	2.10	0.00	0.000E-01	293.	8.	
0.87	2.10	4.11	5.381E+13	570.	255.	
0.87	2.10	5.15	9.443E+13	688.	366.	
0.87	2.10	4.14	7.505E+13	637.	325.	
0.87	2.10	4.24	3.828E+13	508.	196.	
0.87	2.10	4.24	2.536E+13	329.	17.	
0.87	2.10	7.06	3.388E+13	597.	266.	
0.87	2.10	7.72	4.717E+13	680.	345.	
0.87	2.10	4.05	4.838E+13	574.	263.	
0.87	2.10	1.51	7.955E+12	311.	16.	
0.87	2.10	4.33	3.294E+13	490.	177.	
0.87	2.10	6.40	3.135E+13	532.	206.	
0.87	2.10	47.08	5.727E+13	784.	194.	
0.87	2.10	37.19	5.381E+13	910.	384.	
0.87	2.10	36.49	4.492E+13	920.	399.	
0.87	2.10	48.96	1.029E+14	1207.	605.	
0.87	2.10	0.00	0.000E-01	274.	-11.	
0.87	2.10	0.00	0.000E-01	295.	10.	
0.87	2.10	12.48	2.246E+13	412.	46.	
0.87	2.10	69.68	1.451E+14	1752.	1015.	
0.87	2.10	6.78	9.452E+12	310.	-19.	$
0.87	2.10	240.11	6.111E+13	2148.	307.	$
0.87	2.10	100.75	0.000E-01	978.	40.	#
0.87	2.10	97.93	0.000E-01	899.	-21.	#
0.87	2.10	43.78	0.000E-01	523.	-46.	#

$ NET RATE LESS THAN 50 PERCENT OF H2O2 RATE
# PURE H2O2 RUNS FOR THIS DATE:
17-JULY-80

OH + PERNITRIC ACID DATA--Series B

TEMP = 273. KELVIN
HELIUM TOTAL PRESSURE = 3.80 TORR
NO2 SENSITIVITY = 3.306E+11 MOLECULES/CC/MV
NO2/PNA SENSITIVITY RATIO = 7.48

APPROXIMATE NO2/H2O2 SENSITIVITY RATIO = 0.5800

H2O2 PHENOMENOLOGICAL RATE LEAST-SQUARES:
SLOPE = 5.7000
INTERCEPT = 307.0 SEC-1

O3(MTORR)	H2X E-15	H2O2(ARB. UNITS)	PNA(MOLEC./CC)	OBS. RATE(SEC-1)	NET RATE(SEC-1)	
0.23	3.40	20.01	0.000E-01	446.	25.	#
0.23	3.40	31.78	0.000E-01	478.	-10.	#
0.23	3.40	62.62	0.000E-01	607.	-57.	#
0.23	3.40	86.16	0.000E-01	710.	-88.	#
0.23	3.40	3.06	5.303E+13	369.	45.	
0.23	3.40	1.98	6.807E+13	492.	174.	
0.23	3.40	1.41	3.959E+13	467.	152.	
0.23	3.40	0.94	1.550E+13	260.	-52.	
0.23	3.40	3.77	4.291E+13	562.	234.	
0.23	3.40	12.19	1.387E+14	929.	553.	
0.23	3.40	0.00	0.000E-01	237.	-70.	
0.70	3.40	0.00	0.000E-01	297.	-10.	
0.70	3.40	0.00	0.000E-01	322.	15.	
0.70	3.40	9.65	4.640E+13	412.	50.	
0.70	3.40	10.59	4.595E+13	438.	71.	
0.70	3.40	35.31	1.591E+14	1274.	766.	
0.70	3.40	12.95	6.189E+13	576.	195.	
0.70	3.40	8.94	5.124E+13	469.	111.	
0.70	3.40	3.77	2.212E+13	317.	-11.	
0.70	3.40	3.30	1.460E+13	297.	-29.	
0.70	3.40	44.26	0.000E-01	660.	101.	#
0.60	3.40	40.02	0.000E-01	544.	9.	#
0.60	3.40	74.39	0.000E-01	782.	51.	#
0.60	3.40	77.21	0.000E-01	776.	29.	#
0.60	3.40	0.00	0.000E-01	310.	3.	

$ NET RATE LESS THAN 50 PERCENT OF H2O2 RATE
# PURE H2O2 RUNS FOR THIS DATE:
18-JULY-80

OH + PERNITRIC ACID DATA--Series B

TEMP = 316. KELVIN
HELIUM TOTAL PRESSURE = 3.78 TORR
NO2 SENSITIVITY = 2.303E+11 MOLECULES/CC/MV
NO2/PNA SENSITIVITY RATIO = 7.48

APPROXIMATE NO2/H2O2 SENSITIVITY RATIO = 0.4203

H2O2 PHENOMENOLOGICAL RATE LEAST-SQUARES:
SLOPE = 5.4800
INTERCEPT = 289.0 SEC-1

O3(MTORR)	H2X E-15	H2O2(ARB. UNITS)	PNA(MOLEC./CC)	OBS. RATE(SEC-1)	NET RATE(SEC-1)	
0.75	3.20	48.49	0.000E-01	556.	1.	@
0.75	3.20	131.82	0.000E-01	1063.	52.	@
0.75	3.20	73.44	0.000E-01	635.	-56.	@
0.75	3.20	74.39	0.000E-01	674.	-23.	@
0.75	3.20	40.49	0.000E-01	688.	-23.	@
0.75	3.20	0.00	0.000E-01	344.	55.	
0.75	3.20	0.00	0.000E-01	279.	-10.	
0.75	3.20	54.61	1.524E+14	1374.	786.	
0.75	3.20	44.26	8.924E+13	890.	358.	
0.75	3.20	35.31	5.851E+13	855.	373.	
0.75	3.20	13.42	1.943E+13	383.	20.	@
0.75	3.20	0.00	0.000E-01	295.	6.	
0.75	3.20	12.24	2.017E+13	425.	69.	
0.75	3.20	8.94	1.658E+13	413.	75.	
0.75	3.20	16.48	4.003E+13	645.	266.	
0.75	3.20	25.42	5.239E+13	739.	311.	
0.75	3.20	43.31	6.464E+13	867.	341.	
0.75	3.20	83.80	9.357E+13	1229.	481.	

@ NET RATE LESS THAN 50 PERCENT OF H2O2 RATE
@ PURE H2O2 RUNS FOR THIS DATE:
19-JULY-80

OH + PERNITRIC ACID DATA--Series B

TEMP = 251. KELVIN
HELIUM TOTAL PRESSURE = 3.94 TORR
NO2 SENSITIVITY = 2.560E+11 MOLECULES/CC/MV
NO2/PNA SENSITIVITY RATIO = 7.48

APPROXIMATE NO2/H2O2 SENSITIVITY RATIO = 0.5378

H2O2 PHENOMENOLOGICAL RATE LEAST-SQUARES:
SLOPE = 4.7600
INTERCEPT = 290.0 SEC-1

O3(MTORR)	H2X E-15	H2O2(ARB. UNITS)	PNA(MOLEC./CC)	OBS. RATE(SEC-1)	NET RATE(SEC-1)	
0.80	2.11	0.00	0.000E-01	253.	-37.	
0.80	2.11	0.00	0.000E-01	296.	6.	
0.80	2.11	17.66	0.000E-01	309.	-65.	@
0.80	2.11	28.25	0.000E-01	387.	-37.	@
0.80	2.11	71.56	0.000E-01	637.	6.	@
0.80	2.11	49.43	0.000E-01	495.	-30.	@
0.80	2.11	90.39	0.000E-01	828.	108.	@
0.80	2.11	111.11	0.000E-01	760.	-59.	@
0.80	2.11	0.00	0.000E-01	308.	18.	
0.80	2.11	0.00	0.000E-01	307.	17.	
0.80	2.11	64.97	1.369E+14	1163.	564.	
0.80	2.11	10.59	3.391E+13	486.	146.	
0.80	2.11	14.59	4.380E+13	523.	164.	
0.80	2.11	25.89	5.817E+13	665.	252.	
0.80	2.11	53.20	7.255E+13	765.	222.	
0.80	2.11	16.48	2.684E+13	448.	80.	
0.80	2.11	0.00	0.000E-01	361.	71.	

@ NET RATE LESS THAN 50 PERCENT OF H2O2 RATE
@ PURE H2O2 RUNS FOR THIS DATE:
20-JUL-80

OH + PERNITRIC ACID DATA--Series C

TEMP = 298. KELVIN
HELIUM TOTAL PRESSURE = 9.80 TORR
NO2 SENSITIVITY = 7.033E+13 MOLECULES/CC/MV
NO2/PNA SENSITIVITY RATIO = 4.44

APPROXIMATE NO2/H2O2 SENSITIVITY RATIO = 1.4427

H2O2 PHENOMENOLOGICAL RATE LEAST-SQUARES:
SLOPE = 78.0000
INTERCEPT = 505.0 SEC-1

O3(MTORR)	H2O(MTORR)	H2O2(ARB. UNITS)	PNA(MOLEC./CC)	OBS. RATE(SEC-1)	NET RATE(SEC-1)	
0.30	80.00	7.00	0.000E-01	1060.	9.	@
0.30	80.00	3.80	0.000E-01	780.	-21.	@
0.30	80.00	2.20	0.000E-01	684.	7.	@
0.30	80.00	0.90	0.000E-01	574.	-1.	@
0.30	80.00	0.00	0.000E-01	510.	5.	
0.30	80.00	0.69	3.326E+13	689.	130.	
0.30	80.00	12.30	2.471E+14	2450.	986.	
0.30	80.00	14.10	1.204E+14	1796.	191.	#
0.30	80.00	9.40	7.128E+13	1380.	142.	#
0.30	80.00	3.20	5.069E+13	886.	131.	
0.30	80.00	15.00	1.806E+14	2163.	488.	#

NET RATE LESS THAN 50 PERCENT OF H2O2 RATE
@ PURE H2O2 RUNS FOR THIS DATE:
12-NOV-80

OH + PERNITRIC ACID DATA--Series C

TEMP = 298. KELVIN
HELIUM TOTAL PRESSURE = 5.06 TORR
NO2 SENSITIVITY = 9.367E+13 MOLECULES/CC/MV
NO2/PNA SENSITIVITY RATIO = 4.44

APPROXIMATE NO2/H2O2 SENSITIVITY RATIO = 2.0587

H2O2 PHENOMENOLOGICAL RATE LEAST-SQUARES:
SLOPE = 72.8000
INTERCEPT = 807.4 SEC-1

O3(MTORR)	H2O(MTORR)	H2O2(ARB. UNITS)	PNA(MOLEC./CC)	OBS. RATE(SEC-1)	NET RATE(SEC-1)	
0.31	80.00	9.30	0.000E-01	1504.	20.	@
0.31	80.00	12.00	0.000E-01	1729.	48.	@
0.31	80.00	18.60	0.000E-01	2124.	-37.	@
0.31	80.00	1.53	0.000E-01	888.	-31.	@
0.31	80.00	4.30	0.000E-01	1123.	3.	@
0.31	80.00	0.08	8.861E+12	795.	-19.	
0.31	80.00	0.04	2.004E+13	782.	-28.	
0.31	80.00	0.01	3.354E+12	782.	-26.	
0.31	80.00	6.70	1.266E+14	1605.	310.	
0.31	80.00	6.30	1.793E+14	1799.	533.	
0.31	80.00	5.70	2.532E+14	2149.	927.	
0.31	80.00	4.60	1.118E+14	1572.	430.	
0.31	80.00	9.90	1.097E+14	1889.	361.	
0.31	80.00	10.50	1.899E+14	2302.	730.	
0.31	80.00	10.50	1.730E+14	2124.	552.	
0.31	80.00	1.20	4.747E+13	1027.	132.	
0.31	80.00	0.60	3.924E+13	1062.	211.	
0.31	80.00	0.30	2.848E+13	858.	29.	
0.31	80.00	0.10	7.384E+12	822.	7.	
0.31	80.00	6.10	1.435E+14	1618.	367.	
0.31	80.00	6.30	2.595E+14	2160.	894.	
0.31	80.00	4.60	2.089E+14	1837.	695.	
0.31	80.00	2.61	1.076E+14	1243.	246.	
0.31	80.00	1.20	4.873E+13	957.	62.	
0.31	80.00	0.75	3.038E+13	853.	-9.	#

NET RATE LESS THAN 50 PERCENT OF H2O2 RATE
@ PURE H2O2 RUNS FOR THIS DATE:
13-NOV-80

OH + PERNITRIC ACID DATA--Series C

TEMP = 298. KELVIN
HELIUM TOTAL PRESSURE = 10.15 TORR
NO2 SENSITIVITY = 7.280E+13 MOLECULES/CC/MV
NO2/PNA SENSITIVITY RATIO = 4.44

APPROXIMATE NO2/H2O2 SENSITIVITY RATIO = 1.4726

H2O2 PHENOMENOLOGICAL RATE LEAST-SQUARES:
SLOPE = 79.1000
INTERCEPT = 467.0 SEC-1

O3(MTORR)	H2O(MTORR)	H2O2(ARB. UNITS)	PNA(MOLEC./CC)	OBS. RATE(SEC-1)	NET RATE(SEC-1)	
0.30	80.00	4.50	0.000E-01	859.	36.	#
0.30	80.00	8.10	0.000E-01	1238.	130.	#
0.30	80.00	15.90	0.000E-01	1782.	57.	#
0.30	80.00	19.20	0.000E-01	1946.	-40.	#
0.30	80.00	12.00	0.000E-01	1315.	-101.	#
0.30	80.00	1.71	0.000E-01	520.	-82.	#
0.30	80.00	0.22	2.263E+13	595.	111.	
0.30	80.00	0.54	6.559E+13	735.	225.	
0.30	80.00	16.20	1.722E+14	2317.	569.	#
0.30	80.00	15.90	1.541E+14	2200.	475.	#
0.30	80.00	0.20	2.607E+13	510.	27.	
0.30	80.00	0.15	5.411E+13	622.	143.	
0.30	80.00	0.12	1.082E+14	953.	477.	
0.30	80.00	0.60	5.739E+13	712.	198.	
0.30	80.00	3.60	1.672E+14	1406.	654.	
0.30	80.00	2.10	1.312E+14	1091.	458.	
0.30	80.00	0.90	7.050E+13	779.	241.	
0.30	27.00	2.50	7.378E+13	886.	221.	
0.30	27.00	7.20	1.279E+14	1401.	364.	
0.30	27.00	0.90	5.739E+13	704.	166.	
0.30	27.00	2.40	1.164E+14	1084.	427.	
0.30	27.00	3.40	1.426E+14	1216.	480.	
0.30	27.00	6.60	1.623E+14	1495.	506.	

NET RATE LESS THAN 50 PERCENT OF H2O2 RATE
@ PURE H2O2 RUNS FOR THIS DATE:
14-NOV-80

OH + PERNITRIC ACID DATA--Series C

TEMP = 298. KELVIN
HELIUM TOTAL PRESSURE = 10.10 TORR
NO2 SENSITIVITY = 6.330E+13 MOLECULES/CC/MV
NO2/PNA SENSITIVITY RATIO = 4.44

APPROXIMATE NO2/H2O2 SENSITIVITY RATIO = 1.3817

H2O2 PHENOMENOLOGICAL RATE LEAST-SQUARES:
SLOPE = 73.3000
INTERCEPT = 464.0 SEC-1

O3(MTORR)	H2O(MTORR)	H2O2(ARB. UNITS)	PNA(MOLEC./CC)	OBS. RATE(SEC-1)	NET RATE(SEC-1)	
0.40	80.00	5.20	0.000E-01	894.	49.	#
0.40	80.00	10.80	0.000E-01	1393.	137.	#
0.40	80.00	22.80	0.000E-01	2548.	413.	#
0.40	80.00	33.00	0.000E-01	3003.	120.	#
0.40	80.00	4.50	0.000E-01	742.	-52.	#
0.40	80.00	1.32	0.000E-01	577.	16.	#
4.00	80.00	7.30	0.000E-01	960.	-39.	#
4.00	80.00	9.90	0.000E-01	1196.	6.	#
4.00	80.00	63.00	0.000E-01	5076.	-6.	#
4.00	80.00	35.00	0.000E-01	2996.	-34.	#
4.00	80.00	25.80	0.000E-01	2432.	77.	#
4.00	80.00	1.35	1.668E+14	1267.	704.	
4.00	80.00	13.80	2.139E+14	2070.	594.	
4.00	80.00	1.80	1.155E+14	1084.	488.	
4.00	80.00	1.14	6.984E+13	849.	301.	
4.00	80.00	0.75	5.132E+13	769.	250.	
4.00	80.00	0.60	3.678E+13	759.	251.	
4.00	80.00	18.90	1.925E+14	2538.	689.	#
4.00	80.00	4.40	1.141E+14	1243.	456.	
4.00	80.00	5.00	1.255E+14	1214.	383.	
4.00	80.00	3.00	8.411E+13	1029.	345.	
4.00	80.00	1.80	4.990E+13	851.	255.	
4.00	80.00	0.60	2.695E+13	691.	183.	
4.00	80.00	6.00	1.711E+14	1757.	853.	
4.00	80.00	5.40	1.411E+14	1500.	640.	
4.00	80.00	5.40	1.411E+14	1505.	645.	

NET RATE LESS THAN 50 PERCENT OF H2O2 RATE
@ PURE H2O2 RUNS FOR THIS DATE:
17-NOV-80

OH + PERNITRIC ACID DATA--Series C

TEMP = 298. KELVIN
HELIUM TOTAL PRESSURE = 15.10 TORR
NO2 SENSITIVITY = 7.920E+13 MOLECULES/CC/MV
NO2/PNA SENSITIVITY RATIO = 4.44

APPROXIMATE NO2/H2O2 SENSITIVITY RATIO = 1.6143

H2O2 PHENOMENOLOGICAL RATE LEAST-SQUARES:
SLOPE = 78.5000
INTERCEPT = 427.0 SEC-1

O3(MTORR)	H2O(MTORR)	H2O2(ARB. UNITS)	PNA(MOLEC./CC)	OBS. RATE(SEC-1)	NET RATE(SEC-1)	
0.30	80.00	0.00	0.000E-01	342.	-85.	
0.30	80.00	17.40	0.000E-01	1900.	107.	#
0.30	80.00	10.80	0.000E-01	1336.	61.	#
0.30	80.00	61.00	0.000E-01	5187.	-29.	#
0.30	80.00	40.00	0.000E-01	3558.	-9.	#
0.30	80.00	24.90	0.000E-01	2387.	5.	#
0.30	80.00	13.50	0.000E-01	1475.	-12.	#
0.30	80.00	4.80	0.000E-01	771.	-33.	#
0.30	80.00	26.70	2.836E+14	3515.	992.	$
0.30	80.00	5.60	2.248E+14	1580.	713.	
0.30	80.00	2.10	1.712E+14	1133.	541.	
0.30	80.00	1.14	1.195E+14	846.	330.	
0.30	80.00	0.72	8.741E+13	691.	207.	
0.30	80.00	0.36	6.778E+13	613.	158.	

$ NET RATE LESS THAN 50 PERCENT OF H2O2 RATE
# PURE H2O2 RUNS FOR THIS DATE:
18-NOV-80

OH + PERNITRIC ACID DATA† --Series C

TEMP = 298. KELVIN
HELIUM TOTAL PRESSURE = 15.10 TORR
NO2 SENSITIVITY = 9.080E+13 MOLECULES/CC/MV
NO2/PNA SENSITIVITY RATIO = 4.44

APPROXIMATE NO2/H2O2 SENSITIVITY RATIO = 1.8507

H2O2 PHENOMENOLOGICAL RATE LEAST-SQUARES:
SLOPE = 78.5000
INTERCEPT = 427.0 SEC-1

O3(MTORR)	H2O(MTORR)	H2O2(ARB. UNITS)	PNA(MOLEC./CC)	OBS. RATE(SEC-1)	NET RATE(SEC-1)	
0.30	86.00	0.45	9.612E+13	573.	111.	
0.30	86.00	0.90	1.452E+14	745.	247.	
0.30	86.00	2.40	2.331E+14	1095.	480.	
0.30	86.00	22.80	3.374E+14	2547.	330.	$
0.30	86.00	2.70	1.902E+14	972.	333.	
0.30	86.00	1.65	1.432E+14	810.	253.	
0.30	86.00	26.70	3.006E+14	2725.	202.	$
0.30	86.00	7.50	2.270E+14	1434.	418.	
0.10	86.00	7.50	2.270E+14	1361.	345.	
0.30	0.00	7.50	2.270E+14	1457.	441.	
0.30	0.00	1.65	1.063E+14	721.	164.	
0.30	0.00	1.10	7.567E+13	559.	46.	

$ NET RATE LESS THAN 50 PERCENT OF H2O2 RATE
# PURE H2O2 RUNS FOR THIS DATE:
18-NOV-80 H2 DATA

† Test data; not used in evaluation of rate constant.

OH + PERNITRIC ACID DATA--Series C

TEMP = 267. KELVIN
HELIUM TOTAL PRESSURE = 10.10 TORR
NO2 SENSITIVITY = 6.040E+13 MOLECULES/CC/MV
NO2/PNA SENSITIVITY RATIO = 4.44

APPROXIMATE NO2/H2O2 SENSITIVITY RATIO = 1.2187

H2O2 PHENOMENOLOGICAL RATE LEAST-SQUARES:
SLOPE = 79.3000
INTERCEPT = 448.0 SEC-1

O3(MTORR)	H2O(MTORR)	H2O2(ARB. UNITS)	PNA(MOLEC./CC)	OBS. RATE(SEC-1)	NET RATE(SEC-1)	
0.35	80.00	2.90	2.367E+14	1734.	1056.	
0.35	80.00	2.20	1.755E+14	1592.	970.	
0.35	80.00	1.90	1.469E+14	1417.	818.	
0.35	80.00	1.50	1.333E+14	1281.	714.	
0.35	80.00	1.20	1.197E+14	1179.	636.	
0.35	80.00	0.78	9.931E+13	1051.	541.	
0.35	80.00	0.66	8.706E+13	978.	478.	
0.35	80.00	0.60	6.938E+13	874.	378.	
0.35	80.00	0.57	5.577E+13	773.	280.	
0.35	80.00	0.39	4.489E+13	663.	184.	
0.35	80.00	0.24	3.551E+13	622.	155.	
0.35	80.00	0.20	2.408E+13	561.	97.	
0.35	80.00	0.10	1.428E+13	530.	74.	
0.35	80.00	0.00	1.020E+13	473.	25.	
0.35	80.00	19.20	2.612E+14	2382.	411.	$
0.35	80.00	0.54	3.142E+13	652.	161.	
0.35	80.00	0.93	9.795E+13	1003.	481.	
0.35	80.00	0.60	6.530E+13	797.	301.	
0.35	80.00	3.50	1.673E+14	1463.	737.	
0.35	80.00	11.10	1.673E+14	2052.	724.	
0.35	80.00	5.40	1.306E+14	1522.	646.	
0.35	80.00	3.70	1.088E+14	1212.	471.	
0.35	80.00	2.30	7.754E+13	977.	347.	
0.50	80.00	11.10	0.000E-01	1329.	1.	#
0.50	80.00	22.50	0.000E-01	2210.	-22.	#
0.50	80.00	17.40	0.000E-01	1878.	50.	#
0.50	80.00	15.60	0.000E-01	1706.	21.	#
0.50	80.00	7.30	0.000E-01	984.	-43.	#
0.50	80.00	3.80	0.000E-01	774.	25.	#
0.50	80.00	4.10	0.000E-01	750.	-23.	#
0.50	80.00	5.70	0.000E-01	975.	75.	#
0.50	80.00	9.70	0.000E-01	1134.	-83.	#

$ NET RATE LESS THAN 50 PERCENT OF H2O2 RATE
# PURE H2O2 RUNS FOR THIS DATE:
20-NOV-80

OH + PERNITRIC ACID DATA--Series C

TEMP = 324. KELVIN
HELIUM TOTAL PRESSURE = 10.10 TORR
NO2 SENSITIVITY = 6.290E+13 MOLECULES/CC/MV
NO2/PNA SENSITIVITY RATIO = 4.44

APPROXIMATE NO2/H2O2 SENSITIVITY RATIO = 1.4649

H2O2 PHENOMENOLOGICAL RATE LEAST-SQUARES:
SLOPE = 68.7000
INTERCEPT = 588.0 SEC-1

O3(MTORR)	H2O(MTORR)	H2O2(ARB. UNITS)	PNA(MOLEC./CC)	OBS. RATE(SEC-1)	NET RATE(SEC-1)	
0.30	80.00	13.20	0.000E-01	1680.	185.	#
0.30	80.00	41.00	0.000E-01	3378.	-27.	#
0.30	80.00	29.70	0.000E-01	2603.	-25.	#
0.30	80.00	21.00	0.000E-01	2044.	13.	#
0.30	80.00	16.50	0.000E-01	1698.	-24.	#
0.30	80.00	9.90	0.000E-01	1266.	-2.	#
0.30	80.00	8.30	0.000E-01	1110.	-48.	#
0.30	80.00	2.70	0.000E-01	749.	-24.	#
0.30	80.00	0.00	0.000E-01	540.	-48.	
0.30	80.00	3.50	1.530E+14	1429.	601.	
0.30	80.00	2.80	1.275E+14	1198.	418.	
0.30	80.00	2.10	1.133E+14	1135.	403.	
0.30	80.00	1.56	8.783E+13	1016.	321.	
0.30	80.00	1.26	6.942E+13	909.	234.	
0.30	80.00	0.90	5.242E+13	825.	175.	
0.30	80.00	0.60	3.783E+13	747.	118.	
0.30	80.00	0.33	2.678E+13	705.	94.	
0.30	80.00	0.00	1.615E+13	637.	49.	
0.30	80.00	1.05	1.062E+14	1133.	473.	
0.30	80.00	1.80	1.360E+14	1341.	629.	
0.30	80.00	6.00	2.338E+14	1845.	845.	
0.30	80.00	21.00	2.295E+14	2887.	856.	
0.30	80.00	2.34	1.148E+14	1286.	537.	
0.30	80.00	3.10	1.318E+14	1395.	594.	
0.30	80.00	7.20	1.743E+14	1720.	637.	
0.30	80.00	3.60	1.204E+14	1341.	506.	
0.30	80.00	1.32	6.375E+13	1035.	356.	
0.30	80.00	0.57	3.612E+13	853.	226.	

$ NET RATE LESS THAN 50 PERCENT OF H2O2 RATE
# PURE H2O2 RUNS FOR THIS DATE:
24-NOV-80

OH + PERNITRIC ACID DATA--Series C

TEMP = 246. KELVIN
HELIUM TOTAL PRESSURE = 10.10 TORR
NO2 SENSITIVITY = 6.950E+13 MOLECULES/CC/MV
NO2/PNA SENSITIVITY RATIO = 4.44

APPROXIMATE NO2/H2O2 SENSITIVITY RATIO = 1.4140

H2O2 PHENOMENOLOGICAL RATE LEAST-SQUARES:
SLOPE = 78.6000
INTERCEPT = 513.0 SEC-1

O3(MTORR)	H2O(MTORR)	H2O2(ARB. UNITS)	PNA(MOLEC./CC)	OBS. RATE(SEC-1)	NET RATE(SEC-1)	
0.30	80.00	9.20	0.000E-01	1271.	35.	#
0.30	80.00	8.30	0.000E-01	1152.	-13.	#
0.30	80.00	6.50	0.000E-01	1019.	-5.	#
0.30	80.00	5.10	0.000E-01	912.	-2.	#
0.30	80.00	4.40	0.000E-01	821.	-38.	#
0.30	80.00	3.80	0.000E-01	798.	-14.	#
0.30	80.00	3.40	0.000E-01	780.	-0.	#
0.30	80.00	2.80	0.000E-01	699.	-34.	#
0.30	80.00	2.19	0.000E-01	708.	23.	#
0.30	80.00	1.92	0.000E-01	663.	-1.	#
0.30	80.00	1.77.	0.000E-01	674.	22.	#
0.30	80.00	1.62	0.000E-01	654.	14.	#
0.30	80.00	1.38	0.000E-01	629.	8.	#
0.30	80.00	8.10	2.019E+14	2695.	1545.	
0.30	80.00	5.75	1.096E+14	1641.	676.	
0.30	80.00	4.00	8.922E+13	1295.	468.	
0.30	80.00	2.80	6.418E+13	1017.	284.	
0.30	80.00	1.90	5.166E+13	912.	250.	
0.30	80.00	3.00	1.972E+14	1738.	989.	
0.30	80.00	2.19	3.600E+13	722.	37.	#
0.30	80.00	1.50	1.691E+14	1557.	926.	
0.30	80.00	1.00	1.518E+14	1332.	740.	
0.30	80.00	1.80	1.346E+14	1260.	606.	
0.30	80.00	1.50	1.127E+14	1158.	527.	
0.30	80.00	1.50	8.766E+13	1023.	392.	
0.30	80.00	1.23	7.200E+13	964.	354.	
0.30	80.00	0.90	2.477E+13	632.	48.	
0.30	80.00	1.30	1.096E+14	1209.	594.	
0.30	80.00	2.00	1.503E+14	1439.	769.	
0.30	80.00	1.80	1.346E+14	1285.	631.	
0.30	80.00	0.75	3.522E+13	796.	224.	
0.30	80.00	0.99	4.461E+13	853.	262.	
0.30	80.00	1.05	7.827E+13	1021.	425.	
0.30	80.00	0.81	2.536E+13	720.	143.	
0.30	80.00	2.30	1.550E+14	1446.	752.	

NET RATE LESS THAN 50 PERCENT OF H2O2 RATE
@ PURE H2O2 RUNS FOR THIS DATE:
25-NOV-80

OH + PERNITRIC ACID DATA--Series C

TEMP = 246. KELVIN
HELIUM TOTAL PRESSURE = 15.10 TORR
NO2 SENSITIVITY = 5.740E+13 MOLECULES/CC/MV
NO2/PNA SENSITIVITY RATIO = 4.44

APPROXIMATE NO2/H2O2 SENSITIVITY RATIO = 1.4330

H2O2 PHENOMENOLOGICAL RATE LEAST-SQUARES:
SLOPE = 44.0900
INTERCEPT = 532.0 SEC-1

O3(MTORR)	H2O(MTORR)	H2O2(ARB. UNITS)	PNA(MOLEC./CC)	OBS. RATE(SEC-1)	NET RATE(SEC-1)	
0.50	80.00	2.40	0.000E-01	724.	38.	#
0.50	80.00	1.05	0.000E-01	593.	-6.	#
0.50	80.00	1.58	0.000E-01	632.	-1.	#
0.50	80.00	10.20	0.000E-01	989.	-197.	#
0.50	80.00	8.20	0.000E-01	879.	-179.	#
0.50	80.00	7.20	0.000E-01	1207.	214.	#
0.50	80.00	6.30	0.000E-01	1176.	240.	#
0.50	80.00	5.75	0.000E-01	1064.	163.	#
0.50	80.00	4.50	0.000E-01	924.	104.	#
0.50	80.00	2.79	0.000E-01	532.	-179.	#
0.50	80.00	2.25	0.000E-01	491.	-185.	#
0.50	80.00	12.90	0.000E-01	1347.	-12.	#
0.50	80.00	1.92	5.430E+13	1055.	400.	
0.50	80.00	1.59	6.852E+13	1165.	531.	
0.50	80.00	1.35	7.498E+13	1177.	558.	
0.50	80.00	1.80	1.086E+14	1039.	392.	
0.50	80.00	2.30	1.319E+14	1146.	467.	
0.50	80.00	4.50	1.629E+14	1473.	653.	
0.50	80.00	10.50	1.978E+14	1088.	683.	

NET RATE LESS THAN 50 PERCENT OF H2O2 RATE
@ PURE H2O2 RUNS FOR THIS DATE:
05-DEC-80

OH + PERNITRIC ACID DATA--Series D

TEMP = 245. KELVIN
HELIUM TOTAL PRESSURE = 15.10 TORR
NO2 SENSITIVITY = 9.600E+12 MOLECULES/CC/MV
NO2/PNA SENSITIVITY RATIO = 5.07

APPROXIMATE NO2/H2O2 SENSITIVITY RATIO = 0.7797

H2O2 PHENOMENOLOGICAL RATE LEAST-SQUARES:
SLOPE = 19.7000
INTERCEPT = 303.0 SEC-1

O3(MTORR)	H2O(MTORR)	H2O2(ARB. UNITS)	PNA(MOLEC./CC)	OBS. RATE(SEC-1)	NET RATE(SEC-1)	
0.60	80.00	0.00	0.000E-01	280.	-23.	
0.60	80.00	7.20	0.000E-01	457.	12.	#
0.60	80.00	12.00	0.000E-01	607.	68.	#
0.60	80.00	17.70	0.000E-01	619.	-33.	#
0.60	80.00	9.10	0.000E-01	440.	-42.	#
0.60	80.00	5.60	0.000E-01	386.	-27.	#
0.60	80.00	3.90	0.000E-01	428.	48.	#
0.60	80.00	2.40	0.000E-01	357.	7.	#
0.60	80.00	1.20	0.000E-01	314.	-13.	#
0.60	80.00	2.25	4.147E+13	543.	196.	
0.60	80.00	3.80	7.763E+13	840.	462.	
0.60	80.00	12.60	1.307E+14	1181.	630.	
0.60	80.00	24.00	1.628E+14	1409.	633.	
0.60	80.00	80.00	1.875E+14	2383.	504.	#
0.60	80.00	52.00	1.628E+14	1756.	429.	#
0.60	80.00	41.00	1.458E+14	1400.	289.	#
0.60	80.00	24.00	1.136E+14	1087.	311.	
0.60	80.00	12.00	6.817E+13	736.	197.	
0.60	80.00	9.00	5.340E+13	651.	171.	
0.60	80.00	6.00	3.408E+13	518.	97.	
0.60	80.00	4.50	1.647E+13	433.	41.	#
0.60	80.00	22.50	1.307E+14	1100.	354.	
0.60	80.00	20.00	1.098E+14	939.	242.	
0.60	80.00	5.50	2.556E+13	561.	150.	
0.60	80.00	11.70	8.899E+13	898.	365.	
0.60	80.00	15.00	1.079E+14	956.	358.	

NET RATE LESS THAN 50 PERCENT OF H2O2 RATE
@ PURE H2O2 RUNS FOR THIS DATE:
11-DEC-80

OH + PERNITRIC ACID DATA--Series D

TEMP = 254. KELVIN
HELIUM TOTAL PRESSURE = 15.10 TORR
NO2 SENSITIVITY = 2.020E+13 MOLECULES/CC/MV
NO2/PNA SENSITIVITY RATIO = 5.07

APPROXIMATE NO2/H2O2 SENSITIVITY RATIO = 0.7340

H2O2 PHENOMENOLOGICAL RATE LEAST-SQUARES:
SLOPE = 44.0300
INTERCEPT = 175.0 SEC-1

O3(MTORR)	H2O(MTORR)	H2O2(ARB. UNITS)	PNA(MOLEC./CC)	OBS. RATE(SEC-1)	NET RATE(SEC-1)	
0.80	80.00	37.00	0.000E-01	1758.	-46.	@
0.80	80.00	31.00	0.000E-01	1573.	33.	@
0.80	80.00	28.50	0.000E-01	1443.	13.	@
0.80	80.00	26.10	0.000E-01	1343.	19.	@
0.80	80.00	20.10	0.000E-01	1074.	14.	@
0.80	80.00	15.90	0.000E-01	863.	-12.	@
0.80	80.00	11.40	0.000E-01	663.	-14.	@
0.80	80.00	9.00	0.000E-01	533.	-38.	@
0.80	80.00	7.10	0.000E-01	491.	3.	@
0.80	80.00	5.00	0.000E-01	425.	30.	@
0.80	80.00	4.40	0.000E-01	362.	-7.	@
0.80	80.00	1.00	7.650E+13	323.	104.	
0.80	80.00	1.50	1.873E+14	589.	348.	
0.80	80.00	4.50	2.869E+14	1510.	1137.	
0.80	80.00	7.50	2.630E+14	1550.	1045.	
0.80	80.00	16.80	3.267E+14	1937.	1022.	
0.80	80.00	1.80	7.172E+13	513.	259.	
0.80	80.00	3.40	1.235E+14	781.	456.	
0.80	80.00	4.50	1.673E+14	923.	550.	
0.80	80.00	6.00	2.032E+14	1098.	659.	
0.80	80.00	9.00	2.550E+14	1345.	774.	
0.80	80.00	14.10	2.988E+14	1544.	748.	
0.80	80.00	3.00	5.857E+13	474.	167.	
0.80	80.00	1.00	1.634E+13	290.	71.	
0.80	80.00	1.00	4.781E+13	385.	166.	
0.80	80.00	5.10	1.634E+14	819.	419.	
0.80	80.00	12.60	2.271E+14	1312.	582.	
0.80	80.00	4.50	1.355E+14	759.	386.	
0.80	80.00	6.60	1.793E+14	924.	458.	
0.80	80.00	3.50	9.323E+13	571.	242.	
0.80	80.00	2.50	7.172E+13	508.	223.	
0.80	80.00	6.00	1.594E+14	782.	343.	
0.80	80.00	19.50	2.151E+14	1323.	289.	#

NET RATE LESS THAN 50 PERCENT OF H2O2 RATE
@ PURE H2O2 RUNS FOR THIS DATE:
22-DEC-80

E. References (Appendix D)

1. R. Simonaitis and J. Heicklen, J. Phys. Chem., 80, 1 (1976).

2. H. Niki, P. D. Maker, C. M. Savage, and L. P. Breitenbach, Chem. Phys. Letters, 45, 564 (1977).

3. C. J. Howard, J. Chem. Phys., 67, 5258 (1977).

4. R. A. Graham, A. M. Winer, and J. N. Pitts, Jr., Chem. Phys. Letters, 51, 215 (1977); J. Chem. Phys., 68, 4505 (1978).

5. A. C. Baldwin and D. M. Golden, J. Phys. Chem., 82, 644 (1978).

6. A. C. Baldwin, J. R. Barker, D. M. Golden, and D. G. Hendry, J. Phys. Chem., 81, 2483 (1977).

7. R. A. Graham, A. M. Winer, and J. N. Pitts, Geophys. Res. Lett., 5, 909 (1978).

8. R. A. Cox and K. Patrick, Int. J. Chem. Kinetics, 11, 635 (1979).

9. L. T. Molina and M. J. Molina, 14th Informal Conference on Photochemistry, March 30-April 3, 1980, paper C2; M. J. Molina, Report No. FAA-EE-80-07, US Department of Transportation, Federal Aviation Administration, 1980.

10. J. S. Chang, P. L. Trevor, and J. R. Barker, submitted.

11. P. L. Trevor and J. R. Barker, submitted.

12. P. L. Trevor and J. E. Davenport, submitted.

13. (a) R. Cicerone and S. Walters, 14th Informal Conference on Photochemistry, March 30-April 3, 1980, paper C6;
    (b) W. H. Duewer and D. J. Wuebbles, Ibid., paper J6;
    (c) J. Steed, private communication;
    (d) S. C. Liu, private communication.

14. Preliminary results for the flow-tube data were presented earlier: P. Trevor, J. S. Chang, and J. R. Barker, 14th Informal Conference on Photochemistry, March 30-April 3, 1980, paper C3.

15. J. S. Chang and J. R. Barker, J. Phys. Chem., 83, 3059 (1979).

16. J. S. Chang, J. R. Barker, J. E. Davenport, and D. M. Golden, Chem. Phys. Lett., 60, 385 (1979).

17. R. L. Kenley, P. L. Trevor, and B. Y. Lan, J. Amer. Chem. Soc., in press.

18. M. Griggs, J. Chem. Phys., 49, 857 (1968).

19. J. A. Davidson, H. I. Schiff, G. E. Streit, J. R. McAfee, A. L. Schmeltekopf, and C. J. Howard, J. Chem. Phys., 67, 5021 (1977).

20. Preliminary results obtained in experiment Series C were reported earlier: J. R. Barker, G. Black, and P. L. Trevor, 1980 American Geophysical Union Fall Meeting, San Francisco, CA, 8-12 December 1980.

21. K. H. Gericke and F. J. Canes, Chem. Phys. Letters, 74, 63 (1980).

22. (a) N. R. Geiner, J. Chem. Phys., 53, 1070 (1970);
(b) K. R. Darnall, R. Atkinson, and J. N. Pitts, Jr., J. Phys. Chem., 82, 1581 (1978) and references cited therein.

23. For example, see reference 24(b).

24. (a) For a summary, see R. F. Hampson, Jr., and D. Garvin, NBS Special Publication No. 513 (1977).
(b) P. H. Wine, N. M. Kreutter, and A. R. Ravishankara, J. Phys. Chem. 83, 3191 (1979).

25. R. J. Cvetanovic, R. P. Overend, and G. Paraskevopoulous, Int. J. Chem. Kinetics, Symp. 1, 249 (1975); R. J. Cvetanovic, D. L. Singleton, and G. Paraskevopoulos, J. Phys. Chem., 83, 50 (1979).

26. D. Littlejohn and H. S. Johnston, 1980 American Geophysical Union Fall Meeting, San Francisco, CA, 8-12 December 1980.

27. P. H. Wine, A. R. Ravishankara, N. M. Kreutter, R. C. Shah, J. M. Nicovich, R. L. Thompson, and D. J. Wuebbles, "Rate of Reaction of OH with HNO_3," J. Geophys. Res., in press.

28. W. J. Marinelli, H. H. Nelson, and H. S. Johnston, 1980 American Geophysical Union Fall Meeting, San Francisco, CA, 8-12 December 1980.

29. L. F. Keyser, J. Phys. Chem., 84, 1659 (1980).

30. U. C. Sridharan, B. Reisnann, and F. Kaufman, J. Chem. Phys., 73, 1286 (1980).

31. R. A. Cox, R. G. Derwent, and P. M. Holt, JCS Faraday I, 72, 2031 (1976).

32. This material is based upon work supported by the National Science Foundation under Grant No. CHE79-16250 awarded to the University of California at Berkeley in collaboration with Stanford University. Any opinions, finding and conclusions or recommendations expressed in this publication are those of the author(s) and do not necessarily reflect the views of the National Science Foundation, University of California at Berkeley, or Stanford University.

CAPTIONS

1 Schematic Diagram of Fast-Flow-Discharge-Tube Apparatus.

2 Schematic Diagram of Laser Flash Photolysis Resonance-Fluorescence Experimental Apparatus. For experiment Series B, a KrF excimer laser (248 nm) was used, and for experiment Series C and D, the quadrupled output (266 nm) of a Nd:YAG laser was used.

3 First-Order Plot of Log I_f versus Time. Rate data giving $k^I = 1155\ s^{-1}$ are for $[PNA] = 1.06 \times 10^{14}$ molecules/cm^2 and $[H_2O_2]$ = 1.05 arbitrary units. Data giving $k^I = 2531\ s^{-1}$ are for $[PNA] = 1.51 \times 10^{14}$ molecules/cm^3 and $[H_2O_2]$ = 21.9 arbitrary units (too high for use in second-order analysis). Both sets of data are from experiment Series C, T = 324 K.

4 Second-Order Plot of k^I versus $[H_2O_2]$ from Experiment Series C, 324 K (uncertainties shown are 1σ).

5 Second-Order Plot of k^I versus $[NO_2]$. The effective bimolecular rate constant is $k^{II} = (9.23 \pm 0.22) \times 10^{-13}$ cm^3 s^{-1} (uncertainties shown are 1σ).

6 Second-Order Plot of k^I versus [PNA] for Experiment Series C, T = 298 K.

7 Second-Order Plot of k^I versus [PNA] for Experiment Series C, T = 246 K.

8 Arrhenius Plot of Log k versus 1000/T
- Δ - Experiment Series B
- $\bullet$ - Experiment Series C
- o - Experiment Series D

The solid error-bars are the 2σ statistical uncertainties not including calibration errors; the dashed error-bars are the total 2σ statistical uncertainties from all sources.

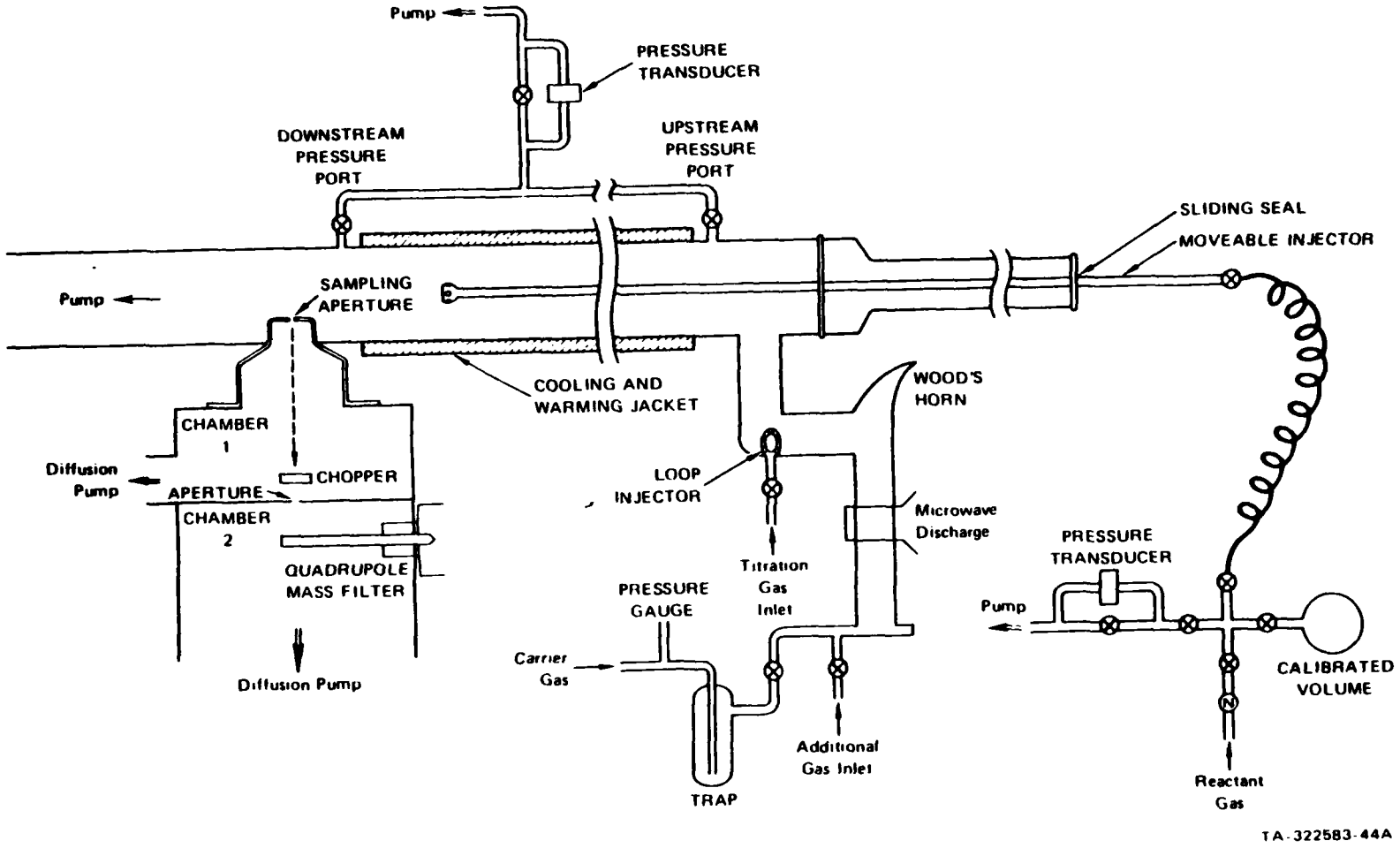
Pump
PRESSURE TRANSDUCER
DOWNSTREAM PRESSURE PORT
UPSTREAM PRESSURE PORT
SLIDING SEAL
MOVEABLE INJECTOR
Pump
SAMPLING APERTURE
COOLING AND WARMING JACKET
WOOD'S HORN
CHAMBER 1
Diffusion Pump
APERTURE
CHOPPER
CHAMBER 2
QUADRUPOLE MASS FILTER
LOOP INJECTOR
Microwave Discharge
PRESSURE TRANSDUCER
Titration Gas Inlet
PRESSURE GAUGE
Pump
CALIBRATED VOLUME
Carrier Gas
Diffusion Pump
Additional Gas Inlet
TRAP
Reactant Gas
TA-322583-44A

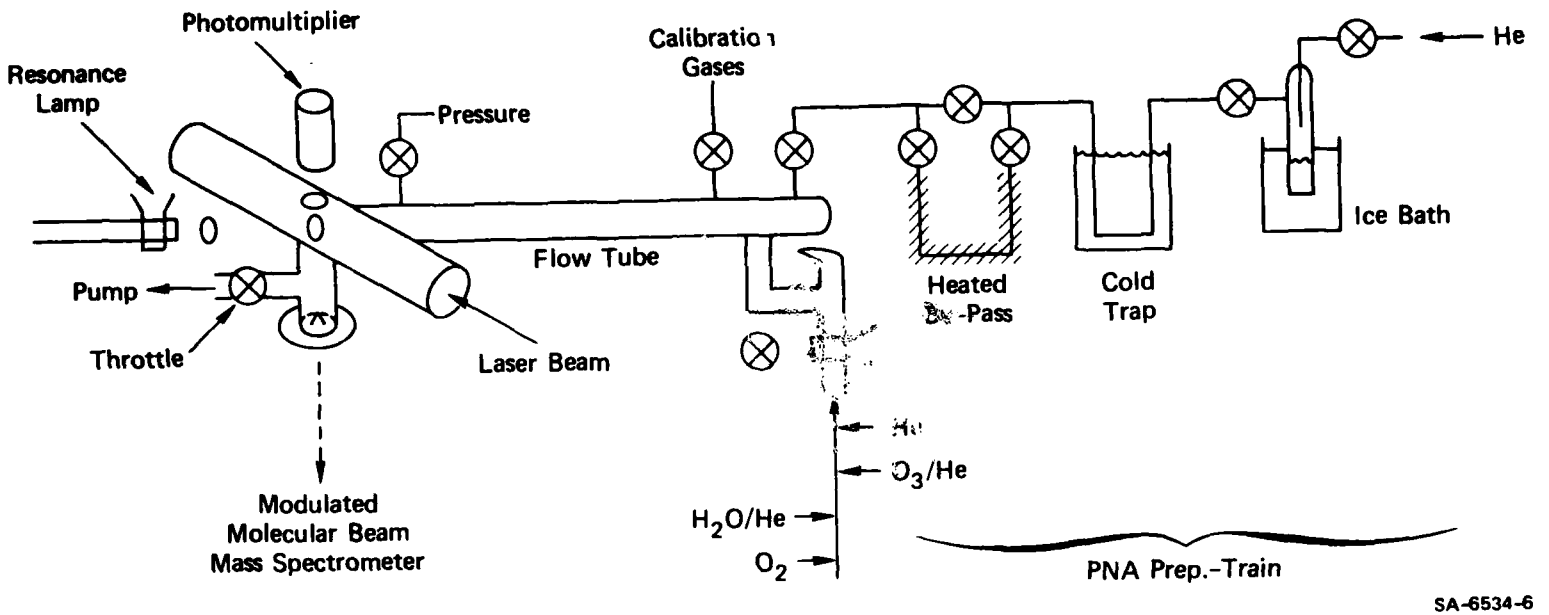
Photomultiplier
Resonance Lamp
Pressure
Calibration Gases
He
Ice Bath
Flow Tube
Heated By-Pass
Cold Trap
Pump
Throttle
Laser Beam
O_3/He
H_2O/He
O_2
Modulated Molecular Beam Mass Spectrometer
PNA Prep.-Train
SA-6534-6

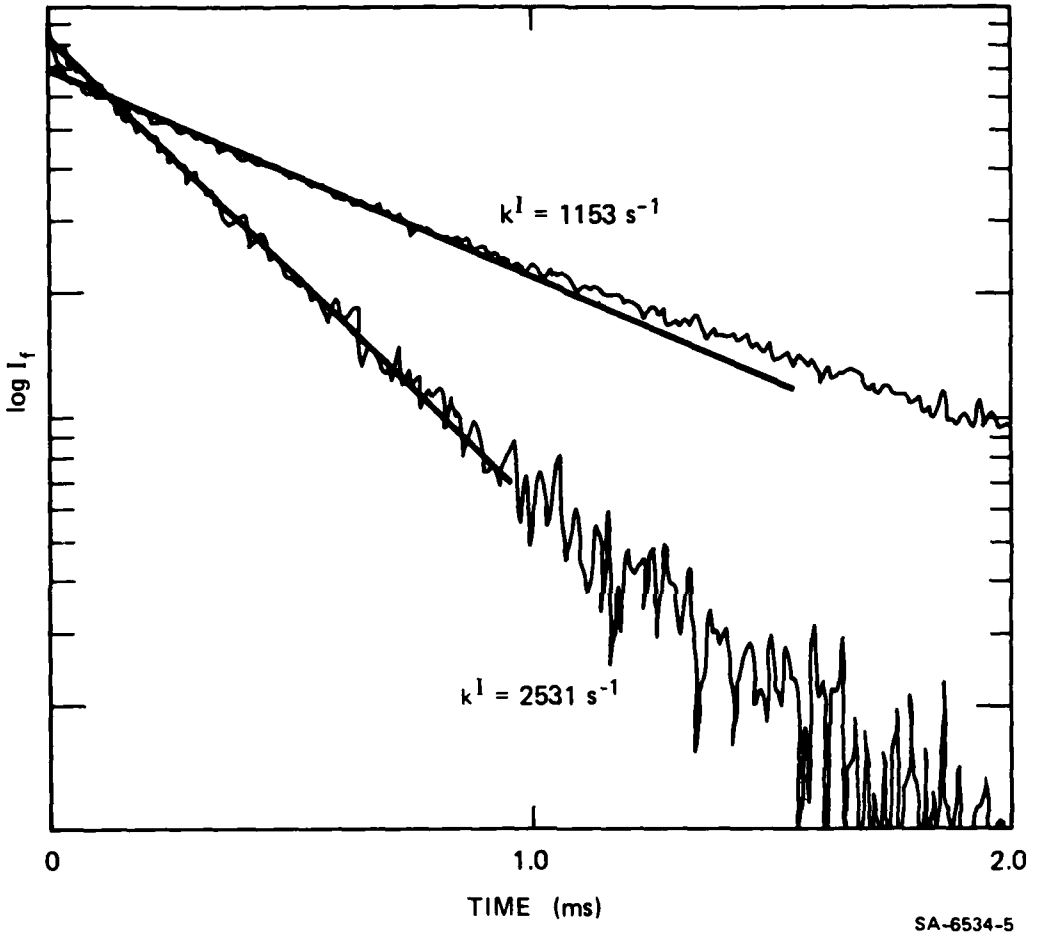
k^I = 1153 s^{-1}
k^I = 2531 s^{-1}
log I_f
0
1.0
2.0
TIME (ms)
SA-6534-5

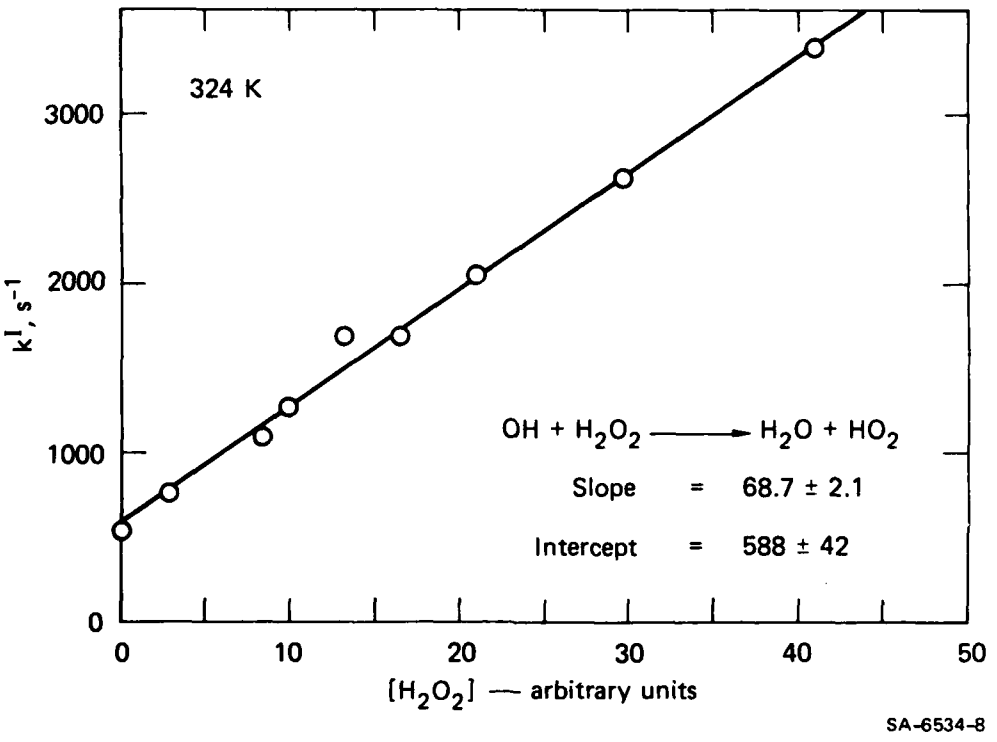
324 K
3000
2000
1000
0
k^1, s^{-1}
0
10
20
30
40
50
$[H_2O_2]$ — arbitrary units
$OH + H_2O_2 \longrightarrow H_2O + HO_2$
Slope = 68.7 ± 2.1
Intercept = 588 ± 42
SA-6534-8

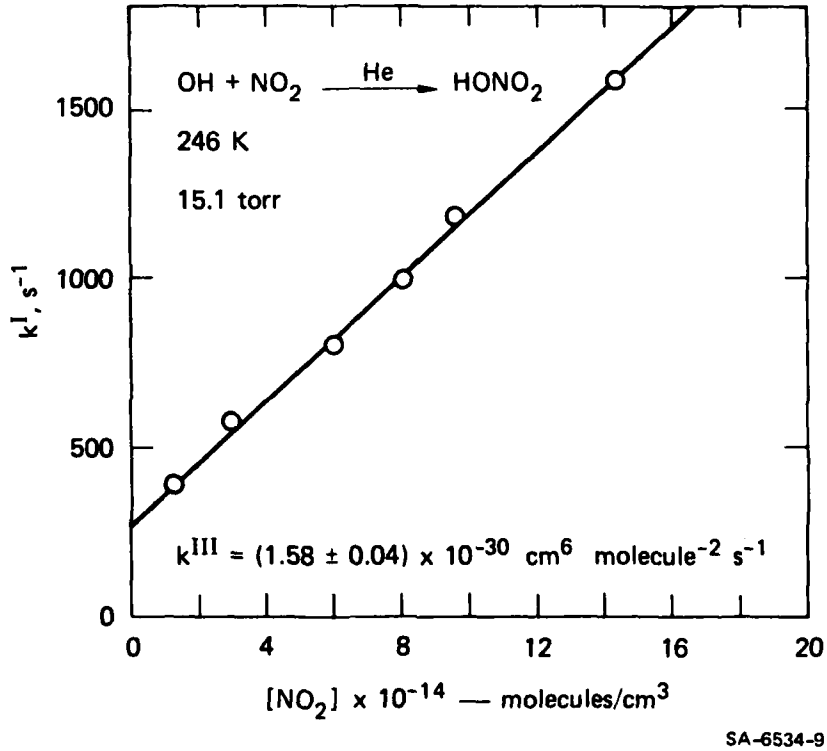
OH + NO2 —He→ HONO2
246 K
15.1 torr
k^III = (1.58 ± 0.04) x 10^-30 cm^6 molecule^-2 s^-1
k^I, s^-1
0
500
1000
1500
0
4
8
12
16
20
[NO2] x 10^-14 — molecules/cm^3
SA-6534-9

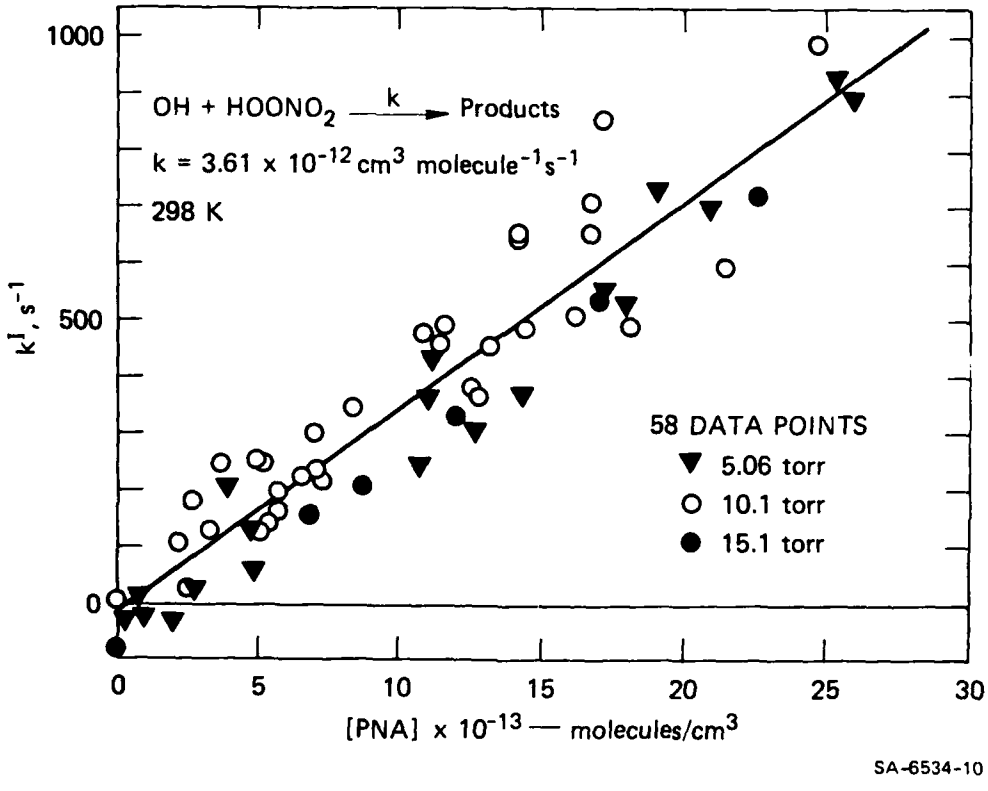
1000
500
0
k^1, s^{-1}
OH + $HOONO_2$ $\xrightarrow{k}$ Products
$k = 3.61 \times 10^{-12}$ cm^3 $molecule^{-1}s^{-1}$
298 K
58 DATA POINTS
5.06 torr
10.1 torr
15.1 torr
0
5
10
15
20
25
30
[PNA] x 10^{-13} — molecules/cm^3
SA-6534-10

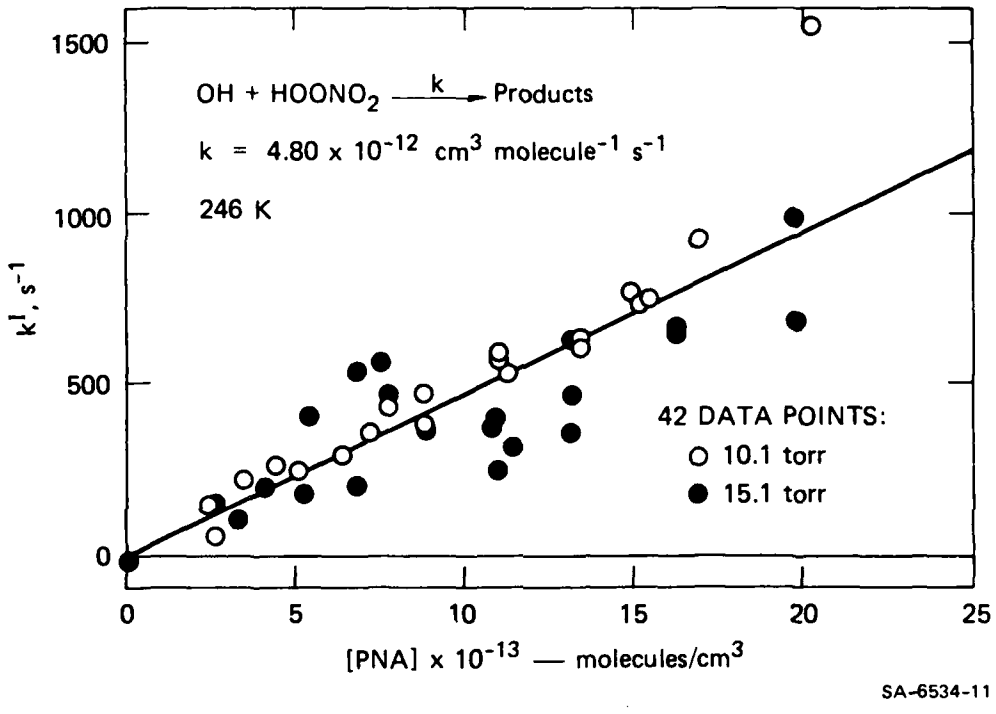
1500
1000
500
0
k^1, s^{-1}
$OH + HOONO_2 \xrightarrow{k}$ Products
$k = 4.80 \times 10^{-12}$ cm^3 molecule^{-1} s^{-1}
246 K
42 DATA POINTS:
○ 10.1 torr
● 15.1 torr
0
5
10
15
20
25
[PNA] x 10^{-13} — molecules/cm^3
SA-6534-11

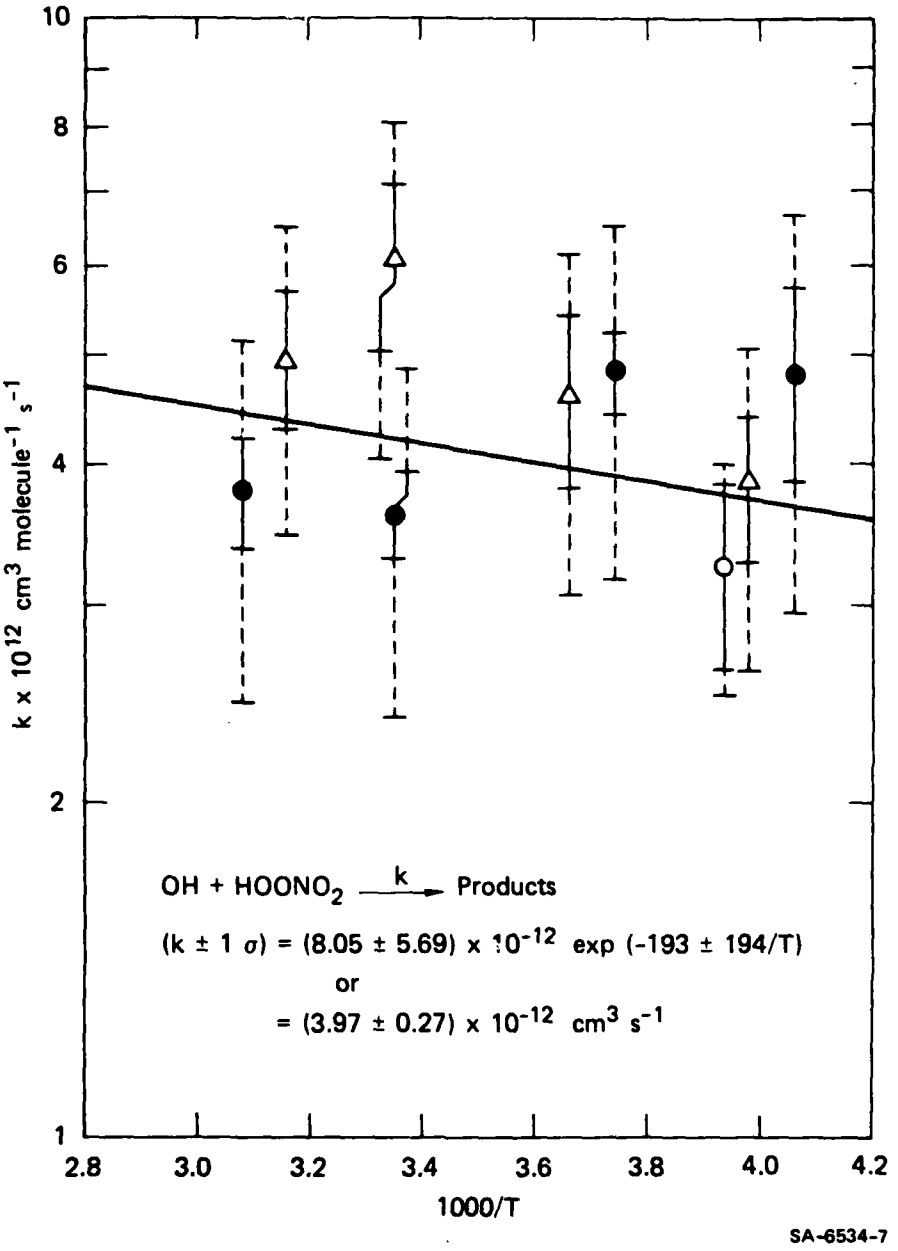
10
8
6
4
2
1
k x 10^12 cm^3 molecule^-1 s^-1
2.8
3.0
3.2
3.4
3.6
3.8
4.0
4.2
1000/T
OH + HOONO2 —k→ Products
(k ± 1 σ) = (8.05 ± 5.69) x 10^-12 exp (-193 ± 194/T)
or
= (3.97 ± 0.27) x 10^-12 cm^3 s^-1
SA-6534-7

Appendix E

O_3 + $HOONO_2$ → PRODUCTS. AN UPPER LIMIT FOR THE RATE CONSTANT

(Paula L. Trevor and John E. Davenport)

A. Introduction

The importance of reactions of pernitric acid ($HOONO_2$) for understanding atmospheric chemistry has been recognized since its formation by reaction (1) was suggested [Simonaitis and Heicklen, 1976]:

$$HO_2 + NO_2 + M \rightleftarrows HOONO_2 + M \qquad (1)$$

After $HOONO_2$ was directly observed in the infrared [Niki et al., 1977], a concerted effort was initiated to investigate $HOONO_2$ reactions [Howard, 1977; Graham, Winer, and Pitts, 1977 and 1978] and to determine the various loss mechanisms that affect its residence time in the stratosphere [Baldwin and Golden, 1978; Graham et al., 1978; Cox and Patrick, 1979; Molina and Molina, 1980]. Because ozone is one of the most important minor species in the stratosphere, and because of the role $HOONO_2$ could play in decreasing the concentration of catalytic destroyers of ozone, it is of interest to examine potential reactions between ozone and $HOONO_2$. In this letter, we describe our determination of the upper limit to the rate constant for the reaction of $HOONO_2$ with ozone and discuss the significance of this limit to our understanding of atmospheric chemistry.

B. Experimental

A static system was used to investigate the reaction kinetics since a slow reaction rate was anticipated. The apparatus consisted of a 20-m variable pathlength Monel cell (Wilks) fitted with a sample inlet and a rotary pump for evacuation; an additional inlet was added to facilitate expansion of O_3 into the cell. A constant temperature circulating bath was attached to cooling coils around the cell to maintain a temperature of 5°C, as measured by an iron-constantan thermocouple on the outer cell surface underneath the outer fiberglass insulating layer. A Perkin-Elmer 467 scanning IR spectrophotometer was used to record spectra of species in the cell.

Ozone was prepared by tesla discharge in O_2 and was stored and purified on silica gel. The infrared absorption at 1000 cm^{-1} showed that the O_3 was $\geq$ 95% pure (O_2 was probably the major impurity). Its concentration in the cell was determined by expansion of a known pressure of the gas from a calibrated volume ($V_{vol}/V_{cell} = 4.5 \times 10^{-3}$), assuming that the O_3 was pure. It was also assumed that no significant change in the O_3 concentration occurred during the experiments. The O_3 concentration was always at least 10 times greater than the $HOONO_2$ concentration at the time of the O_3 addition. Because of the small absorption coefficient [Herzberg, 1945], (506 $l \cdot mole^{-1} \cdot m^{-1}$) at 1000 cm^{-1} for O_3 and interference from $NaNO_3$ (NaCl windows were used for

several experiments) at ~ 1000 cm^{-1}, O_3 concentration measurements by IR were not used in the data analysis. However, the O_3 concentration obtained by the IR absorption at 1000 cm^{-1} agreed within ± 30% of the value calculated by expansion of a pure sample.

$HOONO_2$ was prepared by the addition of 0.6 g (4.5×10^{-3} mol) of solid NO_2BF_4 (Alfa-Ventron) in approximately 5-mg portions with vigorous stirring to 2 g (5.3×10^{-2} mol) 90% H_2O_2 (FMC) at 0°C. This reaction mixture was pipeted into a 10-ml bulb connected as close as possible to the inlet of the IR cell. The mixture was allowed to warm to ambient room temperature. Argon (~ 60 cm^3/min) was then bubbled through the reaction mixture, and the effluent was passed into the previously evacuated 20-m cell until the desired $HOONO_2$ concentration was obtained. More Ar was then added from a separate inlet to raise the cell pressure to the desired value. An IR spectrum was obtained using the preparative method described above and a flow-through 10-cm pathlength cell; the spectrum is shown in Figure 1. This spectrum indicates a low level of impurity from HNO_3 (840 cm^{-1}) and NO_2 (1620 cm^{-1}). Because $HOONO_2$ and HNO_3 have strong absorptions at 1720 cm^{-1}, the $HOONO_2$ absorption at 803 cm^{-1}, $\epsilon = (1.26 \times 10^5\ l \cdot mole^{-1} \cdot m^{-1})$ [Graham et al., 1977 and 1978] was monitored for the experimental measurements. It was observed that HNO_3 increased after $HOONO_2$ contacted the Monel cell walls.

Throughout the study, it was clear that even after passivation of the cell walls, the $HOONO_2$ reacted heterogeneously. Not only was a green substance

($Ni(NO_3)_2 \cdot x\ H_2O$?) deposited on the walls, but the mirror surfaces were attacked, apparently through disintegration of the epoxy that bonded the gold mirror coating to the glass substrate.

Because of the nonreproducible behavior of the heterogeneous reaction, we performed experiments with ozone according to the following sequence. As previously described, the $HOONO_2$ was swept into the cell and then buffered to a total pressure of $\sim$ 13 torr with Ar (P_T^0); the IR spectrum was quickly scanned from 1800 cm^{-1} - 700 cm^{-1}. If the $HOONO_2$ proved to be relatively pure, the spectrometer was set at 803 cm^{-1} and the absorbance was recorded as a function of time with a strip-chart recorder. When sufficient time had elapsed to determine the $HOONO_2$ half-life in the cell (k^0_{obs}), the contents of a 25-ml bulb of O_3 gas ($\geq$ 95%) attached to the inlet system were flushed into the cell with Ar to a total pressure of $\sim$ 15 torr (P_T). The $HOONO_2$ decay continued to be monitored until the new $HOONO_2$ half-life was established (k_{obs}) and no more significant change was observed.

C. Results and Discussion

Experiments with only $HOONO_2$ and Ar were performed according to the procedure described in the preceding section; a typical result is shown in Figure 2. Under these conditions, we assumed the following reactions were taking place in the cell:

$$HOONO_2 + M \rightarrow HO_2 + NO_2 + M \quad (2)$$

$$HO_2 + NO_2 + M \rightarrow HOONO_2 + M \quad (3)$$

$$HOONO_2 \xrightarrow{\text{wall}} \text{Loss} \quad (4)$$

This mechanism implies that the observed first-order decay rate constant of $HOONO_2$, k^o_{obs}, is a direct measure of k_4. Wall loss of HO_2 was considered unimportant since experimental evidence indicated that the first-order loss rate of $HOONO_2$ was not affected by the addition of up to 1 torr of NO_2. This is also consistent with the fact that with the estimated impurity level of NO_2 ($[NO_2] \cong 0.1\,[HOONO_2]$), reaction (3) occurs faster than diffusion to the walls ($t_{diff} \cong 5$ sec). By analogy with other HO_2 reactions [Lloyd, 1974], reactions of HO_2 and $HOONO_2$ were judged to be too slow for inclusion in the above scheme.

When ozone was added to the cell, according to the procedure given in the previous section, the first-order loss rate of $HOONO_2$ was increased. A typical experimental run demonstrating this effect is shown in Figure 3; a summary of the experimental data is given in Table 1. Besides reactions (2), (3), and

Table 1

$HOONO_2 + O_3 \rightarrow$ PRODUCTS; SUMMARY OF EXPERIMENTAL DATA AT 278 K (see text for details

Experiment	$[HO_2NO_2]$ (molecule cm^{-3})	P_T^0 (torr)	k^0_{obs} (sec^{-1})	$[O_3]_0$ (molecule cm^{-3})	P_T (torr)	k_{obs} (sec^{-1})	$[NO_2]_{max}$ (molecule cm^{-3}
1 *	2.5×10^{15}	11.8	3.40×10^{-4}	5.8×10^{16}	13.3	8.43×10^{-4}	2.5×10^{16}
2	2.0×10^{15}	13.1	5.78×10^{-4}	4.9×10^{16}	11.1	5.54×10^{-4}	2.0×10^{16}
3	1.8×10^{15}	13.6	8.75×10^{-4}	9.1×10^{16}	16.5	1.99×10^{-3}	1.8×10^{16}
4	1.1×10^{15}	13.4	6.79×10^{-4}	9.8×10^{16}	16.5	6.08×10^{-4}	1.1×10^{15}
5	2.4×10^{15}	12.8	7.70×10^{-4}	3.3×10^{16}	14.5	7.22×10^{-4}	2.4×10^{16}
6 *	1.9×10^{15}	13.8	3.73×10^{-4}	1.6×10^{16}	14.8	5.50×10^{-4}	1.9×10^{16}
7 *	2.1×10^{15}	11.8	4.81×10^{-4}	1.3×10^{17}	16.1	2.89×10^{-3}	2.1×10^{16}
8	1.7×10^{15}	13.4	5.02×10^{-4}	8.3×10^{16}	16.5	1.54×10^{-3}	1.7×10^{16}
9	3.4×10^{15}	13.1	1.16×10^{-3}	6.6×10^{16}	15.5	1.75×10^{-3}	3.4×10^{16}

* Denotes simulated experimental run.

(4), we included the following reactions in the mechanism:

$$HO_2 + O_3 \rightarrow OH + 2O_2 \quad (5)$$

$$HOONO_2 + O_3 \xrightarrow{?} OH + 2O_2 + NO_2 \quad (6)$$

$$OH + HOONO_2 \xrightarrow{?} H_2O + NO_2 + O_2 \quad (7)$$

$$OH + NO_2 + M \rightarrow HNO_3 + M \quad (8)$$

$$OH + O_3 \rightarrow HO_2 + O_2 \quad (9)$$

Wall loss and disproportionation of OH were ignored in view of the fast homogeneous reactions involving OH and the large concentrations of both O_3 and $HOONO_2$ in the cell. Although the products of reaction (7) have not been measured directly, no experimental evidence indicates otherwise [Trevor et al., 1981; Littlejohn and Johnston, 1980]. Products were not measured in this kinetic study; however, those listed for reaction (6) seemed most likely. Since k^o_{obs} indicated that the wall loss of $HOONO_2$ ($t_{wall} \geq 150$ sec) occurred more slowly than diffusion to the walls and thus was not diffusion controlled, we assumed that the pressure increase due to the introduction of ozone into the system had no measurable effect on k_4.

The three experimental runs that best represented the range of ozone concentrations were simulated by means of a computer program employing Gear's method [Gear, 1971] to integrate the set of differential equations corresponding to reactions (2) through (9). The input parameters consisted of the rate constants for the reactions in the kinetic scheme given above and all initial non-zero reactant concentrations. Literature values were used for k_2, k_3, k_5, k_7, k_8,

and k_9 (see Table 2); k^0_{obs} was substituted for k_4 for each of the simulation runs. The measured initial concentrations of ozone and HOONO used are listed in Table 1. Because the NO_2 concentration was not directly monitored, three different concentration values were used for each set of experimental conditions, while all other input parameters remained the same. The three NO_2 concentrations chosen were: (1) the most probable value; (2) zero; and, (3) the maximum possible value. The most probable NO_2 concentration was determined by taking the difference between the $HOONO_2$ initially present and the $HOONO_2$ remaining after k^0_{obs} had been determined, just prior to the addition of ozone. The zero concentration was chosen simply to bracket the extreme cases. The maximum possible NO_2 concentration was chosen by taking ten times the total $HOONO_2$ concentration. At these high values, the computer simulations indicated deviations from first-order decay rates at low $HOONO_2$ which were not observed in any of the experimental data. Thus, these values do indeed represent the limiting cases for the initial NO_2 concentration.

The rate constant of interest, k_6, was allowed to assume values of zero, 1×10^{-20} cm^3 s^{-1}, 2×10^{-20} cm^3 s^{-1}, and 5×10^{-20} cm^3 s^{-1}. During the actual simulation, the $HOONO_2$ concentration was monitored as a function of time and a first-order decay rate constant was calculated for all of the situations previously discussed. These results are listed in Table 3. For the three experiments studied, it was observed that if k_6 was as large as 2×10^{-20} cm^3 s^{-1}, k_{calc} was larger than k_{obs} for all cases investigated. In order to allow for random

Table 2

REFERENCES FOR REACTION SCHEME

Reaction	Reference
(2) $HOONO_2 \rightarrow HO_2 + NO_2$ $k_2 = 4.40 \times 10^{-4}\ s^{-1}$	Graham, et al., 1977 Graham, et al., 1978
(3) $HO_2 + NO_2 + M \rightarrow HOONO_2 + M$ $k_3 = 3.07 \times 10^{-31}\ cm^6\ molecule^{-2} s^{-1}$	Graham, et al., 1977 Graham, et al., 1978 Baldwin and Golden, 1978
(5) $HO_2 + O_3 \rightarrow OH + 2\ O_2$ $k_5 = 1.74 \times 10^{-15}\ cm^3\ s^{-1}$	Zahniser and Howard, 1980
(7) $OH + HOONO_2 \rightarrow H_2O + NO_2 + O_2$ $k_7 = 4.0 \times 10^{-12}\ cm^3\ s^{-1}$	Barker et al., 1980 Trevor et al., 1981
(8) $OH + NO_2 + M \rightarrow HNO_3 + M$ $k_8 = 3.24 \times 10^{-30}\ cm^6\ molecule^{-2}\ s^{-1}$	Atkinson, et al., 1976 Anastasi and Smith, 1976 Wine, et al., 1979
(9) $OH + O_3 \rightarrow HO_2 + O_2$ $k_9 = 5.44 \times 10^{-14}\ cm^3\ s^{-1}$	Anderson and Kaufman, 1973 Ravishankara, et al., 1979

Table 3

SUMMARY OF GEAR ROUTINE RESULTS (k_{calc}‡)
k_{calc} versus NO_2, k_6 (see text for details)

Experiment 1 $k_{obs} = 8.43 \times 10^{-4}$ s^{-1}

**k_6	$[NO_2]$* 0	7.6×10^{14}	2.5×10^{16}
0	7.31×10^{-4}	5.82×10^{-4}	3.51×10^{-4}
1.0×10^{-20}	1.28×10^{-3}	1.23×10^{-3}	9.41×10^{-4}
2.0×10^{-20}	1.74×10^{-3}	1.75×10^{-3}	1.49×10^{-3}
5.0×10^{-20}	3.44×10^{-3}	3.79×10^{-3}	3.12×10^{-3}

Experiment 6 $k_{obs} = 5.50 \times 10^{-4}$ s^{-1}

**k_6	0	8.0×10^{14}	1.9×10^{16}
0	6.28×10^{-4}	4.83×10^{-4}	3.78×10^{-4}
1.0×10^{-20}	8.09×10^{-4}	6.94×10^{-4}	5.52×10^{-4}
2.0×10^{-20}	9.88×10^{-4}	8.88×10^{-4}	7.18×10^{-4}
5.0×10^{-20}	1.46×10^{-3}	1.39×10^{-3}	1.19×10^{-3}

Experiment 7 $k_{obs} = 2.89 \times 10^{-3}$ s^{-1}

**k_6	0	1.4×10^{15}	2.1×10^{16}
0	9.06×10^{-4}	6.92×10^{-4}	5.10×10^{-4}
1.0×10^{-20}	2.14×10^{-3}	1.74×10^{-3}	1.70×10^{-3}
2.0×10^{-20}	2.98×10^{-3}	3.03×10^{-3}	2.94×10^{-3}
5.0×10^{-20}	5.95×10^{-3}	5.75×10^{-3}	6.17×10^{-3}

*Units are molecules cm^{-3}

**Units are cm^3 s^{-1}

‡Units are s^{-1}.

experimental fluctuations and the influence of systematic uncertainties, we estimated that 5×10^{-20} cm^3 s^{-1} is a conservative upper limit for the rate constant k_6 for the reaction of ozone with $HOONO_2$.

D. Conclusions

The potential importance of $HOONO_2$ is due to its ability to act as a reservoir for both HO_2 and NO_2. This unique role underlines its potential importance and makes it difficult to estimate its effects without detailed modeling calculations. Although $HOONO_2$ can be shown not to influence tropospheric photochemical smog [Baldwin et al., 1977], it potentially has a large effect in the stratosphere because the lower temperatures and pressures combine to give it a much longer lifetime with respect to unimolecular decomposition. Table 4 briefly summarizes several of the effects of various processes on the first-order loss rate of $HOONO_2$ in the atmosphere. The photolysis rates (J_{hv}) are based on those for H_2O_2, multiplied by 1.5 to approximate the absorption cross sections of $HOONO_2$ recently measured by Molina [1980]. If the correct cross sections are the larger ones measured by Graham et al. [1978], the photolysis rate of H_2O_2 should be multiplied by ~ 6.

From inspection of Table 4, it is clear from the derived upper limit to the rate constant for reaction of ozone with $HOONO_2$ that this reaction should have no direct effect of atmospheric importance.

Acknowledgment: Support by the High Altitude Pollution Program of the Office of Environment and Energy, Federal Aviation Administration, De Department of Transportation under contract DOT-FA78WA-4228 is gratefully acknowledged. We also wish to thank J. R. Barker, A. C. Baldwin, R. A. Kenley, H. S. Johnston, and D. M. Golden for helpful discussions.

Table 4

ATMOSPHERIC $HOONO_2$ FIRST-ORDER LOSS RATES (s^{-1})

Altitude (km)	Thermal[a]	$J_{h\nu}$ [b]	$k_6(O_3)$ [c]	Total	Lifetime (hr)
0	2.8(−2)	9.3(−6)	≤ 5 (−8)	2.8(−2)	0.01
20	2.6(−8)	5.2(−6)	≤ 3 (−7)	≤ 5.5(−6)	51
30	2.4(−7)	1.1(−5)	≤ 2 (−7)	1.1(−5)	2.5
40	1.3(−5)	5.2(−5)	≤ 4.5(−8)	6.5(−5)	4.3

[a] [Graham et al., 1977 and 1978; Baldwin and Golden, 1978].

[b] Based on $J(H_2O_2)$ x 1.5 [R. D. Hudson, 1977].

[c] O_3 concentration from [Luther et al., 1979, as quoted from U.S. Standard Atmosphere, 1976], rate constant limit from present work.

E. References (Appendix E)

Anastasi, C., P. P. Bemand, and I.W.M. Smith, Rate constants for: OH + NO_2 (+ N_2) → HNO_3 (+ N_2) between 220 and 358 K, Chem. Phys. Lett., 37, 370, 1976.

Anastasi, C. and I.W.M. Smith, Rate measurements of reactions of OH by resonance absorption, J. Chem. Soc. Faraday Trans. II, 72, 1459, 1976.

Anderson, J. G. and F. Kaufman, Kinetics of the reaction OH(v=0) + O_3 → HO_2 + O_2, Chem. Phys. Lett., 19, 483, 1973.

Atkinson, R., R. A. Perry, and J. N. Pitts, Jr., Rate constants for the reactions of the OH radical with NO_2 (M = Ar and N_2) and SO_2 (M = Ar), J. Chem. Phys., 65, 306, 1976.

Baldwin, A. C., J. R. Barker, D. M. Golden, and D. G. Hendry, Photochemical smog. Rate parameter estimates and computer simulations, J. Phys. Chem. 81, 2483, 1977.

Baldwin, A. C. and D. M. Golden, Application of RRKM theory using a hindered rotational Gorin model transition state to the reaction HO_2NO_2 + N_2 ⇄ HO_2 + NO_2 + N, J. Phys. Chem. 82, 644, 1978.

Barker, J. R., G. Black, and P. L. Trevor, Rate constant measurements for the reaction $HOONO_2$ + OH → Products, 1980 Geophysical Union Fall Meeting, San Francisco, CA, 8-12 December 1980.

Cox, R. A. and K. Patrick, Kinetics of the reaction HO_2 + NO_2 (+ M) ⇄ HO_2NO_2 (+ M) using molecular modulation spectrometry, Int. J. Chem. Kinetics, 11, 635, 1979.

Gear, C. W., Numerical Initial Value Problems in Ordinary Differential Equations, Prentice Hall, New Jersey, 1971.

Graham, R. A., A. M. Winer, and J. N. Pitts, Jr., Temperature dependence of the unimolecular decomposition of pernitric acid and its atmospheric implications, Chem. Phys. Lett., 51, 215, 1977.

Graham, R. A., A. M. Winer, and J. N. Pitts, Jr., Ultraviolet and infrared absorption cross sections of gas-phase HO_2NO_2, Geophys. Res. Lett., 5, 909, 1978.

Graham, R. A., A. M. Winer, and J. N. Pitts, Jr., Pressure and temperature dependence of the unimolecular decomposition of HO_2NO_2, J. Chem. Phys., 68, 4505, 1978.

Herzberg, Gerhard, Infrared and Raman Spectra, Vol. II, van Nostrand Reinhold Company, 1945, p. 286.

Howard, C. J., Kinetics of the reaction of HO_2 with NO_2, J. Chem. Phys., 67, 5258, 1977.

Hudson, R. D., Ed., Chlorofluoromethanes and the Stratosphere, NASA Ref. Pub., 1010, NTIS, 1977.

Littlejohn, D. and H. S. Johnston, 1980 American Geophysical Union Fall Meeting, San Francisco, CA, 8-12 December 1980.

Lloyd, Alan C., Evaluated and estimated kinetic data for gas-phase reactions of the hydroperoxyl radical, Int. J. Chem. Kinetics, 6, 169, 1974.

Luther, F. M., J. S. Chang, W. H. Duewer, J. E. Penner, R. L. Tarp, and D. J. Wuebbles, Potential Environmental Effects of Aircraft Emissions, Lawrence Livermore Laboratory Report No. UCRL-52861, 1979.

Molina, L. T. and M. J. Molina, Ultraviolet absorption cross sections of HO_2NO_2 vapor, 14th Informal Conference on Photochemistry, Newport Beach, CA, 30 March-3 April, 1980.

Niki, H., P. D. Maker, C. M. Savage, and L. P. Breitenbach, Fourier transform IR spectroscopic observation of pernitric acid formed via $HOO + NO_2 \rightarrow HOONO_2$, Chem. Phys. Lett., 45, 564, 1977.

Ravishankara, A. R., P. H. Wine, and A. O. Langford, Absolute rate constant for the reaction $OH(v=0) + O_3 \rightarrow HO_2 + O_2$ over the temperature range 238-357 K, J. Chem. Phys., 70, 984, 1979.

Simonaitis, R. and J. Heicklen, Reactions of HO_2 with NO and NO_2 and of OH with NO, J. Phys. Chem., 80, 1, 1976.

Trevor, P. L., G. Black, and J. R. Barker, The reaction rate constant for OH + $HOONO_2$ → Products over the temperature range 246 K to 324 K, J. Phys. Chem., submitted.

United States Standard Atmosphere, ICAO, Geneva, Switzerland, 1976.

Wine, P. H., N. M. Kreutter, and A. R. Ravishankara, Flash photolysis-resonance fluorescence kinetics study of the reaction OH + NO_2 + M → HNO_3 + M, J. Phys. Chem., 83, 3191, 1979.

Zahniser, M. S. and C. J. Howard, Kinetics of the reaction of HO_2 with ozone, J. Chem. Phys., 73, 1620, 1980.

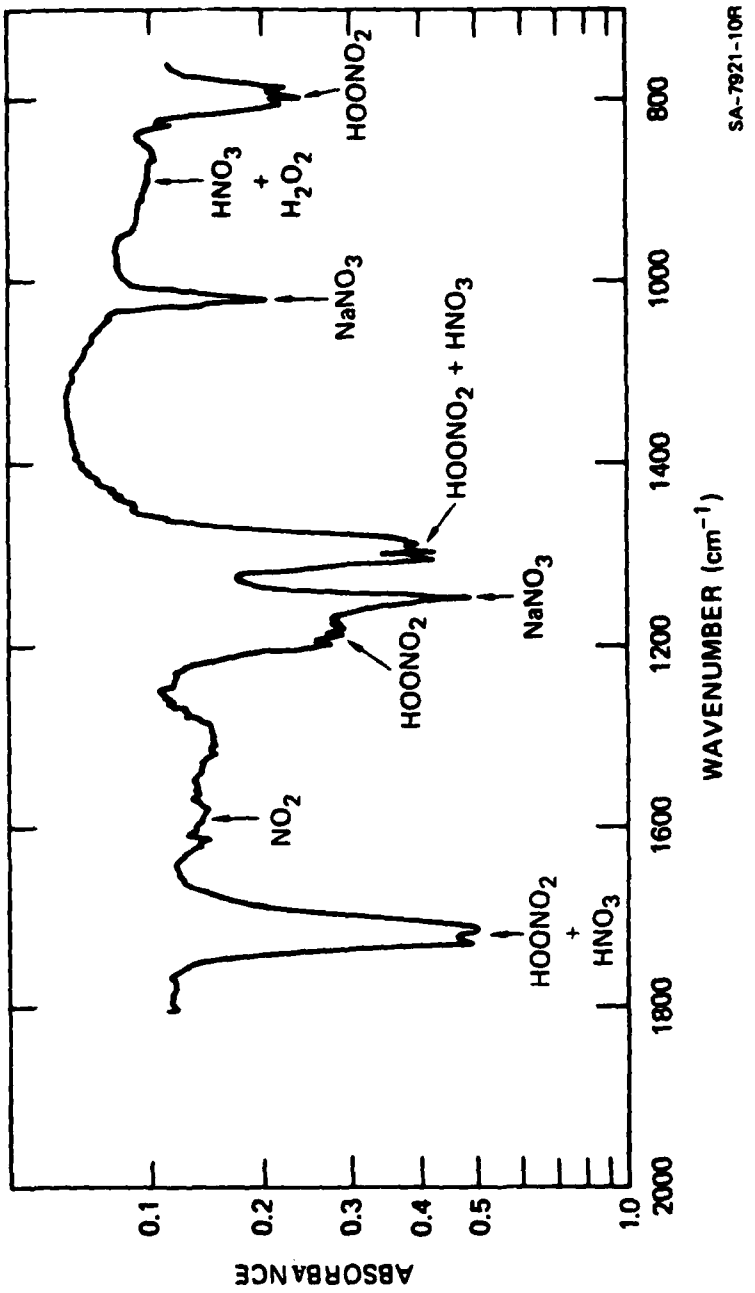

FIGURE 1 INFRARED SPECTRUM OF $HOONO_2$ PREPARED AS DESCRIBED IN TEXT

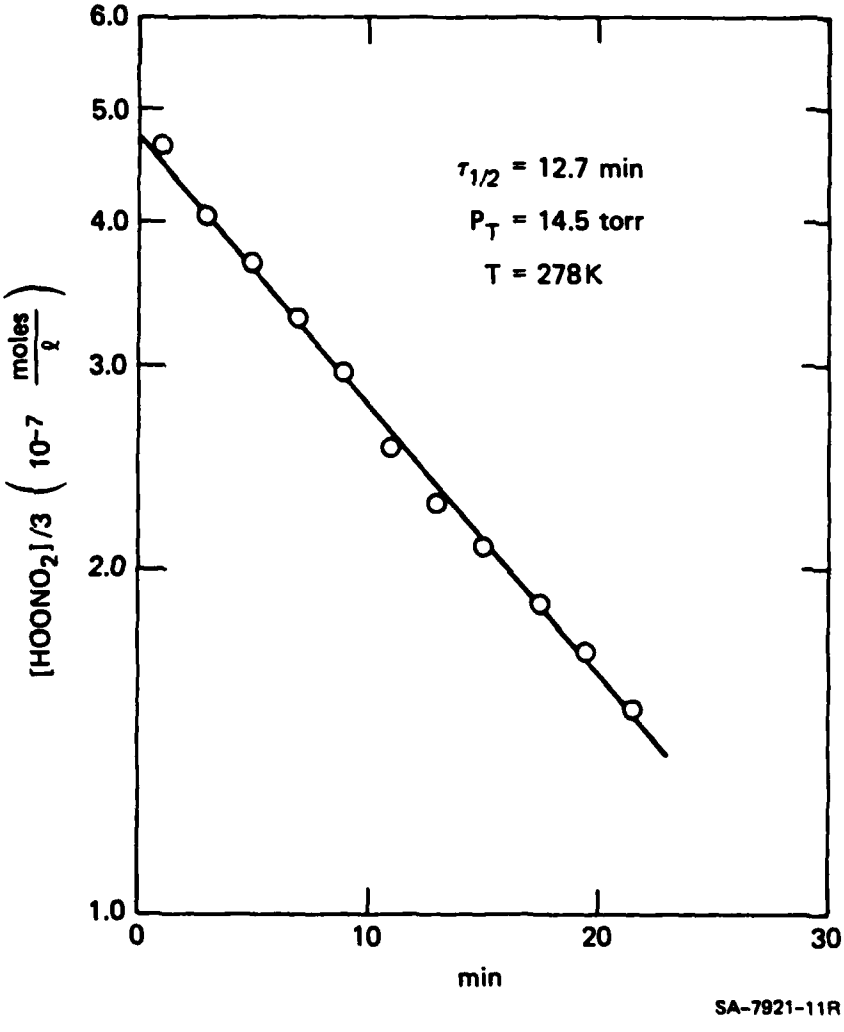

FIGURE 2 SEMI-LOGARITHMIC PLOT OF $HOONO_2$ DECAY
Typical result for Argon buffer gas.

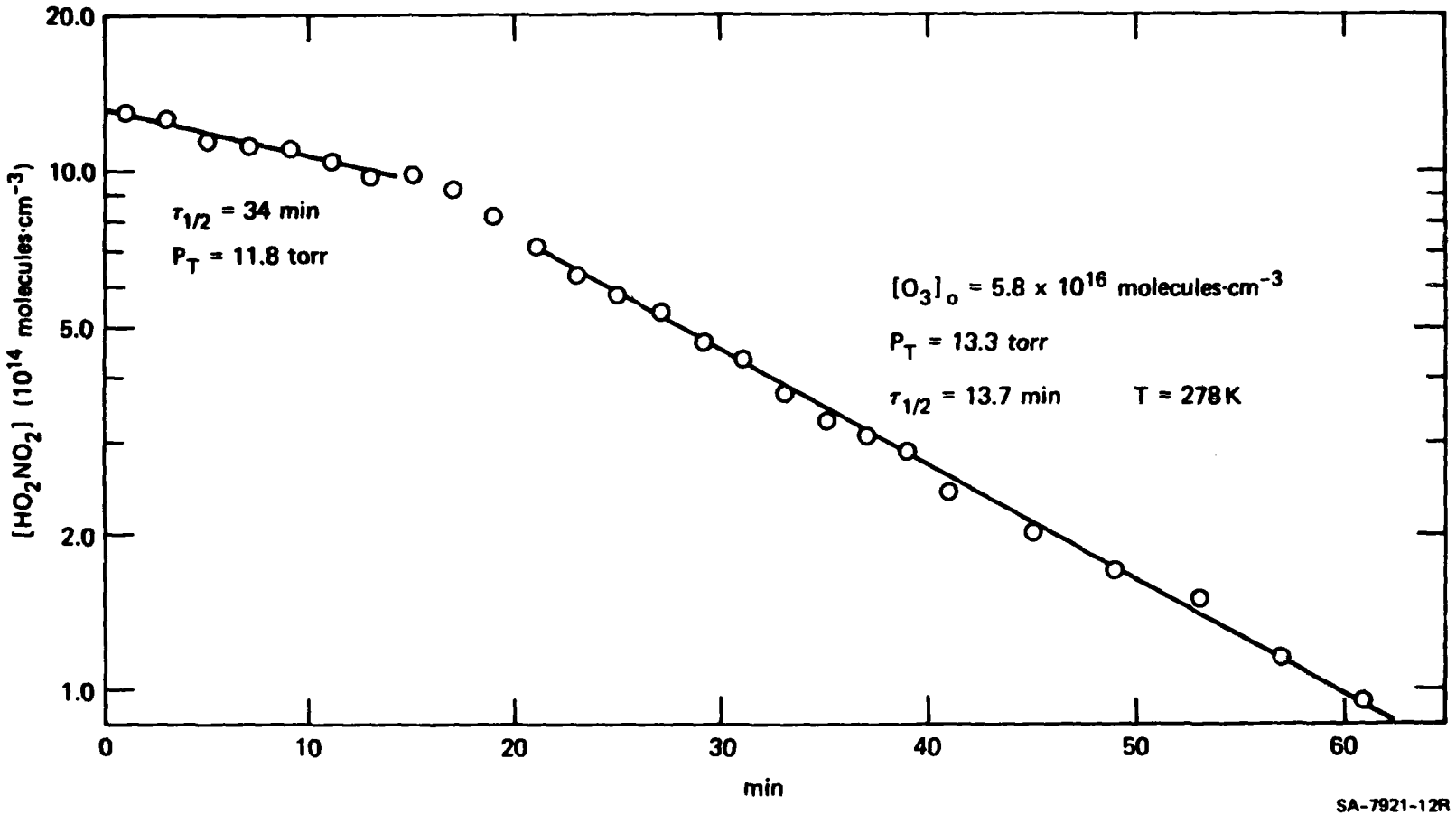

FIGURE 3 TYPICAL EXPERIMENTAL RUN SHOWING INCREASED RATE OF $HOONO_2$ LOSS AFTER ADDITION OF O_3 (AT ~18 MINUTES)